

QUANTUM MECHANICS OF LEPTOGENESIS

Dissertation
zur Erlangung des Doktorgrades
des Departments Physik
der Universität Hamburg

vorgelegt von

Sebastián Mendizabal Cofré

aus Santiago, Chile

Hamburg

2010

Gutachter der Dissertation: Prof. Dr. W. Buchmüller
Prof. Dr. J. Bartels
Gutachter der Disputation: Prof. Dr. W. Buchmüller
Prof. Dr. K. Fredenhagen
Datum der Disputation: 09.07.2009
Vorsitzender des Prüfungsausschusses: Prof. Dr. G. Sigl
Vorsitzender des Promotionsausschusses: Prof. Dr. J. Bartels
Dekan der Fakultät MIN: Prof. Dr. H. Graener

Abstract

Leptogenesis is an attractive mechanism that simultaneously explains the matter-antimatter asymmetry of the universe as well as the small masses of the standard model neutrinos. This is performed by naturally extending the standard model with the insertion of right handed neutrinos. Leptogenesis is usually studied via the semi-classical Boltzmann equations. However, these equations suffer from basic conceptual problems and they lack to include many quantum phenomena, such as memory effects and coherence oscillations. In order to fully describe leptogenesis, a full quantum treatment is required. In this work we show how to address leptogenesis systematically in a purely quantum way. We start by studying scalar and fermionic excitations in a plasma by solving the Kadanoff-Baym equations of motion for Green's functions, with significant emphasis on the initial and boundary conditions of the solutions. We compute analytically the asymmetry generated from the departure of equilibrium of a particle in a thermal bath. The comparison with the semi-classical Boltzmann approach is also analysed, leading to a qualitative difference between both methods. The non-locality of the Kadanoff-Baym equations shows how off-shell effects can have a huge impact on the generated asymmetry, effects that cannot be studied with the Boltzmann equations. The insertion of standard model interactions like the decay widths for the particles of the bath is also discussed. We explain how with a trivial insertion of these widths we regain locality on the processes, i.e. we regain the Boltzmann equations.

Zusammenfassung

Leptogenese ist ein attraktiver Mechanismus zur gleichzeitigen Erklärung der Materie-Antimaterie-Asymmetrie des Universums sowie der kleinen Massen der Standardmodellneutrinos. Er beruht auf der natürlichen Erweiterung des Standardmodells um rechtshändige Neutrinos. Leptogenese wird üblicherweise mittels semiklassischer Boltzmann-Gleichungen studiert, welche jedoch mit prinzipiellen Schwierigkeiten einhergehen und bei der Beschreibung von Quantenphänomenen fehlschlagen. Solche Effekte, wie etwa Gedächtniseffekte und kohärente Oszillationen, sind wesentlich für die vollständige Beschreibung der Leptogenese. In dieser Arbeit zeigen wir wie sich Leptogenese systematisch durch rein quantenmechanische Methoden untersuchen lässt. Zunächst lösen wir dazu die Kadanoff-Baym-Bewegungsgleichungen für Greensfunktionen skalarer und fermionischer Anregungen in einem Plasma, wobei wir besonders die Bedeutung von Anfangs- und Randbedingungen für die Lösungen betonen. Wir berechnen die Asymmetrie, welche durch die Entfernung eines Teilchens aus dem Gleichgewicht in einem thermischen Bad generiert wird, analytisch. Der Vergleich mit der semiklassischen Boltzmann-Beschreibung wird ebenfalls durchgeführt und zeigt die qualitativen Unterschiede beider Methoden auf. Die Nichtlokalität der Kadanoff-Baym-Gleichungen belegt den großen Einfluss von Off-shell-Effekten auf die generierte Asymmetrie, Effekte, welche nicht mittels Boltzmann-Gleichungen studiert werden können. Die Einführung von Standardmodellwechselwirkungen, etwa von Zerfallsbreiten der Teilchen im Bad, wird ebenfalls diskutiert. Eine triviale Berücksichtigung dieser Breiten ist gleichbedeutend mit der Wiedergewinnung der Lokalität der Prozesse, führt also zurück zur Beschreibung durch Boltzmann-Gleichungen.

Acknowledgments

I would like to thank my supervisor Wilfried Buchmüller for his support, guidance and helpful discussions throughout this thesis.

I would also like to thank Jochen Bartels and Klaus Fredenhagen for refereeing this thesis and my defense.

Especially, I would like to thank the DAAD for its support and the opportunity to study in Germany.

I am very grateful with my collaborators Marco Drewes and Alexey Anisimov, with whom all of the results from this thesis were achieved.

Furthermore, I would like to thank Clare Burrage, Tom Brown, Jonas Schmidt, Cecelie Hector, Christoph Weniger and Christian Hambrock for helping me proof-reading this thesis.

Thanks to all the members of the DESY theory group for the helpful discussions and for the nice, friendly and cheerful atmosphere.

I would like to thank the members of my band *The Bob Morrison Experience*, Chloe Papineau, Christoph Weniger, Javier Redondo and Thomas Danckaert, for the great rehearsals and the most outstanding concerts.

Thanks to my office mates Christian Hambrock, Cecelie Hector, Hao Zou and Sergei Bobrovskiy for making a great and enjoyable office.

A big kiss to my family, specially my mother for her patience, hope and her great support.

A special thank to Valeria del Campo for her support from the distance.

Finally I would like to thank Elizabeth Ortega for her happiness, belief and joy that she gave to me during these years.

To everyone who believes that physics should be simple...

Contents

Introduction	1
Outline	5
1 Thermal leptogenesis	7
1.1 Baryon asymmetry in the universe (BAU)	7
1.2 Sakharov's conditions	8
1.3 Type I seesaw mechanism	9
1.4 Other seesaw models	11
1.5 Sphalerons	12
1.6 Boltzmann equations	15
1.7 CP asymmetry	16
1.8 Semi-classical leptogenesis	17
1.9 Effective model	19
2 Non-equilibrium thermal field theory	21
2.1 Keldysh-Schwinger formalism for scalars	22
2.1.1 Kadanoff-Baym equations for scalars	22
2.1.2 Solutions for the KB equations	26
2.1.3 Thermalization	31
2.1.4 Model example	34
2.2 Keldysh-Schwinger formalism for Fermions	41
2.2.1 Kadanoff-Baym equations for fermions	41
2.2.2 Solutions for the KB equations	44
2.2.3 Properties of the solutions	50
2.3 Keldysh-Schwinger formalism for standard model leptons	52
2.4 Keldysh-Schwinger formalism for Majorana fermions	53
3 Thermal leptogenesis	57
3.1 Boltzmann formalism	57
3.1.1 Boltzmann equation for the production of Majorana fermions	57

3.1.2	Boltzmann equations for the production of a the lepton asymmetry	59
3.2	Quantum formalism	62
3.2.1	Simple exemplary case	62
3.2.2	Kadanoff-Baym equations for leptons	64
3.2.3	Asymmetry from the quantum formalism	69
3.2.4	Comparison with Boltzmann	72
3.3	Introducing SM widths	73
4	Future work	75
4.1	Including expansion of the universe	75
4.2	Wash-out terms	75
4.3	Non-perturbative regime	76
4.4	Resonant leptogenesis	76
5	Conclusions	79
A	Notation and conventions	83
A.1	Conventions	83
A.2	Scalars Green's functions	84
A.3	Fermionic Green's functions	85
B	Scalar theory	89
B.1	Self Energy	89
B.2	Breit-Wigner	91
B.3	Time translational invariance	92
C	Fermion theory	95
C.1	2 flavour structure matrix Inverse	95
C.2	Calculation of the 1-loop self-energy	97
C.3	Computation of Γ	108
C.4	Calculation of the 2-loop self-energy	110
D	List of propagators	115

Introduction

One of the few parameters from the early universe that we can measure today with high accuracy, is the *Baryon Asymmetry of the Universe* (BAU). The baryon asymmetry density per photon density has been determined from *Big-Bang-Nucleosynthesis* (BBN) to be [1]

$$\eta^{BBN} = \frac{n_B - n_{\bar{B}}}{n_\gamma} = (5.1 - 6.5) \times 10^{-10}. \quad (0.0.1)$$

The same parameter has also been measured with great accuracy by the *Wilkinson Microwave Anisotropy Probe* (WMAP) with a very similar result [2]

$$\eta^{WMAP} = (6.19 \pm 0.15) \times 10^{-10}. \quad (0.0.2)$$

In order to explain this asymmetry a variety of different methods have been developed, like *GUT baryogenesis* [3–10], *electroweak baryogenesis* [11–19], *Affleck-Dine baryogenesis* [20–22], *ν MSMM mechanism* [23] among others. The common aspect from these models is, that they need to fulfill the Sakharov conditions [24].¹ The *standard model* (SM) can in principle satisfy this conditions and generate an asymmetry. However, the asymmetry created by the SM is too small to explain the data. It is necessary to extend the SM and allow for new possible sources to generate sufficient asymmetry. One of the most simple and natural ways of extending it is to embed an additional neutrino with right-hand chirality, giving rise to *Thermal Leptogenesis* [25–28]. With the help of the *see-saw mechanism* [29,30], thermal leptogenesis can in principle explain the BAU and also the smallness of the SM neutrino masses.

Thermal leptogenesis has been a very popular model to explain the BAU during the past couple of decades. This model describes the BAU via a previous asymmetry on the leptonic sector and then translated to a baryon-asymmetry via processes called *Sphalerons* [31,32]. The principal idea of leptogenesis is to create an asymmetry with the decay of the heavy Majorana neutrinos that appear after the seesaw mechanism is used. These CP-violating decays become important when the temperature is of the order of the mass of the decaying particle ($\sim 10^9$ GeV), below this threshold they are exponentially suppressed. Such high reheating temperatures can have important cosmological consequences. In supersymmetric scenarios where the mass of the gravitino lies below 10 TeV its late decay typically destroys the successful predictions of the

¹see Sec. 1.2 for more details.

Standard Big Bang Nucleosynthesis (BBN) scenario [33, 34]. However, if the gravitino is itself the LSP and hence stable, the late decay of the NLSP again causes similar problems [35–42]. Many ways of circumventing these problems have been proposed, like the small violation of R-parity [43], the decay of the NLSP into hidden sector particles [44, 45] or the production of entropy before BBN [46].

The dynamics of leptogenesis is commonly described with the Boltzmann equations. These are first order differential equations that characterise the time evolution of number particle densities or distribution functions. The Boltzmann equations are well known to work for describing the creation of light elements such as H and He, and for the decoupling of the *cosmic microwave background* (CMB) from the primordial plasma [47, 48]. However, they are semi-classical equations and may fail to describe strongly coupled systems or quantum phenomena such as coherent oscillations or quantum interference. Since leptogenesis originates from quantum effects, a full quantum treatment to leptogenesis is indispensable.

In order to obtain a better understanding of leptogenesis, many authors have upgraded the Boltzmann equations to the so-called *quantum Boltzmann* [49–52] or the *full quantum Boltzmann* equations [53–58] equations. In this scenario, many properties have been studied, for example in [59–67] flavour effects are taken into account. In [68–71] it was also demonstrated, that the CP-violating parameter is resonantly enhanced if two of the heavy Majorana neutrinos have a difference in mass comparable to their decay widths. The basic idea behind *quantum-* or *full-quantum* Boltzmann equations is to promote the scattering matrix elements inside the collision term of the Boltzmann equations to contain matrix elements calculated from *quantum field theory*. This type of procedure is valid only when particles in the thermal bath can be represented as quasi-particles with well defined thermal masses and widths. However, when the temperature is increased, the quasi-particle or thermal Breit-Wigner representation breaks down [72]. This happens when the imaginary part of the self-energy, i.e. the decay width, becomes non-negligible with respect to the mass scale of the system.

The quantum Boltzmann equations represent a first order approximation to a full quantum theory [73]. They are only valid when the width of the generated particle in the plasma is small. However, taking the first order approximation is not well justified. Because leptogenesis is a purely quantum phenomenon, quantum interference is a crucial factor where off-shell effects can be important. When only the first order approximation is taken into account, all off-shell effects in the quantum interference are neglected, leading to an erroneous result.

The full treatment of non-equilibrium processes in quantum field theory is usually based either on Kadanoff-Baym equations [74] and the Schwinger-Keldysh formalism [75–80] or on stochastic Langevin equations [81–84]. The Kadanoff-Baym equations are the thermal analogs to the Schwinger-Dyson equations [85], and its first order solution in an expansion around its center of mass coordinate after a Wigner transformation gives back the normal Boltzmann equations. Again, making this approximation, i.e.

neglecting higher order solutions in this derivative expansion, is only valid when the non-equilibrium process is very close to equilibrium. However, leptogenesis is generated from far from equilibrium process, and quantum effects that come from the interference between the center of mass of the non-equilibrium field and the thermal bath are very important.

In our work, we solve exactly the Kadanoff-Baym equations for the excitations in a plasma. We concentrate our analysis on the evolution of correlation functions instead of particle number densities or distribution functions, with special focus on the boundary and initial conditions of the correlators. The understanding of the non-equilibrium dynamics of this excitations is one of the most important aspect of our work in order to be able to move towards a complete quantum theory of leptogenesis. In this scenario, a non-equilibrium Majorana neutrino is created in thermal bath, and its quantum interference with the plasma explains the expected asymmetry.

In order to be able to solve the Kadanoff-Baym equations some important simplifications need to be made: a) the thermal bath is homogenous and isotropic, b) the temperature of the bath varies much slower than the expansion of the universe, so the bath remains in equilibrium, c) the thermal bath is strongly coupled and its many degrees of freedom make back-reaction of the out-of-equilibrium particle negligible. We will show how the time-translation invariance of the self-energy of the bath that comes from these three conditions, allows us to solve analytically the Kadanoff-Baym equations. However, for the case of leptogenesis, the self-energy is not time-translational invariant due to the non-equilibrium decay of the Majorana neutrino within the bath. Here an expansion around equilibrium can be performed by considering the asymmetry to be generated close to equilibrium. This, however, does not contradict the fact that the Majorana neutrino is produced far away from equilibrium.

In this work we are able to stretch the understanding of full quantum leptogenesis by studying the dynamics of a weakly coupled Majorana neutrino to a thermal bath, which explains the observed matter-antimatter asymmetry. The Kadanoff-Baym equations give us all the information of the quantum dynamics of the asymmetry, where now all on-shell and off-shell effects can be clearly studied. In order to understand the differences between the semi-classical formalism and a full quantum one, there is no need to perform a quantitative calculation, but a qualitative comparison is enough to see how important off-shell effects are, and how quantum interference plays a crucial role.

Outline

In Chapter 1, we briefly summarise the ingredients to successfully produce a baryon asymmetry in the universe. We start in Sec. 1.1 by describing different models for baryogenesis. Through Sec. 1.2 to 1.8, we explain different mechanisms commonly used for an asymmetry generating model, such as the seesaw mechanism, sphaleron processes, Boltzmann equations and the introduction of a CP violating parameter. In Sec. 1.9 and 1.10, we discuss the fundamentals of thermal leptogenesis and its limitations to be a full quantum theory.

In Chapter 2, we describe the non-equilibrium dynamics of particles in a thermal bath. We show a quantum description via the Kadanoff-Baym equations of the creation and subsequent thermalization of a particle. In Sec. 2.1 we concentrate on scalar particles in order to study the special characteristics of this quantum model for a simple system. In Sec. 2.2 and 2.3, the same procedure is performed for fermionic particles, first for a general massive fermion, and is afterwards extended to massless leptons and Majorana fermions. We obtained an analytical solution with well defined boundary and initial conditions for non-equilibrium propagators for a particle which is created in a thermal bath.

In Chapter 3, we apply the previously discussed non-equilibrium dynamics to thermal leptogenesis. In Sec. 3.1 the Boltzmann procedure is used for coupled differential equations describing the production of Majorana particle and the lepton asymmetry. The solution is obtained for a system with neglected wash-out terms. The full quantum procedure for leptogenesis is described in Sec. 3.2. We start by showing the coupled Kadanoff-Baym equations, with one of them already solved in Chapter 2. In Sec. 3.2.4, the generated asymmetry is defined for the full quantum treatment, and the solution is compared to the Boltzmann solution given in Sec. 3.2.5, pointing out the qualitative differences between both methods. In Sec. 3.3, we discuss the problem of introducing standard model correction to the particles inside the thermal bath, and in Sec. 3.4 we present the possibility of having a flavour structure in the Majorana sector.

In Chapter 4, we summarise the results and discuss the possibility of expanding the work by including more realistic aspects of leptogenesis, such as flavour structure, expansion of the universe and non-perturbative standard model corrections. The results of this work have previously been published in [86] and [87].

Chapter 1

Thermal leptogenesis

In this chapter we will describe the basic aspects of thermal leptogenesis. An overview description about its fundamental principles is given. Ingredients such as the seesaw mechanism, sphaleron processes and Boltzmann equations are described in order to outline the actual context of the problem.

1.1 Baryon asymmetry in the universe (BAU)

Many different models have been developed to explain the BAU, Although none of them have been experimentally confirmed, many suffer from theoretical cosmological problems. As an example for baryogenesis models we can start by looking at the following

GUT baryogenesis [3–10]

GUT baryogenesis is a good start for understanding leptogenesis, since both approaches are mathematically quite similar. In this scenario, baryogenesis could be created from the non-equilibrium decay of heavy bosons in Grand Unified Theories. B violation is also satisfied by the decay and CP violation comes from the complex Yukawa couplings. This models are today almost ruled out because they requires higher reheating temperature from inflation than is required. Unwanted relics as monopoles and heavy gravitinos are generated. The GUT baryogenesis has also difficulties with the non-observation of proton decay, which puts a lower bound on the mass of the decaying boson, and therefore on the reheating temperature. Furthermore, in the simplest GUTs, $B + L$ is violated but $B - L$ is not. Consequently, the $B + L$ violating SM sphalerons, which are in equilibrium at $T \sim 10^{12}$ GeV, would destroy this asymmetry.

Electroweak baryogenesis [11–19]

Electroweak baryogenesis is the name for a class of models where the departure from thermal equilibrium is provided by the electroweak phase transition. In principle, the SM belongs to this class, but the phase transition is not strongly first order and the CP violation is too small. Thus, viable models of electroweak baryogenesis need

a modification of the scalar potential such that the nature of the electroweak phase transition changes, and new sources of CP violation. One example insertion of two Higgs doublet, where the Higgs potential has more parameters and, unlike the SM potential, violates CP. Another interesting example is the MSSM (minimal supersymmetric SM), where a light stop modifies the Higgs potential in the required way and where there are new, flavour-diagonal, CP violating phases. Electroweak baryogenesis and, in particular, MSSM baryogenesis, might soon be subject to experimental tests at the LHC.

The Affleck-Dine mechanism [20–22]

In the Affleck-Dine baryogenesis the asymmetry arises in a classical scalar field, which later decays to particles. In a SUSY model, this field could be some combination of squark, Higgs and slepton fields. The field starts with a large expectation value, and rolls towards the origin in its scalar potential. At the initial large distances from the origin, there can be contributions to the potential from baryon or lepton number violating interactions (mediated, for instance, by heavy particles). These impart a net asymmetry to the rolling field. This generic mechanism could produce an asymmetry in any combination of B and L .

Thermal leptogenesis [25–27]

Thermal leptogenesis describes the baryon asymmetry via a previous asymmetry generated in the leptonic sector. Which is later partially converted to a baryon asymmetry via sphaleron processes. In order to obtain a lepton asymmetry, the SM needs to be extended by introducing a right-handed neutrino. The use of the seesaw mechanism will generate heavy Majorana neutrinos which will decay out-of-equilibrium and violate CP in the process.

In this work we will focus on the mechanics on thermal leptogenesis by describing the generation of an out-of equilibrium heavy Majorana neutrino. In what follows we will describe the basics of thermal leptogenesis.

1.2 Sakharov’s conditions

To successfully produce a baryon asymmetry, Andrei Sakharov [24] summarised the three conditions that must be satisfied:

1. Baryon number violation,
2. C-symmetry and CP-symmetry violation,
3. Out of equilibrium dynamics.

These three conditions can already be found to be satisfied in the SM, although the generated baryon asymmetry turns out to be small. Each of the three conditions can be fulfilled separately

1. Baryon number is violated in the standard model via the triangle anomaly [31], where a selection rule is obeyed, $\Delta B = \Delta L = \pm 3$. The amplitude of this baryon number violating process is proportional, at zero temperature, to $e^{-2\pi/\alpha} \sim \mathcal{O}(10^{-170})$. For large temperatures ($T \sim 10^3$ GeV) this suppression disappears.
2. C-symmetry and CP-symmetry violation occur in the weak interactions of the SM via the Kobayashi-Maskawa mechanism [88]. Because of the smallness of the masses involved, the amount of asymmetry that arises with this CP violating mechanism is not sufficient to explain the asymmetry of the universe.
3. Out of equilibrium dynamics in the SM are present, if the electro-weak phase transition is of first order [11]. However, this phase transition is not as strong as required by baryogenesis.

All of this indicates the standard model must be extended with a new source of CP violating processes and a departure from equilibrium that gives us a successful model for baryogenesis. The most simple scenario to extend the SM will give rise to thermal leptogenesis, where the three Sakharov conditions are fulfilled:

1. Lepton number violation occurs due to the Majorana mass that arises from the see-saw mechanism. Afterwards this lepton number asymmetry will translate to a baryon asymmetry via sphaleron processes.
2. Flavour interactions of the massive Majorana neutrinos with the SM particles will give us the right amount of C and CP asymmetry necessary (These interactions come from the quantum interference between one-loop and tree level diagrams).
3. Expansion rate of the universe is much faster than the reaction rate which generates the asymmetry, this will guarantee that the processes are out of equilibrium.

1.3 Type I seesaw mechanism

The seesaw mechanism [29, 30] is a renormalizable model that not only explains the smallest of the neutrino masses but also provides us with all the ingredients for explaining the baryon asymmetry in the universe.

The basic idea is to include three heavy right-handed neutrino singlets to the SM. Because these new neutrinos are electro-weak singlets, we can introduce a Majorana mass term in the Lagrangian without affecting chirality and gauge properties of the SM. The new Lagrangian that includes the new mass and Yukawa term reads

$$-\mathcal{L} = Y_\nu \bar{\ell}_L \phi \nu_R + \frac{M_R}{2} \overline{(\nu_R)^c} \nu_R + h.c. , \quad (1.3.1)$$

where M_R is the mass for the RH neutrino. The coupling to the Dirac neutrinos (Y_ν) will give rise to small Dirac masses. In order to see this, we first notice that the size of

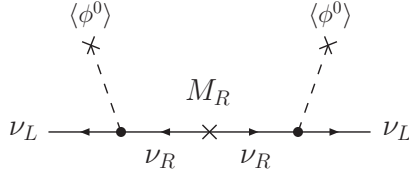


Figure 1.1: Diagram representing the type I seesaw realisation of the small Majorana mass for the LH neutrino with $m_\nu \simeq \langle \phi^0 \rangle^2 Y_\nu M_R^{-1} Y_\nu^T$ (up to a multiplicative constant).

M_R is arbitrary and we can assume that it is very large. As a quick computation we can integrate out the heavy RH field, obtaining the effective Lagrangian

$$\mathcal{L}_{eff} = \frac{Y_\nu^2}{2M_R} \bar{\ell}_L \phi \phi^T \ell_L^c, \quad (1.3.2)$$

In this way we can obtain an effective small mass for the Dirac neutrinos (for $M_R \gg \langle \phi^0 \rangle$ see figure 1.1).

$$m_\nu = \langle \phi^0 \rangle^2 Y_\nu M_R^{-1} Y_\nu^T. \quad (1.3.3)$$

The effective mass of the neutrinos is inverse proportional to the mass of the right handed neutrinos, hence the name see-saw. To be more precise, one can obtain the above result by rearranging the mass terms of the Lagrangian (1.3.1) in a matrix form

$$-\mathcal{L} = \frac{1}{2} \sum_{i,j}^n [\bar{\nu}_{iL} (m_D)_{ij} \nu_{jR} + \overline{(\nu_{jR})^c} (m_D)_{ji} \nu_{iL}^c + \overline{(\nu_{Ri})^c} (M_R)_{ij} \nu_{jR}] + h.c., \quad (1.3.4)$$

where $m_D = Y_\nu \langle \phi^0 \rangle$ and we have used the fact that $\bar{\nu}_{iL} \nu_{jR} = \overline{(\nu_{jR})^c} (\nu_{iL})^c$. Then the above equation can be factorised as

$$\mathcal{L} = \frac{1}{2} (\bar{\nu}_L, \bar{\nu}_R^c) M \begin{pmatrix} \nu_L^c \\ \nu_R \end{pmatrix} + h.c., \quad (1.3.5)$$

with

$$M = \begin{pmatrix} M^L & m_D \\ m_D & M^R \end{pmatrix}. \quad (1.3.6)$$

where $\nu_L = (\nu_{1L}, \dots, \nu_{nL})^T$ and $\nu_R = (\nu_{1R}, \dots, \nu_{nR})^T$. Assuming that the eigenvalues of m_D are much less than those of M_R , the neutrino mass matrix in (1.3.6) may be diagonalized (to first order in $M_R^{-1} m_D^T$) by

$$V M V^T \approx \begin{pmatrix} m_D M_R^{-1} m_D^T & 0 \\ 0 & M_R \end{pmatrix}, \quad (1.3.7)$$

where

$$V = \begin{pmatrix} I & (M_R^{-1} m_D^T)^\dagger \\ -M_R^{-1} m_D^T & I \end{pmatrix} \begin{pmatrix} iI & 0 \\ 0 & I \end{pmatrix}. \quad (1.3.8)$$

The second matrix in the definition of (1.3.8) is included to ensure all mass eigenvalues are positive. If we let $(\nu', N')^T = (\nu_L, \nu_R^c)^T V^T$ and define a set of Majorana fields:

$$\begin{pmatrix} \nu \\ N \end{pmatrix} \equiv \begin{pmatrix} \nu' + (\nu')^c \\ N' + (N')^c \end{pmatrix}, \quad (1.3.9)$$

then the mass terms of the Lagrangian become

$$\begin{aligned} -\mathcal{L}_\nu &= \frac{1}{2}(m_D M_R^{-1} m_D^T) \bar{\nu} \nu + M_R \bar{N} N + h.c., \\ &= m_\nu \bar{\nu} \nu + M_R \bar{N} N + h.c. . \end{aligned} \quad (1.3.10)$$

It is easy to see that this model gives rise to two sets of Majorana neutrinos: the light ones (ν) with mass matrix $m_\nu \approx m_D M_R^{-1} m_D^T = \langle \phi^0 \rangle Y_\nu M_R^{-1} Y_\nu^T$, and the heavy ones (N) with mass $M_N \equiv M_R$. A particularly attractive feature, is that the smallness of m_ν is a direct consequence of the large mass scale of M_R , which may have its origin from higher unification theories.

1.4 Other seesaw models

Beside Type I seesaw, there exist other extensions to the SM which lead to effective Majorana masses. These seesaw models provide alternative ways to understand the smallness of neutrino masses, and hence are of great interest to model builders. We will briefly review them here despite the fact that they play no direct role in our current work.

Type II seesaw

Instead of extending the SM by adding heavy singlet fermions, one can make use of the fact that $\bar{\ell}_L \ell_L^c$ is an $SU(2)_L$ triplet and introduce a heavy triplet scalar to the Higgs sector [89–91], so that a gauge invariant and renormalisable $\bar{\ell}_L \ell_L^c$ -type mass term can be formed. Specifically, suppose we have a heavy $SU(2)_L$ triplet scalar field Δ with hypercharge $Y = -2$ and a convenient 2×2 matrix parametrization given by

$$\Delta = \begin{pmatrix} \Delta^-/\sqrt{2} & \Delta^{--} \\ \Delta^0 & -\Delta^-/\sqrt{2} \end{pmatrix}, \quad (1.4.1)$$

then the Lagrangian

$$-\mathcal{L}_{\text{type-II}} = \frac{Y_\Delta}{2} \bar{\ell}_L i\tau_2 \Delta \ell_L^c + \mu_\Delta \phi^T \Delta \phi + M_\Delta^2 \Delta^\dagger \Delta + h.c. , \quad (1.4.2)$$

will give rise to the process depicted in Fig. 1.2a. This then leads to an effective mass term

$$m_{\text{eff}}^{\text{II}} \simeq \mu_\Delta Y_\Delta \frac{\langle \phi^0 \rangle^2}{M_\Delta^2},$$

$$= \lambda_\Delta Y_\Delta \frac{\langle \phi^0 \rangle^2}{M_\Delta}, \quad \text{after setting } \mu_\Delta \equiv \lambda_\Delta M_\Delta. \quad (1.4.3)$$

In this expression the coupling $\lambda_\Delta Y_\Delta$ plays the role of Y_ν^2 in the Type I seesaw. So, when $M_\Delta \gg \langle \phi^0 \rangle$, small neutrino masses can be induced. This mechanism is known as type II seesaw

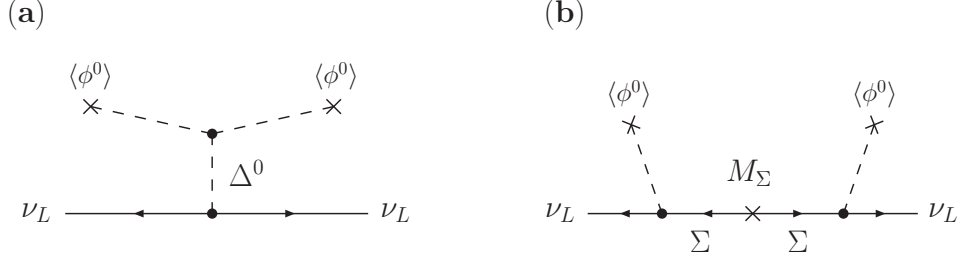


Figure 1.2: **(a)** The process induced by the type II seesaw Lagrangian that will give rise to small neutrino Majorana masses. **(b)** The corresponding process in the type III seesaw case with heavy triplet fermion Σ instead.

Type III seesaw

Another possibility is to replace the RH neutrinos with heavy triplet fermions and allow them to interact with the ordinary lepton doublets via Yukawa couplings [92–94]. In this scenario, the Higgs sector is unmodified, and a set of self-conjugate $SU(2)_L$ triplets of exotic leptons with hypercharge $Y = 0$ are added:

$$\Sigma = \begin{pmatrix} \Sigma^- & \Sigma^0/\sqrt{2} \\ \Sigma^0/\sqrt{2} & \Sigma^+ \end{pmatrix}. \quad (1.4.4)$$

The corresponding Lagrangian for this model is given by

$$-\mathcal{L}_{\text{type-III}} = Y_\Sigma \bar{\ell}_L i\tau_2 \Sigma \phi + M_\Sigma \text{Tr}(\bar{\Sigma}^c \Sigma) + \text{h.c.}, \quad (1.4.5)$$

This gives rise to the diagram shown in Fig. 1.2b, and after integrating out the heavy Σ field, one obtains the desired form for the seesaw neutrino mass

$$m_{\text{eff}}^{\text{III}} \simeq Y_\Sigma \frac{\langle \phi^0 \rangle^2}{M_\Sigma} Y_\Sigma^T. \quad (1.4.6)$$

Hence by setting $M_\Sigma \gg \langle \phi^0 \rangle$, one can explain the smallness of neutrino masses, and as a result, this is often referred to as the type III seesaw mechanism.

1.5 Sphalerons

It is well known that the standard model possesses a gauge symmetry group $SU(3) \times SU(2) \times SU(1)$, and all of its observables are gauge independent. However, it has two

other approximate global symmetries that come from the freedom of rotating the phase of all lepton or quark fields. These symmetries $U(1)_L$ and $U(1)_B$ are associated to the lepton and baryon conserved currents J_μ^B and J_μ^L . If we define the quark doublets and singlets as

$$q = \begin{pmatrix} u & s & t \\ d & c & b \end{pmatrix}_L, \quad (1.5.1)$$

$$u = (u \ s \ t)_R, \quad (1.5.2)$$

$$d = (d \ c \ b)_R, \quad (1.5.3)$$

then the baryonic and leptonic currents are given by

$$J_\mu^B = \frac{1}{3}(\bar{q}_i \gamma_\mu q_i - \bar{u}_i \gamma_\mu u_i - \bar{d}_i \gamma_\mu d_i), \quad (1.5.4)$$

$$J_\mu^L = \bar{l}_i \gamma_\mu l_i - \bar{r}_i \gamma_\mu r_i, \quad (1.5.5)$$

with l_i a left chiral lepton doublet and r_i a right chiral lepton singlet. These correspond to the baryon and lepton number. In fact no laboratory experiment has recorded violation of baryon or lepton number. It was realised later that through the Adler-Bell-Jackiw-triangle-anomaly these symmetries are nevertheless broken, and as a result the baryonic and leptonic currents are anomalous. Their derivatives are then given by

$$\partial_\mu J_B^\mu = \partial_\mu J_L^\mu = \frac{N_g}{32\pi^2}(g^2 \text{Tr} W_{\mu\nu} \tilde{W}^{\mu\nu} - g'^2 \text{Tr} B_{\mu\nu} \tilde{B}^{\mu\nu}), \quad (1.5.6)$$

where N_g is the number of fermion generations, $W_{\mu\nu}$ and $B_{\mu\nu}$ are the field tensors of the $SU(2)$ and $U(1)$ fields respectively, g and g' are their associated coupling constants and trace is taken over the group index. We have also defined the dual of a field tensor by

$$\tilde{W}^{\mu\nu} = \frac{1}{2}\epsilon^{\mu\nu\alpha\beta}W_{\alpha\beta}. \quad (1.5.7)$$

The traces of the field tensors on the RHS of the equation (1.5.6) can be written as a derivative of two quantities,

$$K_\mu = \epsilon^{\mu\nu\alpha\beta} \left(W_{\nu\alpha}^a A_\beta^a - \frac{1}{3}g\epsilon_{abc}A_\nu^a A_\alpha^b A_\beta^c \right), \quad (1.5.8)$$

$$k_\mu = X_{\nu\alpha} A'_\beta. \quad (1.5.9)$$

where the one-index tensors A_μ and A'_μ refer to the vector potentials of the $SU(2)$ and $U(1)$ fields. Then we could define a new current which would have a vanishing derivative,

$$\partial_\mu \left(J_L^\mu - \frac{N_g g^2}{32\pi^2} K^\mu + \frac{N_g g'^2}{32\pi^2} k^\mu \right) = 0. \quad (1.5.10)$$

It would be tempting to define this current as the new baryonic and leptonic number, understanding the addition as baryon and lepton number carried by the gauge fields. This is however not possible, since k_μ and K_μ are not gauge invariant. As we are

interested in the time-evolution of the baryon and lepton numbers, we consider their evolution from an initial time $t = 0$ to some point of time by defining the change in the baryon number

$$\Delta B(t) = N_g [N_{CS}(t) - N_{CS}(0)] , \quad (1.5.11)$$

where we use the Chern-Simons numbers of the $SU(2)$ gauge field

$$N_{CS} = \frac{g^2}{32\pi^2} \int d^3x \epsilon^{\mu\nu\sigma} \left(W_{\mu\nu}^a A_\sigma^a - \frac{g}{3} \epsilon_{abc} A_\mu^a A_\nu^b A_\sigma^c \right) . \quad (1.5.12)$$

Even though the definition of K_μ was not gauge invariant, the change of the divergence of K_μ is gauge invariant. The different values of the Chern-Simons number correspond to different vacuum configurations of the gauge field. The value of the Chern-Simons number in pure gauge configurations, corresponding to vacuum, is an integer, and thus the change in the baryon (and lepton) number corresponding to the change of the vacuum of the gauge field is N_g integer: both the baryon and lepton numbers change in multiples of three. This anomaly induces a 12-fermion operator of the form

$$\prod_{i=1}^3 (q_i q_i q_i l_i) , \quad (1.5.13)$$

coupling to all left-handed fermions. Since the divergences of J_μ^B and J_μ^L are the same, $B - L$ is conserved. In 1976 't Hooft [32] estimated the rate of these baryon number violating processes. He considered the instanton solution between two separate vacua and calculated the action associated with the saddle-point configuration between them. This field configuration is called the sphaleron, from the Greek word meaning ready to fall, as the saddle-point configuration is inherently unstable. The probability of tunneling between the different vacua is approximately

$$\Gamma \sim e^{-S_{instanton}} = e^{-\frac{4\pi}{\alpha}} = \mathcal{O}(10^{-170}) . \quad (1.5.14)$$

This rate is so infinitely small that the sphaleron process is in no contradiction with the practical observation of the lack of violation of B or L . In 1985 Kuzmin, Rubakov and Shaposhnikov [20] pointed out that in thermal bath the transition can happen instead of quantum mechanical tunneling by classical thermal fluctuations over the potential barrier. If the temperature is above the saddle-point energy between the different vacua then the exponential Boltzmann suppression disappears completely. The energy of the saddle-point configuration can be estimated by the sphaleron configurations. Below the electroweak phase transition temperature ($T < T_{EW}$) the transition rate per unit volume was found to be

$$\frac{\Gamma_{sph}}{V} \sim e^{-\frac{M_W}{\alpha T}} , \quad (1.5.15)$$

which is still very much suppressed. In the symmetric phase $T > T_{EW}$, however, the transition rate is no longer suppressed, but rather [95–98]

$$\frac{\Gamma_{sph}}{V} \sim \alpha^5 \ln \alpha^{-1} T^4 . \quad (1.5.16)$$

Sphaleron processes can be in equilibrium when the sphaleron rate Γ_{sph} exceeds the expansion rate of the universe H . Comparison of the estimate for Γ_{sph} to H in radiation dominated universe gives as the temperature interval when sphalerons were in equilibrium as

$$100\text{GeV} < T < 10^{13}\text{GeV} . \quad (1.5.17)$$

Following the terminology of literature, we call the entire $B + L$ -violating process the sphaleron process, even though the sphaleron specifically refers only to the unstable saddle-point configuration.

1.6 Boltzmann equations

The Boltzmann equations are classical equations that describe the evolutions of phase space distribution functions of a given particle by solving the following equation [47, 99]

$$\hat{L}[f_\psi] = \hat{C}[f_\psi] , \quad (1.6.1)$$

where \hat{L} is the Liouville operator and \hat{C} is the collision term. The Liouville operator describes the evolution of the distribution function when there is no interactions, meanwhile the collision term describes the interaction in the system. The non-relativistic form of the Liouville operator is

$$\hat{L}_{NR} = \frac{\partial}{\partial t} + \frac{p_i}{m} \cdot \nabla_x^i + F_i \cdot \nabla_p^i , \quad (1.6.2)$$

where p is the conjugate momentum of the coordinate x , $\nabla_x = \hat{x}_1 \frac{\partial}{\partial x_1} + \hat{x}_2 \frac{\partial}{\partial x_2} + \hat{x}_3 \frac{\partial}{\partial x_3} + \dots + \hat{x}_n \frac{\partial}{\partial x_n}$ and $\nabla_p = \hat{p}_1 \frac{\partial}{\partial p_1} + \hat{p}_2 \frac{\partial}{\partial p_2} + \hat{p}_3 \frac{\partial}{\partial p_3} + \dots + \hat{p}_n \frac{\partial}{\partial p_n}$ in n dimensions. The relativistic version of this operator takes the form

$$\hat{L}_R = p^\alpha \frac{\partial}{\partial x^\alpha} - \Gamma_{\beta\gamma}^\alpha p^\beta p^\gamma \frac{\partial}{\partial p^\alpha} , \quad (1.6.3)$$

here $\Gamma_{\beta\gamma}^\alpha$ are the Christoffel symbols. In a free theory, solving the Boltzmann equations is an easy task, but when interactions are taken into account the operator \hat{C} must be introduced. After defining number density as

$$n_\psi = \frac{g}{(2\pi)^3} \int f_\psi(\mathbf{p}) d^3p , \quad (1.6.4)$$

with g being the total number of internal degrees of freedom, we get that the Boltzmann equation in a Robertson-Walker universe takes the form

$$\begin{aligned} \dot{n}_\psi + 3Hn_\psi &= \int d\Pi_\psi \hat{C}[f_\psi] \\ &= - \int d\Pi_\psi d\Pi_i d\Pi_j \dots d\Pi_a d\Pi_b \dots \end{aligned}$$

$$\times (2\pi^4) \delta^4(p_i + \dots + p_j - p_\psi - p_a - p_b - \dots) |\mathcal{M}|^2, \quad (1.6.5)$$

where the subindices i, \dots, j take into account the initial states and a, \dots, b the final states. The phase space integrals are

$$d\Pi = \frac{g}{(2\pi)^3} \frac{d^3\mathbf{p}}{2E}, \quad (1.6.6)$$

and the squared scattering amplitude $|\mathcal{M}|$

$$\begin{aligned} |\mathcal{M}|^2 = & \quad |\mathcal{M}|_{i+\dots+j \rightarrow \psi+a+\dots+b}^2 f_i \cdots f_j (1 \pm f_\psi)(1 \pm f_a) \cdots (1 \pm f_b) \\ & - |\mathcal{M}|_{\psi+a+\dots+b \rightarrow i+\dots+j}^2 f_\psi f_a \cdots f_b (1 \pm f_i) \cdots (1 \pm f_j), \end{aligned} \quad (1.6.7)$$

which depends on the elements of the S -matrix. The bosonic enhancement or fermionic suppression will give us the right sign for \pm , positive for bosonic enhancement and negative for fermionic suppression (Pauli blocking).

The Boltzmann equations suffer severe limitations when promoted to quantum mechanics. For example, to use these equations one must introduce the S -matrix elements by hand, elements which can be computed from quantum field theory. For equilibrium dynamics, the Boltzmann equations are a good approximation, because all the scattering elements can be computed from the vacuum, but for non-equilibrium processes, these equations lack the properties that come from the plasma, changes that include non-Markovian effects which can lead to big discrepancies. Secondly, in order to use the Boltzmann equations, a number density quantity must be defined, this is not clear in non-equilibrium quantum mechanics, where quantities as number densities are not observables that can be easily defined.

To promote the Boltzmann equations from a classical or semi-classical to a full quantum treatment of the evolution of particle states, one needs to start from a pure quantum formalism that can describe out-of-equilibrium dynamics. In order to do so, the Keldysh formalism using the Kadanoff-Baym equations can be applied, the self-energies of the particles involved will give us the S -matrix elements (via the optical theorem).

1.7 CP asymmetry

The Standard Model contains only two ways to break CP symmetry. The first of these is in the QCD Lagrangian, and has not been found experimentally; but one would expect this to lead to either no CP violation or a CP violation that is many orders of magnitude too large [100]. The second of these, involving the weak force, has been experimentally verified, but can account for only a small portion of CP violation [101]. It is predicted to be sufficient for a net mass of normal matter equivalent to only a single galaxy.

The issue of CP-violating decays of a heavy Majorana neutrino at $T = 0$ was already investigated in [102–105]. Here, the amount of CP violation is given from the interaction between tree-level and one loop Feynman graphs. These interactions involve flavour mixing between the heavy Majorana neutrinos via their Yukawa couplings, and is given by

$$\epsilon_1 = \frac{\Gamma_{Nl} - \Gamma_{N\bar{l}}}{\Gamma_{Nl} + \Gamma_{N\bar{l}}}, \quad (1.7.1)$$

where $\Gamma_{Nl} = \sum_{\alpha,\beta} \Gamma(N \rightarrow l^\alpha H^\beta)$ and $\Gamma_{N\bar{l}} = \sum_{\alpha,\beta} \Gamma(N \rightarrow \bar{l}^\alpha H^\beta)$ are the CP violating processes, with a result given by (for hierarchy masses $M_1 \ll M_2, M_3$)

$$\epsilon_1 \approx \frac{3}{16\pi} \frac{1}{(\lambda\lambda^\dagger)_{11}} \cdot \sum_{i=2,3} \text{Im} \left[(\lambda\lambda^\dagger)_{i1}^2 \right] \frac{M_1}{M_i}, \quad (1.7.2)$$

with λ being the complex Yukawa coupling. As we will see, the effect of temperature is crucial, giving a non-trivial T dependence of the CP violation. The effect of thermal masses was taken into account in [106] using the one-loop finite temperature resummed propagators. We will also see, that this CP-violation parameter will appear naturally when a pure quantum treatment is used, where the CP-asymmetry will come from the two-loop self-energy of the heavy Majorana neutrinos. One can verify via the optical theorem, that interference effects used in [106] are included in the two-loop self energy.

1.8 Semi-classical leptogenesis

Leptogenesis is an elegant theory that involves every aspect explained above (for complete review see [26, 27]). Normally leptogenesis is calculated using the classical Boltzmann equations with quantum processes for the S -matrix elements, and the asymmetry is obtained thanks to the inclusion of three heavy Majorana neutrinos. The Sakharov conditions are well satisfied:

1) The lepton number is broken by the Majorana mass term and then is translated into baryon number via sphalerons processes.

2) The right amount of CP violation is satisfied from the mixing of the Majorana neutrinos in the Yukawa sector.

3) Out-of-equilibrium is obtained because the rate of decays is shorter than the expansion of the universe.

With these three conditions satisfied, one can start by putting everything together. The normal picture is to take a hierarchy in the heavy neutrino masses $M_1 \ll M_2, M_3$, and temperatures in the beginning of order $T > M_1$, in this regime the lightest of the Majorana neutrinos is created in a thermal bath of leptons and Higgs, the Majorana will reach an equilibrium within the bath at temperatures of $T \gtrsim M_1$. Because of the

expansion of the Universe, the temperature will drop, and when $T \sim M_1$ the inverse decay channel of the Majorana neutrino will be blocked, and the neutrinos will decay out-of-equilibrium producing the asymmetry in the leptonic sector. This mechanism is described via a set of two coupled Boltzmann equations, for the number density of the Majorana neutrino, and for the asymmetry in $B - L$

$$\frac{dN_{N_1}}{dz} = -(D + S)(N_{N_1} - N_{N_1}^{eq}), \quad (1.8.1)$$

$$\frac{dN_{B-L}}{dz} = -\epsilon_1 D(N_{N_1} - N_{N_1}^{eq}) - W N_{B-L}, \quad (1.8.2)$$

where $z = M_1/T$. These equations involve decays (D) and scattering (S) processes calculated via Feynman graphs. The CP violating parameter ϵ_1 corresponds to the asymmetry produced by M_1 . In the above equation one can see that there is a race between the decay of the heavy neutrino and the washout term W , that comes from the expansion of the universe. The solution of the above equation considering only decays and inverse decays is given by

$$N_{B-L}(z) = N_{B-L}^i e^{-\int_{z_i}^z dz' W(z')} - \frac{3}{4} \epsilon_1 \kappa(z : \tilde{m}_1, M_1 \tilde{m}_1^2), \quad (1.8.3)$$

with κ a efficiency factor that does not depend on the CP asymmetry. The masses involved are the effective neutrino mass \tilde{m}_1 and the sum of the light neutrino masses \tilde{m}

$$\tilde{m}_1 = \frac{(m_D^\dagger m_D)_{11}}{M_1}, \quad (1.8.4)$$

$$\tilde{m}^2 = m_1^2 + m_2^2 + m_3^2. \quad (1.8.5)$$

The efficiency factor comes from the solution of the first of the Boltzmann equations

$$\kappa(z) = \frac{4}{3} \int_{z_i}^z dz' D(N_{N_1} - N_{N_1}^{eq}) e^{-\int_{z_i}^z dz' W(z')} \quad (1.8.6)$$

$$= -\frac{4}{3} \int_{z_i}^z dz' \frac{D}{D+S} \frac{dN_{N_1}}{dz'} e^{-\int_{z_i}^z dz' W(z')}. \quad (1.8.7)$$

Two regimes can be noticed, first the strong wash-out regime, where the solution will not depend on the initial conditions (N_{B-L}^i) that might be generated by the decay of the two heavy Majorana neutrinos or another mechanism. And the weak wash-out regime, where a great dependence on the initial condition exists.

Our goal is to find quantum version of these equations, a method that will give raise to quantum corrections and to a better understanding of a theory of leptogenesis. The approach will be also satisfied with a comparison between a new set of equations and the Boltzmann equations, in order to really understand the regime of validity of taking quantum effects into consideration.

1.9 Effective model

The scenario which we will consider is referred to in the literature as vanilla leptogenesis, where a hierarchy on the masses of the three Majorana neutrinos after the see-saw mechanism exists (i.e. $M_1 \ll M_2, M_3$). The lepton asymmetry will be created by the interaction of the lightest of the heavy neutrinos with the thermal bath. Because of the hierarchy of the masses, we can integrate out M_2 and M_3 obtaining an effective model for M_1 with a Lagrangian given by (cf. [73])

$$\mathcal{L} = \bar{l}_{Li} \tilde{\phi} \lambda_{i1}^* N + N^T \lambda_{i1} C l_{Li} \phi - \frac{1}{2} M N^T C N + \frac{1}{2} \eta_{ij} l_{Li}^T \phi C l_{Lj} \phi + \frac{1}{2} \eta_{ij}^* \bar{l}_{Li} \tilde{\phi} C \bar{l}_{Lj}^T \tilde{\phi} . \quad (1.9.1)$$

here C is the charge conjugation matrix, $\tilde{\phi} = i\sigma_2 \phi$, and the coupling

$$\eta_{ij} = \sum_{k>1} \lambda_{ik} \frac{1}{M_k} \lambda_{kj}^T . \quad (1.9.2)$$

The effective Lagrangian, which is valid for momenta up to $p < M_2, M_3$, has the advantage that flavour structure is trivial and given by the effective coupling η . We shall consider the case of small Yukawa couplings, $\lambda_{i1} \ll 1$, such that the decay width of N is much smaller than its mass.

From this effective Lagrangian we can obtain the following Feynman rules¹:

- Majorana

$$\bullet \xrightarrow{N} \bullet : iG_{\alpha\beta}(x_1, x_2)$$

$x_{2,\beta} \qquad \qquad \qquad x_{1,\alpha}$

- Lepton

$$\bullet \xrightarrow{l} \bullet : i\delta_{ij} \delta_{ab} S_{\alpha\beta}(x_1, x_2)$$

$x_{2,\beta,b,j} \qquad \qquad \qquad x_{1,\alpha,a,i}$

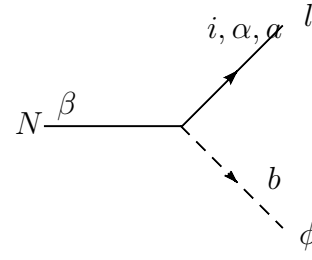
- Scalar

$$\bullet \xrightarrow{\phi} \bullet : i\delta_{ab} \Delta(x_1, x_2)$$

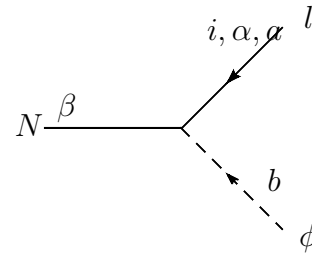
$x_{2,b} \qquad \qquad \qquad x_{1,a}$

¹The exact shape of the propagators will be given in Appendix D

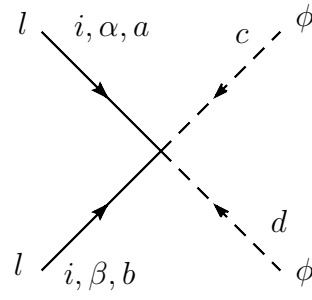
•Vertices



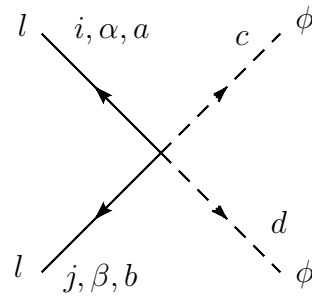
$$: i\lambda_{i1}^* \epsilon_{ab} (P_R)_{\alpha\beta}$$



$$b: i\lambda_{i1} (C P_L)_{\beta\alpha} \epsilon_{ab}$$



$$: i\eta_{ij} (\epsilon_{ac} \epsilon_{bd} + \epsilon_{ad} \epsilon_{bc}) (C P_L)_{\alpha\beta}$$



$$: i\eta_{ij}^* (\epsilon_{ac} \epsilon_{bd} + \epsilon_{ad} \epsilon_{bc}) (P_R C)_{\alpha\beta}$$

For the rest of this thesis we rename $M_1 \rightarrow M$ for simplicity, unless otherwise stated.

Chapter 2

Non-equilibrium thermal field theory

A full quantum treatment for the dynamics for different types of particles is presented. First we will consider a system composed only by scalar particles. This first discussion will give us a qualitative idea of the important issues of the general problem of thermalization of a weakly coupled particle in a thermal bath. These concepts will be then applied to more complicated model composed by fermions.

By definition, the Green's functions are the average of the time ordered product of Heisenberg field operators over some state, i.e.,

$$G(t_1, t_2) = -i \left\langle T(\hat{A}(t_1)\hat{B}(t_2)) \right\rangle . \quad (2.0.1)$$

By going to the interaction picture, we can rewrite the above equation as

$$G(t_1, t_2) = -i \left\langle S^\dagger T(\hat{A}(t_1)\hat{B}(t_2)S) \right\rangle , \quad (2.0.2)$$

where the S -matrix is defined by

$$S \equiv U(\infty, -\infty) = T \exp \left(-i \int_{-\infty}^{\infty} \mathcal{H}_{int}^I(t) dt \right) , \quad (2.0.3)$$

with the interacting Hamiltonian in the interaction picture. If the renormalized ground state is considered we regain the normal many-body theory at zero temperature. This case change when the system is in thermo-equilibrium at different from zero temperature. Here the quantum state is not pure and it is now described by the density matrix operator

$$\hat{\rho} = \exp[\beta(\mathcal{F} - \hat{\mathcal{H}})] , \quad (2.0.4)$$

where β is the inverse of the temperature and \mathcal{F} is the free energy. The thermal average will then be given by

$$\langle O \rangle = \text{Tr}(\hat{\rho}O) . \quad (2.0.5)$$

If we relate β with an imaginary time it , the density matrix will behave like an evolution operator $\exp(-i\hat{\mathcal{H}}t)$. This is the case for the Matsubara formalism [107]. However, the

term S^\dagger is not easy to handle when a non-equilibrium state is considered. To solve this problem, Schwinger proposed in [75] a time contour C that goes from $-\infty$ to ∞ and back (see figure 2.1). So that we can generalize the S -matrix as

$$S_C = T_C \exp \left(-i \int_C \mathcal{H}_{int}^I(t) dt \right) , \quad (2.0.6)$$

where T_C is the time-ordering operator along the path C . In the positive path T_C is identical to the standard T operator, but in the negative branch represents an anti-time-ordering operator. Also, times in the negative branch are always later as times in the positive one. With this countour, a new set of propagators can be defined

$$G_C(t_1, t_2) = -i \left\langle T_C(\hat{A}(t_1)\hat{B}(t_2)) \right\rangle . \quad (2.0.7)$$

Notice that the physical observables will always lay on the positive branch of the contour, but the intermediate steps can be taken to be anywhere. Up to this point the propagator can be chosen to be bosonic or fermionic, we will see how it behaves for different type of particles

2.1 Keldysh-Schwinger formalism for scalars

2.1.1 Kadanoff-Baym equations for scalars

Let us define the scalar propagator Δ_C of a field $\Phi(x)$ in a x^0 -contour (figure 2.1) as

$$\Delta_C(x_1, x_2) = \theta_C(x_1^0, x_2^0) \Delta^>(x_1, x_2) + \theta_C(x_2^0, x_1^0) \Delta^<(x_1, x_2) . \quad (2.1.1)$$

The θ -functions enforce path ordering along the contour C , and $\Delta^>$ and $\Delta^<$ are the correlation functions

$$\Delta^>(x_1, x_2) = \langle \Phi(x_1)\Phi(x_2) \rangle = \text{Tr}(\hat{\rho}\Phi(x_1)\Phi(x_2)) , \quad (2.1.2)$$

$$\Delta^<(x_1, x_2) = \langle \Phi(x_2)\Phi(x_1) \rangle = \text{Tr}(\hat{\rho}\Phi(x_2)\Phi(x_1)) , \quad (2.1.3)$$

where $\hat{\rho}$ is the density matrix of the system at some initial time t_i .

The field Φ is coupled to a thermal bath described by a self-energy Π . The Green's function Δ_C then satisfies the Schwinger-Dyson equation ¹

$$(\square_1 + m^2)\Delta_C(x_1, x_2) + i \int_C d^4x' \Pi_C(x_1, x')\Delta_C(x', x_2) = -i\delta_C(x_1 - x_2) , \quad (2.1.4)$$

where $\square_1 = (\partial^2/\partial x_1^2)$. Like the Green's function, also the self-energy can be decomposed defined in the contour

$$\Pi_C(x_1, x_2) = \theta_C(x_1^0, x_2^0)\Pi^>(x_1, x_2) + \theta_C(x_2^0, x_1^0)\Pi^<(x_1, x_2) . \quad (2.1.5)$$

¹For a consistent definition of the propagators see appendix A.

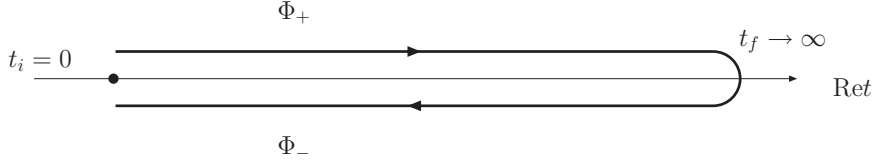


Figure 2.1: Path in the complex time plane for nonequilibrium Green's functions.

Notice that the self energy Π_C is the sum of all 1PI self energies. This type of definition differs from those in [79], but agrees with [80]. However it will be very convenient for the rest of the calculations.

In the Schwinger-Dyson equation the time coordinates of Δ_C and Π_C can be on the upper or lower branch of the contour C , which we denote by the subscripts '+' and '-', respectively. Rewriting

$$\Delta_{-+}(x_1, x_2) = \Delta^>(x_1, x_2), \quad \Delta_{+-}(x_1, x_2) = \Delta^<(x_1, x_2), \quad (2.1.6)$$

$$\Pi_{-+}(x_1, x_2) = \Pi^>(x_1, x_2), \quad \Pi_{+-}(x_1, x_2) = \Pi^<(x_1, x_2), \quad (2.1.7)$$

whereas Δ_{++} , Π_{++} and Δ_{--} , Π_{--} are causal and anti-causal Green functions, respectively. From the Schwinger-Dyson equation (2.1.4) one obtains for the correlation functions $\Delta^<$ and $\Delta^>$,

$$(\square_1 + m^2)\Delta^<(x_1, x_2) = i \int d^4x' (-\Pi_{++}(x_1, x')\Delta^<(x', x_2) + \Pi^<(x_1, x')\Delta_{--}(x', x_2)), \quad (2.1.8)$$

$$(\square_1 + m^2)\Delta^>(x_1, x_2) = i \int d^4x' (-\Pi^>(x_1, x')\Delta_{++}(x', x_2) + \Pi_{--}(x_1, x')\Delta^>(x', x_2)), \quad (2.1.9)$$

where the relative sign in the integrands is due to the anti-causal time ordering on the lower branch of C .

It is convenient to also introduce retarded and advanced Green functions,

$$\Delta^R(x_1, x_2) = \theta(t_1 - t_2)(\Delta^>(x_1, x_2) - \Delta^<(x_1, x_2)) \quad (2.1.10)$$

$$\begin{aligned} &= \theta(t_1 - t_2)\langle[\phi(x_1), \phi(x_2)]\rangle \\ &= \Delta_{++}(x_1, x_2) - \Delta_{+-}(x_1, x_2) \\ &= \Delta_{-+}(x_1, x_2) - \Delta_{--}(x_1, x_2), \end{aligned}$$

$$\Delta^A(x_1, x_2) = -\theta(t_2 - t_1)(\Delta^>(x_1, x_2) - \Delta^<(x_1, x_2)) \quad (2.1.11)$$

$$\begin{aligned} &= -\theta(t_2 - t_1)\langle[\phi(x_1), \phi(x_2)]\rangle \\ &= \Delta_{++}(x_1, x_2) - \Delta_{-+}(x_1, x_2) \\ &= \Delta_{+-}(x_1, x_2) - \Delta_{--}(x_1, x_2), \end{aligned}$$

$$\Pi^R(x_1, x_2) = \theta(t_1 - t_2)(\Pi^>(x_1, x_2) - \Pi^<(x_1, x_2))$$

$$= \Pi_{++}(x_1, x_2) - \Pi_{+-}(x_1, x_2)$$

$$= \Pi_{-+}(x_1, x_2) - \Pi_{--}(x_1, x_2) , \quad (2.1.12)$$

$$\begin{aligned} \Pi^A(x_1, x_2) &= -\theta(t_2 - t_1)(\Pi^>(x_1, x_2) - \Pi^<(x_1, x_2)) \\ &= \Pi_{++}(x_1, x_2) - \Pi_{-+}(x_1, x_2) \\ &= \Pi_{+-}(x_1, x_2) - \Pi_{--}(x_1, x_2) . \end{aligned} \quad (2.1.13)$$

From Eqs. (2.1.8) and (2.1.9) one obtains the Kadanoff-Baym equations for the correlation functions $\Delta^>$ and $\Delta^<$,

$$(\square_1 + m^2)\Delta^>(x_1, x_2) = -i \int d^4x' (\Pi^>(x_1, x')\Delta^A(x', x_2) + \Pi^R(x_1, x')\Delta^>(x', x_2)) , \quad (2.1.14)$$

$$(\square_1 + m^2)\Delta^<(x_1, x_2) = -i \int d^4x' (\Pi^<(x_1, x')\Delta^A(x', x_2) + \Pi^R(x_1, x')\Delta^<(x', x_2)) . \quad (2.1.15)$$

We now define the real symmetric and antisymmetric correlation functions

$$\Delta^+(x_1, x_2) = \frac{1}{2}\langle\{\Phi(x_1), \Phi(x_2)\}\rangle , \quad (2.1.16)$$

$$\Delta^-(x_1, x_2) = i\langle[\Phi(x_1), \Phi(x_2)]\rangle , \quad (2.1.17)$$

and self-energies

$$\Pi^+(x_1, x_2) = \frac{1}{2}(\Pi^>(x_1, x_2) + \Pi^<(x_1, x_2)) , \quad (2.1.18)$$

$$\Pi^-(x_1, x_2) = i(\Pi^>(x_1, x_2) - \Pi^<(x_1, x_2)) , \quad (2.1.19)$$

which also determine the retarded and advanced self-energies,

$$\Pi^R(x_1, x_2) = \theta(t_1 - t_2)\Pi^-(x_1, x_2) , \quad \Pi^A(x_1, x_2) = -\theta(t_2 - t_1)\Pi^-(x_1, x_2) . \quad (2.1.20)$$

Adding and subtracting the Kadanoff-Baym equations (2.1.14) and (2.1.15), one obtains from Eqs. (2.1.10)-(2.1.13) and (2.1.16)-(2.1.19) an homogeneous equation for Δ^- and an inhomogeneous equation for Δ^+ ,

$$(\square_1 + m^2)\Delta^-(x_1, x_2) = - \int d^3\mathbf{x}' \int_{t_2}^{t_1} dt' \Pi^-(x_1, x')\Delta^-(x', x_2) , \quad (2.1.21)$$

$$\begin{aligned} (\square_1 + m^2)\Delta^+(x_1, x_2) &= - \int d^3\mathbf{x}' \int_{t_i}^{t_1} dt' \Pi^-(x_1, x')\Delta^+(x', x_2) \\ &\quad + \int d^3\mathbf{x}' \int_{t_i}^{t_2} dt' \Pi^+(x_1, x')\Delta^-(x', x_2) . \end{aligned} \quad (2.1.22)$$

We shall refer to these as equations as the first and second Kadanoff-Baym equation. Δ^- and Δ^+ are known as spectral function and statistical propagator (cf. [80]). Together they determine the path ordered Green's function,

$$\Delta_C(x_1, x_2) = \Delta^+(x_1, x_2) - \frac{i}{2}\text{sign}_C(x_1^0 - x_2^0)\Delta^-(x_1, x_2) . \quad (2.1.23)$$

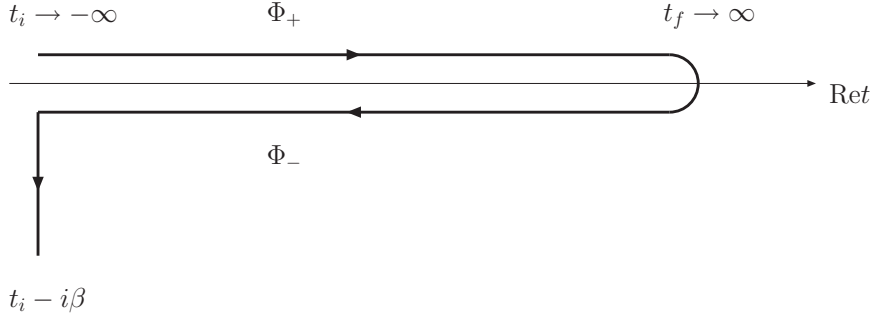


Figure 2.2: Path in the complex time plane for thermal Green's functions.

Δ^- carries information about the spectrum of the system and Δ^+ is related to occupation numbers of different modes.

Using micro-causality and the canonical quantization condition for a real scalar field,

$$[\Phi(x_1), \Phi(x_2)]|_{t_1=t_2} = [\dot{\Phi}(x_1), \dot{\Phi}(x_2)]|_{t_1=t_2} = 0, \quad (2.1.24)$$

$$[\Phi(x_1), \dot{\Phi}(x_2)]|_{t_1=t_2} = i\delta(\mathbf{x}_1 - \mathbf{x}_2), \quad (2.1.25)$$

one obtains from the definitions (2.1.16) and (2.1.17)

$$\Delta^-(x_1, x_2)|_{t_1=t_2} = 0, \quad (2.1.26)$$

$$\partial_{t_1}\Delta^-(x_1, x_2)|_{t_1=t_2} = -\partial_{t_2}\Delta^-(x_1, x_2)|_{t_1=t_2} = \delta(\mathbf{x}_1 - \mathbf{x}_2), \quad (2.1.27)$$

$$\partial_{t_1}\partial_{t_2}\Delta^-(x_1, x_2)|_{t_1=t_2} = 0. \quad (2.1.28)$$

In the following we shall restrict ourselves to systems with spatial translational invariance. In this case all two-point functions only depend on the difference of spatial coordinates, $\mathbf{x}_1 - \mathbf{x}_2$, and it is convenient to perform a Fourier transformation. The Green's functions $\Delta_{\mathbf{q}}^{\pm}(t_1, t_2)$ satisfy the two Kadanoff-Baym equations

$$(\partial_{t_1}^2 + \omega_{\mathbf{q}}^2)\Delta_{\mathbf{q}}^-(t_1, t_2) + \int_{t_2}^{t_1} dt' \Pi_{\mathbf{q}}^-(t_1, t')\Delta_{\mathbf{q}}^-(t', t_2) = 0, \quad (2.1.29)$$

$$(\partial_{t_1}^2 + \omega_{\mathbf{q}}^2)\Delta_{\mathbf{q}}^+(t_1, t_2) + \int_{t_i}^{t_1} dt' \Pi_{\mathbf{q}}^-(t_1, t')\Delta_{\mathbf{q}}^+(t', t_2) = \int_{t_i}^{t_2} dt' \Pi_{\mathbf{q}}^+(t_1, t')\Delta_{\mathbf{q}}^-(t', t_2), \quad (2.1.30)$$

where $\omega_{\mathbf{q}}^2 = \mathbf{q}^2 + m^2$. The initial conditions (2.1.26)-(2.1.28) for the spectral function become

$$\Delta_{\mathbf{q}}^-(t_1, t_2)|_{t_1=t_2} = 0, \quad (2.1.31)$$

$$\partial_{t_1}\Delta_{\mathbf{q}}^-(t_1, t_2)|_{t_1=t_2} = -\partial_{t_2}\Delta_{\mathbf{q}}^-(t_1, t_2)|_{t_1=t_2} = 1, \quad (2.1.32)$$

$$\partial_{t_1}\partial_{t_2}\Delta_{\mathbf{q}}^-(t_1, t_2)|_{t_1=t_2} = 0. \quad (2.1.33)$$

For Green's functions in thermal equilibrium the density matrix in Eqs. (2.1.2), (2.1.3) is $\rho_{\text{eq}} = \exp(-\beta H)$, where H is the Hamiltonian of the system, and $\beta = T^{-1}$ is the inverse temperature. Time coordinates of Green functions now lie on the contour

shown in Figure 2.2, and one has invariance under time translations so that two-point functions only depend on the time difference $t_1 - t_2$. After a Fourier transformation, one obtains the KMS relations [79] for Green's functions and self-energies,

$$\Delta_{\mathbf{q}}^+(\omega) = -\frac{i}{2} \coth\left(\frac{\beta\omega}{2}\right) \Delta_{\mathbf{q}}^-(\omega) , \quad (2.1.34)$$

$$\Pi_{\mathbf{q}}^+(\omega) = -\frac{i}{2} \coth\left(\frac{\beta\omega}{2}\right) \Pi_{\mathbf{q}}^-(\omega) . \quad (2.1.35)$$

The Kadanoff-Baym equations describe the dynamics of a arbitrary non-equilibrium system. Depending on the self-energy and the initial conditions, the solutions will generally be complicated. An enormous simplification is achieved for a large medium such that the back-reaction of the field Φ can be neglected. Furthermore, we assume that the medium is in thermal equilibrium and, therefore, the self energy of Φ is time-translation invariant,

$$\Pi_{\mathbf{q}}(t_1, t_2) = \Pi_{\mathbf{q}}(t_1 - t_2) . \quad (2.1.36)$$

In this case also the spectral function is time-translation invariant, as shown in Appendix B.3. With these simplifications, the Kadanoff-Baym equations become

$$(\partial_{t_1}^2 + \omega_{\mathbf{q}}^2) \Delta_{\mathbf{q}}^-(t_1 - t_2) = - \int_{t_2}^{t_1} dt' \Pi_{\mathbf{q}}^-(t_1 - t') \Delta_{\mathbf{q}}^-(t' - t_2) , \quad (2.1.37)$$

$$\begin{aligned} (\partial_{t_1}^2 + \omega_{\mathbf{q}}^2) \Delta_{\mathbf{q}}^+(t_1, t_2) &= \int_{t_i}^{t_2} dt' \Pi_{\mathbf{q}}^+(t_1 - t') \Delta_{\mathbf{q}}^-(t' - t_2) \\ &\quad - \int_{t_i}^{t_1} dt' \Pi_{\mathbf{q}}^-(t_1 - t') \Delta_{\mathbf{q}}^+(t', t_2) . \end{aligned} \quad (2.1.38)$$

2.1.2 Solutions for the KB equations

Solution for the spectral function

As proven in Appendix B.3, the spectral function is time translation invariant, i.e., it only depends on the time difference $y = t_1 - t_2$. Hence, the first Kadanoff-Baym equation (2.2.18) takes the form

$$(\partial_y^2 + \omega_{\mathbf{q}}^2) \Delta_{\mathbf{q}}^-(y) + \int_0^y dy' \Pi_{\mathbf{q}}^-(y - y') \Delta_{\mathbf{q}}^-(y') = 0 . \quad (2.1.39)$$

This equation can be solved by performing a Laplace transformation,

$$\tilde{\Delta}_{\mathbf{q}}^-(s) = \int_0^\infty dy e^{-sy} \Delta_{\mathbf{q}}^-(y) , \quad (2.1.40)$$

for which one obtains after a straightforward calculation

$$\tilde{\Delta}_{\mathbf{q}}^-(s) = \frac{\partial_y \Delta_{\mathbf{q}}^-(0) + s \Delta_{\mathbf{q}}^-(0)}{s^2 + \omega_{\mathbf{q}}^2 + \tilde{\Pi}_{\mathbf{q}}^R(s)} , \quad (2.1.41)$$

with

$$\tilde{\Pi}_{\mathbf{q}}^R(s) = \int_0^\infty e^{-sy} \Pi_{\mathbf{q}}^R(y) dy = \int_0^\infty e^{-sy} \Pi_{\mathbf{q}}^-(y) dy = \tilde{\Pi}_{\mathbf{q}}^-(s) . \quad (2.1.42)$$

According to (2.1.41), the general solution of (2.1.39) depends on two parameters, the values of $\Delta_{\mathbf{q}}^-$ and $\partial_y \Delta_{\mathbf{q}}^-$ at $y = 0$. Using the inverse Laplace transform one finds

$$\Delta_{\mathbf{q}}^-(y) = (\partial_y \Delta_{\mathbf{q}}^-(0) + \Delta_{\mathbf{q}}^-(0) \partial_y) \int_{\mathcal{C}_B} \frac{ds}{2\pi i} \frac{e^{sy}}{s^2 + \omega_{\mathbf{q}}^2 + \tilde{\Pi}_{\mathbf{q}}^-(s)} . \quad (2.1.43)$$

Here \mathcal{C}_B is the Bromwich contour (see Figure 3): The part parallel to the imaginary axis is chosen such that all singularities of the integrand are to its left; the second part is the semicircle at infinity which closes the contour at $\text{Re}(s) < 0$. Since the integrand of (2.1.43) has singularities only on the imaginary axis, the second part can be deformed to run parallel to the imaginary axis as well: $\mathcal{C}_B \rightarrow \int_{-i\infty+\epsilon}^{i\infty+\epsilon} + \int_{i\infty-\epsilon}^{-i\infty-\epsilon}$.

The spectral function $\Delta_{\mathbf{q}}^-(y)$ satisfies the boundary conditions (2.1.31) and (2.1.32), which implies

$$\Delta_{\mathbf{q}}^-(y) = \int_{\mathcal{C}_B} \frac{ds}{2\pi i} \frac{e^{sy}}{s^2 + \omega_{\mathbf{q}}^2 + \tilde{\Pi}_{\mathbf{q}}^-(s)} . \quad (2.1.44)$$

This result can be further simplified by making use of the analytic properties of the self-energy $\tilde{\Pi}^-(s)$. On the real axis $\tilde{\Pi}^-(s)$ is real, while on the parts of the contour which are parallel to the imaginary axis one has

$$\tilde{\Pi}^-(i\omega \pm \epsilon) = \text{Re} \Pi_{\mathbf{q}}^R(\omega) \pm i \text{Im} \Pi_{\mathbf{q}}^R(\omega) , \quad (2.1.45)$$

with

$$\text{Im} \Pi_{\mathbf{q}}^R(\omega) = \frac{1}{2i} (\Pi_{\mathbf{q}}^R(\omega + i\epsilon) - \Pi_{\mathbf{q}}^R(\omega - i\epsilon)) . \quad (2.1.46)$$

Hence, the expression (2.1.44) takes the form

$$\Delta_{\mathbf{q}}^-(y) = i \int_{-\infty}^{\infty} \frac{d\omega}{2\pi} e^{-i\omega y} \rho_{\mathbf{q}}(\omega) , \quad (2.1.47)$$

where the spectral function $\rho_{\mathbf{q}}(\omega)$ is given in terms of real and imaginary part of the self-energy $\Pi_{\mathbf{q}}^R(\omega)$,

$$\rho_{\mathbf{q}}(\omega) = \frac{-2\text{Im} \Pi_{\mathbf{q}}^R(\omega) + 2\omega\epsilon}{[\omega^2 - \omega_{\mathbf{q}}^2 - \text{Re} \Pi_{\mathbf{q}}^R(\omega)]^2 + [\text{Im} \Pi_{\mathbf{q}}^R(\omega) + \omega\epsilon]^2} = i \tilde{\Delta}_{\mathbf{q}}^-(i\omega) . \quad (2.1.48)$$

Note that $\text{Im} \Pi_{\mathbf{q}}^R(\omega)$ and $\text{Re} \Pi_{\mathbf{q}}^R(\omega)$ are odd and even functions, respectively, which implies that $\Delta_{\mathbf{q}}^-(y)$ is real. Further properties of this solution are discussed in Appendix A. Let us recall that the expression (2.1.48) is obtained after neglecting the backreaction

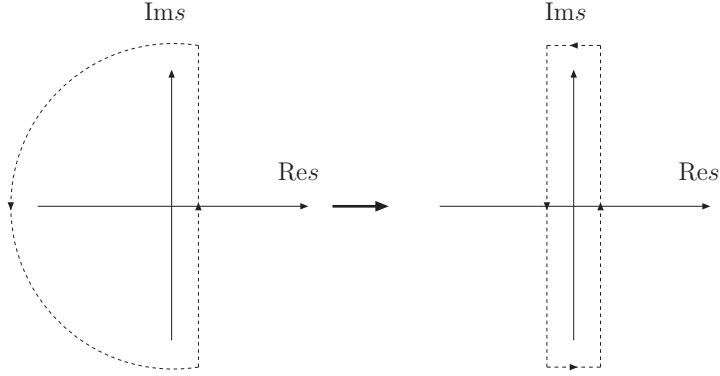


Figure 2.3: Bromwich contour

of the field Φ on the thermal bath. This is the reason why the self-energy and the spectral function are time translation invariant.

The self-energy $\Pi_{\mathbf{q}}^R(\omega)$, and consequently the spectral function $\rho_{\mathbf{q}}(\omega)$, are divergent and have to be renormalized. This can be done by the usual mass and wave function renormalization at zero temperature. In (2.1.48) $\omega_{\mathbf{q}}^2$ is replaced by $\omega_{\mathbf{q}(0)}^2 = m_0^2 + \mathbf{q}^2$, where m_0 is the bare mass of the field Φ . The difference between bare and renormalized mass squared is determined by requiring that at zero temperature the spectral function has a pole at $\omega_{\mathbf{q}}^2 = m^2 + \mathbf{q}^2$,

$$\omega_{\mathbf{q}}^2 - \omega_{\mathbf{q}(0)}^2 - \text{Re}\Pi_{\mathbf{q}}^R(\omega_{\mathbf{q}})|_{T=0} = 0. \quad (2.1.49)$$

Expanding the self-energy around around $\omega_{\mathbf{q}}$, a further divergence can be absorbed in a wave function renormalization constant,

$$\text{Re}\Pi_{\mathbf{q}}^R(\omega) = \text{Re}\Pi_{\mathbf{q}}^R(\omega_{\mathbf{q}})|_{T=0} + (1 - Z^{-1}) (\omega^2 - \omega_{\mathbf{q}}^2) + \text{Re}\hat{\Pi}_{\mathbf{q}}^R(\omega), \quad (2.1.50)$$

where $\text{Re}\hat{\Pi}_{\mathbf{q}}^R(\omega)$ is the finite part and

$$Z^{-1} = 1 - \frac{1}{2\omega_{\mathbf{q}}} \left. \frac{\partial \text{Re}\Pi_{\mathbf{q}}^R(\omega)}{\partial \omega} \right|_{\omega=\omega_{\mathbf{q}}, T=0}. \quad (2.1.51)$$

The spectral function (2.1.48) now takes the form

$$\rho_{\mathbf{q}}(\omega) = Z \frac{-2Z \text{Im}\Pi_{\mathbf{q}}^R(\omega) + 2\omega\epsilon}{\left(\omega^2 - \omega_{\mathbf{q}}^2 - Z \text{Re}\hat{\Pi}_{\mathbf{q}}^R(\omega)\right)^2 + (Z \text{Im}\Pi_{\mathbf{q}}^R(\omega) + \omega\epsilon)^2}. \quad (2.1.52)$$

Introducing the renormalized field operator $\Phi_r = \sqrt{Z}\Phi$, one obtains the renormalized spectral function $\rho_{\mathbf{q}}^r(\omega) = Z\rho_{\mathbf{q}}(\omega)$ in terms of the renormalized self-energy $\Pi_{\mathbf{q}}^{R,r}(\omega) = Z\hat{\Pi}_{\mathbf{q}}^R(\omega)$,

$$\rho_{\mathbf{q}}^r(\omega) = \frac{-2\text{Im}\Pi_{\mathbf{q}}^{R,r}(\omega) + 2\omega\epsilon}{\left(\omega^2 - \omega_{\mathbf{q}}^2 - \text{Re}\Pi_{\mathbf{q}}^{R,r}(\omega)\right)^2 + \left(\text{Im}\Pi_{\mathbf{q}}^{R,r}(\omega) + \omega\epsilon\right)^2}. \quad (2.1.53)$$

The divergencies of spectral function and statistical propagator can be removed in the same way by mass and wave function renormalization at zero temperature. In the following we shall drop the superscript ‘ r ’ to keep the notation simple.

The spectral function describes a quasi-particle resonance at finite temperature with energy $\Omega_{\mathbf{q}}$,

$$\Omega_{\mathbf{q}}^2 - \omega_{\mathbf{q}}^2 - \text{Re}\Pi_{\mathbf{q}}^R(\Omega_{\mathbf{q}}) = 0, \quad \text{quad}\Omega_{\mathbf{q}}^2|_{T=0} = \omega_{\mathbf{q}}^2, \quad (2.1.54)$$

and decay width

$$\Gamma_{\mathbf{q}} \simeq -\frac{1}{\Omega_{\mathbf{q}}} \text{Im}\Pi_{\mathbf{q}}^R(\Omega_{\mathbf{q}}). \quad (2.1.55)$$

For simplicity, we have neglected the effect of $\text{Im}\Pi_{\mathbf{q}}^R$ on the quasi-particle energy.

In a free theory $\text{Im}\Pi_{\mathbf{q}}^R(\omega) = 0$, and (2.1.53) is a representation of the δ -function. The spectral function (2.1.47) then oscillates without damping, i.e., there are no dissipative effects. Dissipation arises either from Φ decays and inverse decays or, similar to Landau damping, from scattering processes with particles in the plasma. Which of these mechanisms dominates the dissipative effects and therefore the equilibration process depends on the position of the quasi-particle pole relative to the masses of particles in the thermal bath. A specific example will be discussed in Section 2.1.4. For small width the spectral function is well approximated by the Breit-Wigner function. The relevant formulae are collected in Appendix D.

Solution for the statistical propagator

We are now ready to solve the second Kadanoff-Baym equation (2.2.24) for the statistical propagator, which for initial time $t_i = 0$ is given by

$$(\partial_{t_1}^2 + \omega_{\mathbf{q}}^2)\Delta_{\mathbf{q}}^+(t_1, t_2) + \int_0^{t_1} dt' \Pi_{\mathbf{q}}^-(t_1 - t')\Delta_{\mathbf{q}}^+(t', t_2) = \zeta(t_1, t_2), \quad (2.1.56)$$

with

$$\zeta(t_1, t_2) = \int_0^{t_2} dt' \Pi_{\mathbf{q}}^+(t_1 - t')\Delta_{\mathbf{q}}^-(t' - t_2). \quad (2.1.57)$$

One easily verifies that the solution can be expressed as

$$\Delta_{\mathbf{q}}^+(t_1, t_2) = \hat{\Delta}_{\mathbf{q}}^+(t_1, t_2) + \int_0^{t_1} dt' \Delta_{\mathbf{q}}^-(t_1 - t')\zeta(t', t_2), \quad (2.1.58)$$

where $\hat{\Delta}_{\mathbf{q}}^+(t_1, t_2)$ satisfies the homogeneous equation

$$(\partial_{t_1}^2 + \omega_{\mathbf{q}}^2)\hat{\Delta}_{\mathbf{q}}^+(t_1, t_2) + \int_0^{t_1} dt' \Pi_{\mathbf{q}}^-(t_1 - t')\hat{\Delta}_{\mathbf{q}}^+(t', t_2) = 0. \quad (2.1.59)$$

The homogeneous equation is identical to (2.1.39), with t_2 playing the role of a parameter. We can therefore read off the general solution from (2.1.43),

$$\hat{\Delta}_{\mathbf{q}}^+(t_1, t_2) = A_{\mathbf{q}}(t_2)\dot{\Delta}_{\mathbf{q}}^-(t_1) + B_{\mathbf{q}}(t_2)\Delta_{\mathbf{q}}^-(t_1) . \quad (2.1.60)$$

Using the symmetry $\hat{\Delta}_{\mathbf{q}}^+(t_1, t_2) = \hat{\Delta}_{\mathbf{q}}^+(t_2, t_1)$, one obtains

$$A_{\mathbf{q}}(t_2)\dot{\Delta}_{\mathbf{q}}^-(t_1) + B_{\mathbf{q}}(t_2)\Delta_{\mathbf{q}}^-(t_1) = A_{\mathbf{q}}(t_1)\dot{\Delta}_{\mathbf{q}}^-(t_2) + B_{\mathbf{q}}(t_1)\Delta_{\mathbf{q}}^-(t_2) . \quad (2.1.61)$$

Together with the boundary conditions (2.1.31)-(2.1.33), $\Delta_{\mathbf{q}}^-(0) = \ddot{\Delta}_{\mathbf{q}}^-(0) = 0$ and $\dot{\Delta}_{\mathbf{q}}^-(0) = 1$, this implies

$$A_{\mathbf{q}}(t) = A_{\mathbf{q}}(0)\dot{\Delta}_{\mathbf{q}}^-(t) + B_{\mathbf{q}}(0)\Delta_{\mathbf{q}}^-(t) , \quad B_{\mathbf{q}}(t) = \dot{A}_{\mathbf{q}}(0)\dot{\Delta}_{\mathbf{q}}^-(t) + \dot{B}_{\mathbf{q}}(0)\Delta_{\mathbf{q}}^-(t) . \quad (2.1.62)$$

Inserting $A_{\mathbf{q}}(t)$ and $B_{\mathbf{q}}(t)$ in (2.1.61) and using the symmetry of $\hat{\Delta}_{\mathbf{q}}^+(t_1, t_2)$, one finds $B_{\mathbf{q}}(0) = \dot{A}_{\mathbf{q}}(0)$. The initial state of the system is therefore characterized by three constants, which can be chosen as

$$\Delta_{\mathbf{q},\text{in}}^+ = \Delta_{\mathbf{q}}^+(t_1, t_2)|_{t_1=t_2=0} = A_{\mathbf{q}}(0) , \quad (2.1.63)$$

$$\dot{\Delta}_{\mathbf{q},\text{in}}^+ = \partial_{t_1}\Delta_{\mathbf{q}}^+(t_1, t_2)|_{t_1=t_2=0} = \partial_{t_2}\Delta_{\mathbf{q}}^+(t_1, t_2)|_{t_1=t_2=0} = B_{\mathbf{q}}(0) = \dot{A}_{\mathbf{q}}(0) , \quad (2.1.64)$$

$$\ddot{\Delta}_{\mathbf{q},\text{in}}^+ = \partial_{t_1}\partial_{t_2}\Delta_{\mathbf{q}}^+(t_1, t_2)|_{t_1=t_2=0} = \dot{B}_{\mathbf{q}}(0) . \quad (2.1.65)$$

From Eqs. (2.1.58), (2.1.60), (2.1.62) and the initial conditions (2.1.98)-(2.1.100) we now obtain the full solution for the statistical propagator,

$$\begin{aligned} \Delta_{\mathbf{q}}^+(t_1, t_2) &= \Delta_{\mathbf{q},\text{in}}^+\dot{\Delta}_{\mathbf{q}}^-(t_1)\dot{\Delta}_{\mathbf{q}}^-(t_2) + \ddot{\Delta}_{\mathbf{q},\text{in}}^+\Delta_{\mathbf{q}}^-(t_1)\Delta_{\mathbf{q}}^-(t_2) \\ &+ \dot{\Delta}_{\mathbf{q},\text{in}}^+\left(\dot{\Delta}_{\mathbf{q}}^-(t_1)\Delta_{\mathbf{q}}^-(t_2) + \Delta_{\mathbf{q}}^-(t_1)\dot{\Delta}_{\mathbf{q}}^-(t_2)\right) \\ &+ \Delta_{\mathbf{q},\text{mem}}^+(t_1, t_2) , \end{aligned} \quad (2.1.66)$$

where

$$\Delta_{\mathbf{q},\text{mem}}^+(t_1, t_2) = \int_0^{t_1} dt' \int_0^{t_2} dt'' \Delta_{\mathbf{q}}^-(t_1 - t') \Pi_{\mathbf{q}}^+(t' - t'') \Delta_{\mathbf{q}}^-(t'' - t_2) . \quad (2.1.67)$$

This contribution to the statistical propagator, which is independent of the initial conditions, is often referred to as *memory integral*. It can be expressed in the form

$$\Delta_{\mathbf{q},\text{mem}}^+(t_1, t_2) = - \int_{-\infty}^{\infty} \frac{d\omega}{2\pi} e^{-i\omega(t_1-t_2)} \mathcal{H}_{\mathbf{q}}^*(t_1, \omega) \mathcal{H}_{\mathbf{q}}(t_2, \omega) \Pi_{\mathbf{q}}^+(\omega) , \quad (2.1.68)$$

where [84]

$$\mathcal{H}_{\mathbf{q}}(t, \omega) = \int_0^t d\tau e^{-i\omega\tau} \Delta_{\mathbf{q}}^-(\tau) . \quad (2.1.69)$$

The expression (2.1.68) will be the basis of our numerical analysis in Section 2.1.4.

2.1.3 Thermalization

Let us now verify that the solution (2.1.66) for the statistical propagator approaches thermal equilibrium at late times. This means that the quantity

$$\Delta_{\mathbf{q}}^+(t, \omega) = \int_{-2t}^{2t} dy e^{i\omega y} \Delta_{\mathbf{q}}^+ \left(t + \frac{y}{2}, t - \frac{y}{2} \right), \quad (2.1.70)$$

which becomes a Fourier transform for $t \rightarrow \infty$, satisfies the KMS condition asymptotically,

$$\Delta_{\mathbf{q}}^+(\infty, \omega) = -\frac{i}{2} \coth \left(\frac{\beta\omega}{2} \right) \Delta_{\mathbf{q}}^-(\omega). \quad (2.1.71)$$

For late times only the memory integral is relevant, since $\Delta_{\mathbf{q}}^-(t)$ and $\dot{\Delta}_{\mathbf{q}}^-(t)$ fall off exponentially for $t \gg 1/\Gamma$. One then obtains

$$\Delta_{\mathbf{q}}^+(\infty, \omega) = \Delta_{\mathbf{q}, \text{mem}}^+(\infty, \omega) = -|\mathcal{H}_{\mathbf{q}}(\infty, \omega)|^2 \Pi_{\mathbf{q}}^+(\omega). \quad (2.1.72)$$

The quantity $\mathcal{H}_{\mathbf{q}}(\infty, \omega)$ is the Laplace transform of the spectral function,

$$\begin{aligned} \mathcal{H}_{\mathbf{q}}(\infty, \omega) &= \int_0^{\infty} d\tau e^{-i(\omega - i\epsilon)\tau} \Delta_{\mathbf{q}}^-(\tau) \\ &= \tilde{\Delta}_{\mathbf{q}}^-(i\omega + \epsilon) \\ &= \frac{1}{s^2 + \omega_{\mathbf{q}}^2 + \tilde{\Pi}_{\mathbf{q}}(s)} \Big|_{s=i\omega+\epsilon} \\ &= -\frac{1}{\omega^2 - \omega_{\mathbf{q}}^2 - \text{Re}\Pi_{\mathbf{q}}^R(\omega) - i\text{Im}\Pi_{\mathbf{q}}^R(\omega)}, \end{aligned} \quad (2.1.73)$$

which yields

$$\begin{aligned} |\mathcal{H}_{\mathbf{q}}(\infty, \omega)|^2 &= \frac{1}{(\omega^2 - \omega_{\mathbf{q}}^2 - \text{Re}\Pi_{\mathbf{q}}^R(\omega))^2 + (\text{Im}\Pi_{\mathbf{q}}^R(\omega))^2} \\ &= -\frac{\rho_{\mathbf{q}}(\omega)}{2 \text{Im}\Pi_{\mathbf{q}}^R(\omega)}. \end{aligned} \quad (2.1.74)$$

Inserting this expression into (2.1.72), using the KMS condition for the self-energy,

$$\Pi_{\mathbf{q}}^-(\omega) = 2i\text{Im}\Pi_{\mathbf{q}}^R(\omega), \quad (2.1.75)$$

one obtains (cf. (2.1.47),(2.1.48)),

$$\begin{aligned} \Delta_{\mathbf{q}}^+(\infty, \omega) &= -\coth \left(\frac{\beta\omega}{2} \right) \frac{\text{Im}\Pi_{\mathbf{q}}^R(\omega)}{(\omega^2 - \omega_{\mathbf{q}}^2 - \text{Re}\Pi_{\mathbf{q}}^R(\omega))^2 + (\text{Im}\Pi_{\mathbf{q}}^R(\omega))^2} \\ &= -\frac{i}{2} \coth \left(\frac{\beta\omega}{2} \right) \Delta_{\mathbf{q}}^-(\omega). \end{aligned} \quad (2.1.76)$$

Hence, our solution for the statistical propagator indeed fulfills the KMS condition (2.1.34) in the limit $t \rightarrow \infty$, which proves that the system reaches thermal equilibrium. For a specific example the approach to equilibrium will be studied numerically in Section 2.1.4.

It is instructive to evaluate the statistical propagator in thermal equilibrium at equal times, i.e., $y = t_1 - t_2 = 0$,

$$\Delta_{\mathbf{q}}^+|_{y=0} = \frac{1}{2} \int_{-\infty}^{\infty} \frac{d\omega}{2\pi} \coth\left(\frac{\beta\omega}{2}\right) \rho_{\mathbf{q}}(\omega) . \quad (2.1.77)$$

For a free field one has

$$\rho_{\mathbf{q}}(\omega) = 2\pi \text{sign}(\omega) \delta(\omega^2 - \omega_{\mathbf{q}}^2) , \quad (2.1.78)$$

which yields the well know result

$$\Delta_{\mathbf{q}}^+|_{y=0} = \frac{1}{\omega_{\mathbf{q}}} \left(\frac{1}{2} + n_{\text{B}}(\omega_{\mathbf{q}}) \right) , \quad (2.1.79)$$

with the temperature dependent Bose-Einstein distribution function

$$n_{\text{B}}(\omega_{\mathbf{q}}) = \frac{1}{e^{\beta\omega_{\mathbf{q}}} - 1} . \quad (2.1.80)$$

Generically, the interaction with the thermal bath changes the energy $\omega_{\mathbf{q}}$ of a free particle to a temperature dependent complex energy $\hat{\Omega}_{\mathbf{q}}$ which appears as a pole of the spectral function $\rho_{\mathbf{q}}(\omega)$ and the integrand of (2.1.77). The spectral function then has two poles in the upper plane, $\hat{\Omega}_{\mathbf{q}}$ and $-\hat{\Omega}_{\mathbf{q}}^*$, which are determined by the condition

$$\hat{\Omega}_{\mathbf{q}} - \left(\omega_{\mathbf{q}}^2 + \Pi_{\mathbf{q}}^R(\hat{\Omega}_{\mathbf{q}}) \right)^{1/2} = 0 . \quad (2.1.81)$$

Assuming that the integral can be closed in the upper half-plane, one obtains for the statistical propagator in equilibrium,²

$$\Delta_{\mathbf{q}}^+|_{y=0} = \text{Re} \left(\frac{1}{\hat{\Omega}_{\mathbf{q}}} \left(\frac{1}{2} + n_{\text{B}}(\hat{\Omega}_{\mathbf{q}}) \right) \right) . \quad (2.1.82)$$

Compared to (2.1.78), the Bose-Einstein distribution function has been replaced by the complex distribution function $n_{\text{B}}(\hat{\Omega}_{\mathbf{q}})$.

At high temperatures, where $\beta\omega_{\mathbf{q}} \ll 1$, the Bose-Einstein distribution has a well-known infrared divergence,

$$n_{\text{B}}(\omega_{\mathbf{q}}) \simeq \frac{1}{\beta\omega_{\mathbf{q}}} \gg 1 . \quad (2.1.83)$$

²Here we restrict ourselves to the case where there are no additional poles.

For quasi-particles, where $\omega_{\mathbf{q}}$ is replaced by $\hat{\Omega}_{\mathbf{q}} = \Omega_{\mathbf{q}} + i\Gamma_{\mathbf{q}}/2$, this divergence is cut off by the finite width,

$$|n_{\text{B}}(\hat{\Omega}_{\mathbf{q}})| \simeq \frac{1}{|\beta(\Omega_{\mathbf{q}} + \frac{i}{2}\Gamma_{\mathbf{q}})|} \leq \frac{2}{\beta\Gamma_{\mathbf{q}}}, \quad (2.1.84)$$

which remains finite even if the real part $\Omega_{\mathbf{q}}$ vanishes.

Comparison of equations (2.1.79) and (2.1.82) suggests that in thermal equilibrium the Φ particles may form a gas of quasi-particles. This question can be clarified by evaluating energy density and pressure of the Φ particles. Since the expectation value of Φ vanishes, one obtains from the energy momentum tensor³

$$T_{\mu\nu} = \partial_{\mu}\Phi\partial_{\nu}\Phi - \eta_{\mu\nu}L \quad (2.1.85)$$

for the contribution of a mode with momentum \mathbf{q} to energy density and pressure,

$$\epsilon_{\mathbf{q}} = \langle T_{00} \rangle |_{\mathbf{q}} = \frac{1}{2} \langle \dot{\Phi}^2 + (\vec{\nabla}\Phi)^2 + m^2\Phi^2 \rangle |_{\mathbf{q}}, \quad (2.1.86)$$

$$p_{\mathbf{q}} = \langle T_{ii} \rangle |_{\mathbf{q}} = \langle \frac{1}{3}(\nabla\Phi)^2 + \frac{1}{2}(\dot{\Phi}^2 - (\nabla\Phi)^2 - m^2\Phi^2) \rangle |_{\mathbf{q}}. \quad (2.1.87)$$

This yields for the energy density

$$\begin{aligned} \epsilon_{\mathbf{q}}(\infty) &= \frac{1}{2} (\partial_{t_1}\partial_{t_2} + \omega_{\mathbf{q}}^2) \Delta_{\mathbf{q}}^+(t_1, t_2) |_{t_1=t_2=\infty} \\ &= \frac{1}{2} (\Omega_{\mathbf{q}}^2 + \omega_{\mathbf{q}}^2) \frac{1}{\Omega_{\mathbf{q}}} \left(\frac{1}{2} + n_{\text{B}}(\Omega_{\mathbf{q}}) \right), \end{aligned} \quad (2.1.88)$$

and for the pressure

$$\begin{aligned} p_{\mathbf{q}}(\infty) &= \left(\frac{1}{3}\mathbf{q}^2 + \frac{1}{2}(\partial_{t_1}\partial_{t_2} - \omega_{\mathbf{q}}^2) \right) \Delta_{\mathbf{q}}^+(t_1, t_2) |_{t_1=t_2=\infty} \\ &= \left(\frac{1}{3}\mathbf{q}^2 + \frac{1}{2}(\Omega_{\mathbf{q}}^2 - \omega_{\mathbf{q}}^2) \right) \frac{1}{\Omega_{\mathbf{q}}} \left(\frac{1}{2} + n_{\text{B}}(\Omega_{\mathbf{q}}) \right), \end{aligned} \quad (2.1.89)$$

where, for simplicity, we have neglected the quasi-particle width.

In summary, the energy momentum tensor in thermal equilibrium can be expressed as sum of a quasi-particle gas contribution and a temperature dependent ‘vacuum’ term,

$$\langle T_{\mu\nu} \rangle |_{\mathbf{q}} = u_{\mu}u_{\nu} (\epsilon_{\mathbf{q}}^{\text{QP}} + p_{\mathbf{q}}^{\text{QP}}) - \eta_{\mu\nu}p_{\mathbf{q}}^{\text{QP}} + \eta_{\mu\nu}\kappa_{\mathbf{q}}^{\text{VAC}}. \quad (2.1.90)$$

Here $u^{\mu} = (1, \vec{0})$ is the 4-velocity of the thermal bath, and

$$\epsilon_{\mathbf{q}}^{\text{QP}} = \Omega_{\mathbf{q}} \left(\frac{1}{2} + n_{\text{B}}(\Omega_{\mathbf{q}}) \right), \quad (2.1.91)$$

³We use the convention $\text{diag}(\eta_{\mu\nu}) = (1, -1, -1, -1)$.

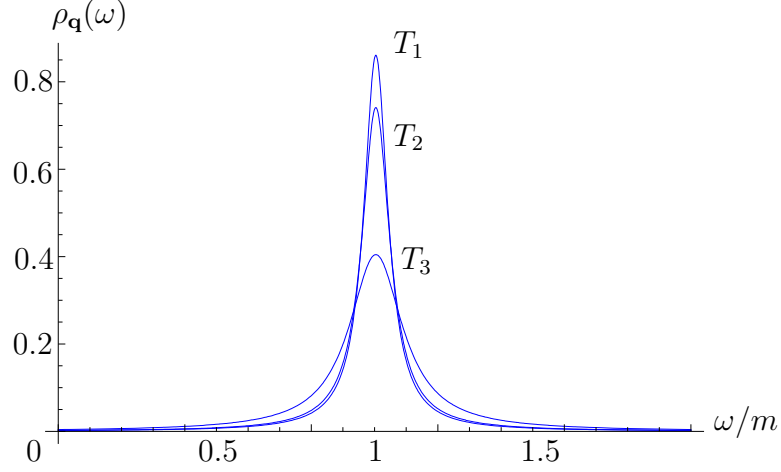


Figure 2.4: Spectral function $\rho_{\mathbf{q}}(\omega)$ for $\mathbf{q} = 0$; case (a) with masses $m_1 = m_2 = 0.2m$ and temperatures $T_1 = 0.1m$, $T_2 = 0.2m$, $T_3 = 0.5m$.

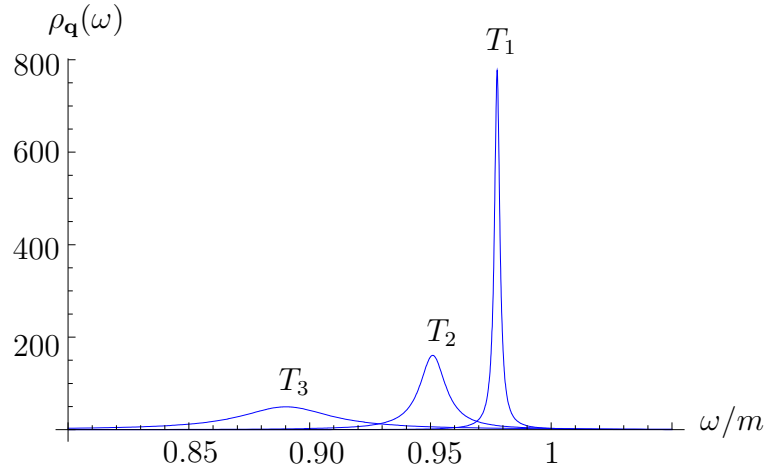


Figure 2.5: Spectral function $\rho_{\mathbf{q}}(\omega)$ for $\mathbf{q} = 0$; case (b) with masses $m_1 = m$, $m_2 = 5m$ and temperatures $T_1 = m$, $T_2 = 2m$, $T_3 = 5m$.

$$p_{\mathbf{q}}^{\text{QP}} = \frac{1}{3} \frac{\mathbf{q}^2}{\Omega_{\mathbf{q}}} \left(\frac{1}{2} + n_{\text{B}}(\Omega_{\mathbf{q}}) \right), \quad (2.1.92)$$

$$\kappa_{\mathbf{q}}^{\text{VAC}} = \frac{\omega_{\mathbf{q}}^2 - \Omega_{\mathbf{q}}^2}{2\Omega_{\mathbf{q}}} \left(\frac{1}{2} + n_{\text{B}}(\Omega_{\mathbf{q}}) \right). \quad (2.1.93)$$

Energy density and pressure of the quasi-particle gas agree with the corresponding expressions for a free gas, with the energy $\omega_{\mathbf{q}}$ of a free particle replaced by the quasi-particle energy $\Omega_{\mathbf{q}}$. The ‘vacuum contribution’ $\kappa_{\mathbf{q}}^{\text{VAC}}$ vanishes for $\Omega_{\mathbf{q}} = \omega_{\mathbf{q}}$. For large thermal effects, i.e. $\Omega_{\mathbf{q}} \gg \omega_{\mathbf{q}}$ or $\Omega_{\mathbf{q}} \ll \omega_{\mathbf{q}}$, the equation of state differs significantly from the one of a free gas. Note that for $\Omega_{\mathbf{q}}^2 < \omega_{\mathbf{q}}^2$, the pressure can even become negative!

2.1.4 Model example

So far we have performed a very general analysis, and the only approximation has been to neglect the backreaction of the field Φ on the thermal bath. Furthermore, we

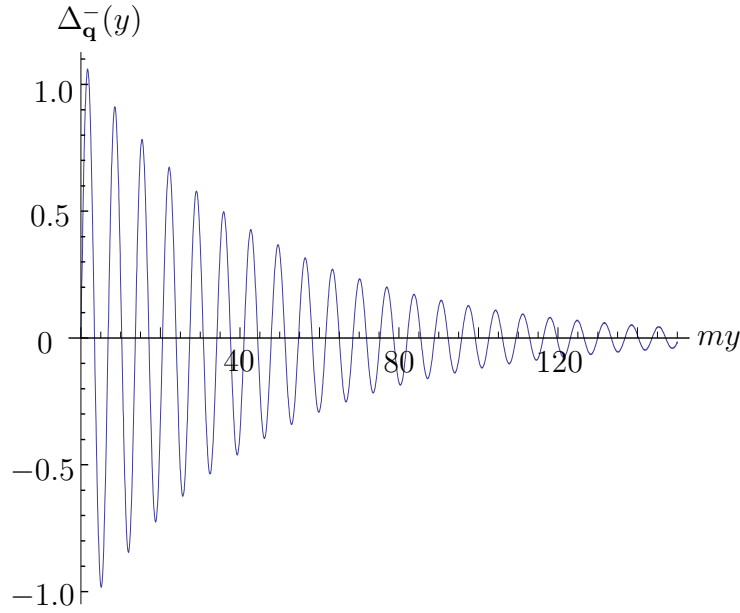


Figure 2.6: Spectral function $\Delta_{\mathbf{q}}^-(y)$ for $\mathbf{q} = 0$; case (b) with masses $m_1 = m$, $m_2 = 5m$ and $T = 10m$.

have restricted our discussion to the case that Φ is linearly coupled to the bath via an interaction term $g\Phi\mathcal{O}(\chi)$. In general, χ represents an arbitrary number of bosonic or fermionic fields with arbitrary couplings including gauge interactions. In order to illustrate the results of the previous sections, we now consider a toy model (cf. [84, 108]), where the quanta of two massive scalar fields represent the thermal bath. The full Lagrangian is given by

$$\mathcal{L} = \frac{1}{2}\partial_\mu\Phi\partial^\mu\Phi - \frac{1}{2}m^2\Phi^2 + \sum_{i=1}^2 \left(\frac{1}{2}\partial_\mu\chi_i\partial^\mu\chi_i - \frac{1}{2}m_i^2\chi_i^2 \right) + g\Phi\chi_1\chi_2 + \mathcal{L}_{\chi\text{int}}. \quad (2.1.94)$$

Note that the coupling g has the dimension of mass. In the following we shall neglect self-interaction of the χ fields and use free thermal propagators for simplicity.

We consider two cases: (a) $m \gg m_1, m_2$ and (b) $m_2 \gg m, m_1$. In the first case, dissipation is dominated by Φ decays and inverse decays, $\Phi \leftrightarrow \chi_1\chi_2$, whereas in the second one χ_2 decays and inverse decays, $\chi_2 \leftrightarrow \Phi\chi_1$, are most important.

In both cases the imaginary part of the self-energy is known analytically [84], the calculation can be seen in Appendix B.1. For $m \gg m_1, m_2$, the decay width of Φ at zero temperature is given by

$$\Gamma = \frac{1}{16\pi} \left(\frac{g}{m} \right)^2 m. \quad (2.1.95)$$

To illustrate thermal effects we shall use a rather large coupling which corresponds to $\Gamma/m = 0.1$.

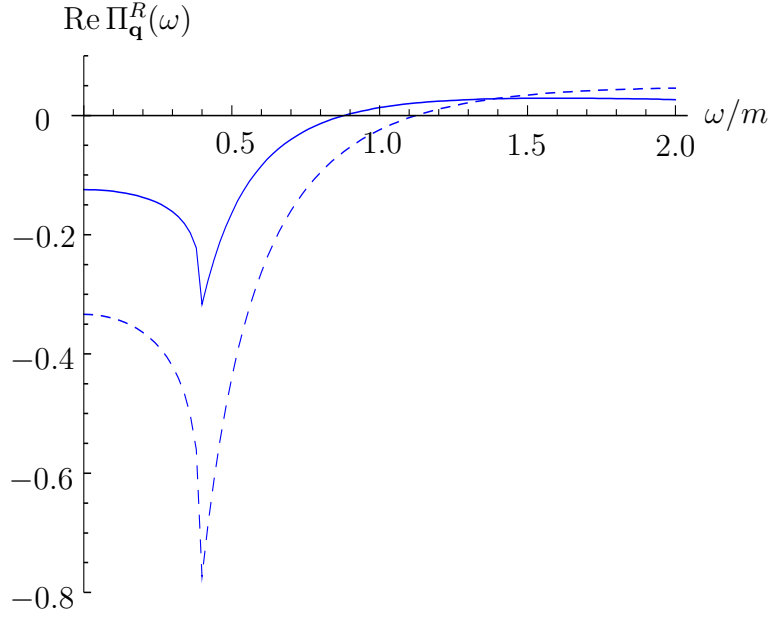


Figure 2.7: Real part of the self-energy $\Pi_{\mathbf{q}}^R(\omega)$ for $\mathbf{q} = 0$; case (a) with masses $m_1 = m_2 = 0.2m$ and temperatures $T_1 = 0.5m$ (solid) and $T_2 = m$ (dashed).

The spectral function $\rho_{\mathbf{q}}(\omega)$ (cf. (2.1.53)) is shown in Figures 2.4 and 2.5 for the two mass patterns (a) and (b), respectively. In case (a), $\Pi_{\mathbf{q}}^R$ has an imaginary part at zero temperature. The width is large, and already at small temperatures the quasi-particle profile becomes broad. On the contrary, in case (b) the zero-temperature width is zero and the finite-temperature width is small. Hence, the quasi-particle profile becomes broad only at much larger temperatures. The spectral function $\Delta_{\mathbf{q}}^-(y)$ is the Fourier transform of $i\rho_{\mathbf{q}}(\omega)$. As Fig. 2.6 illustrates, it approximately represents a damped oscillation with frequency $\Omega_{\mathbf{q}}$ and damping rate $\Gamma_{\mathbf{q}}$.

It is interesting that thermal corrections can increase or decrease the particle mass m . Whether the quasi-particle peak moves to the right or to the left depends on the position of the zero-temperature pole relative to the branch cuts, and it also depends on the temperature. This can be seen by considering the real part of the self-energy, which is displayed for two different temperatures in Fig. 2.7 for case (a). For the smaller temperature one has $\text{Re } \Pi_{\mathbf{q}=0}^R(m) > 0$, whereas $\text{Re } \Pi_{\mathbf{q}=0}^R(m) < 0$ holds for the larger temperature, which corresponds to a shift of the particle mass to the right and to the left, respectively.

The statistical propagator $\Delta_{\mathbf{q}}^+(t_1, t_2)$ depends on the initial conditions. The most general gaussian initial density matrix has five free parameters (cf. [80]). We consider the simplest case of a free field density matrix and vanishing mean values Φ and $\dot{\Phi}$, which implies for each momentum mode,

$$\Phi_{\mathbf{q},\text{in}} = 0, \quad (2.1.96)$$

$$\dot{\Phi}_{\mathbf{q},\text{in}} = 0, \quad (2.1.97)$$

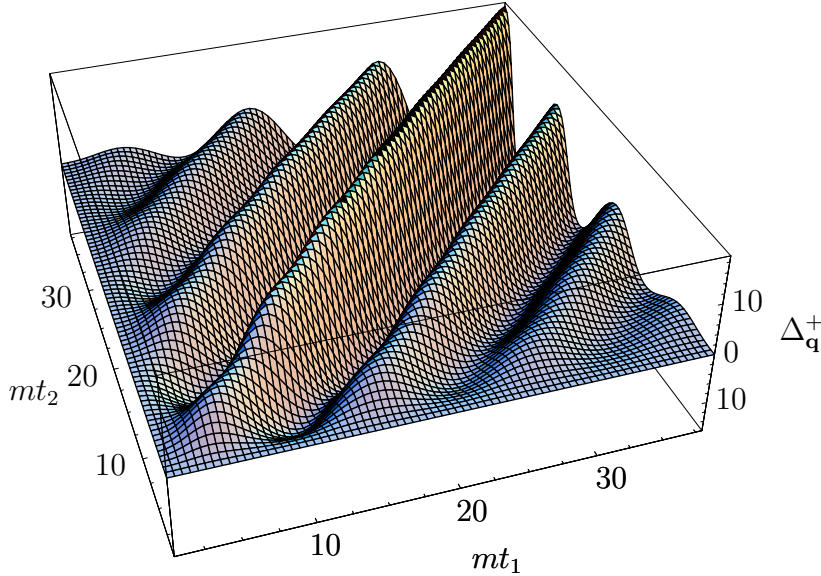


Figure 2.8: Statistical propagator $\Delta_{\mathbf{q}}^+(t_1, t_2)$ for $\mathbf{q} = 0$; case (b) with masses $m_1 = m$, $m_2 = 5m$ and $T = 10m$.

$$\Delta_{\mathbf{q},\text{in}}^+ = \Delta_{\mathbf{q}}^+(t_1, t_2)|_{t_1=t_2=0} = \frac{1}{\omega_{\mathbf{q}}} \left(\frac{1}{2} + n_{\mathbf{q}} \right) , \quad (2.1.98)$$

$$\dot{\Delta}_{\mathbf{q},\text{in}}^+ = \partial_{t_1} \Delta_{\mathbf{q}}^+(t_1, t_2)|_{t_1=t_2=0} = \partial_{t_2} \Delta_{\mathbf{q}}^+(t_1, t_2)|_{t_1=t_2=0} = 0 , \quad (2.1.99)$$

$$\ddot{\Delta}_{\mathbf{q},\text{in}}^+ = \partial_{t_1} \partial_{t_2} \Delta_{\mathbf{q}}^+(t_1, t_2)|_{t_1=t_2=0} = \omega_{\mathbf{q}} \left(\frac{1}{2} + n_{\mathbf{q}} \right) . \quad (2.1.100)$$

The initial state of the system is now characterized by only one parameter $n_{\mathbf{q}}$ which corresponds to an initial number density for a free field.

The general solution (2.1.66) for the statistical propagator $\Delta_{\mathbf{q}}^+(t_1, t_2)$ is shown in Figure 2.8. For fixed $t = (t_1 + t_2)/2$ one sees damped oscillations in $y = t_1 - t_2$. The amplitude increases with increasing time t , as illustrated by Figure 2.9. For fixed $y = t_1 - t_2$ one observes the approach to equilibrium with increasing $t = (t_1 + t_2)/2$. For large times the departure from equilibrium is described by a first-order differential equation, and it decreases exponentially. At small times the evolution is governed by a second-order differential equation, which leads to the oscillations visible in Figure 2.10. The independence of the equilibrium solution from the initial conditions is illustrated by Figure 2.11. The memory of the initial conditions is lost at times $t > 1/\Gamma$.

Finally, it is important to recall that the equilibrium value of the energy differs from the one obtained in the Boltzmann approximation. This is illustrated in Figure 2.12 where the different contributions to the energy are compared as functions of temperature. For the chosen parameters the particle and quasi-particle energies are indistin-

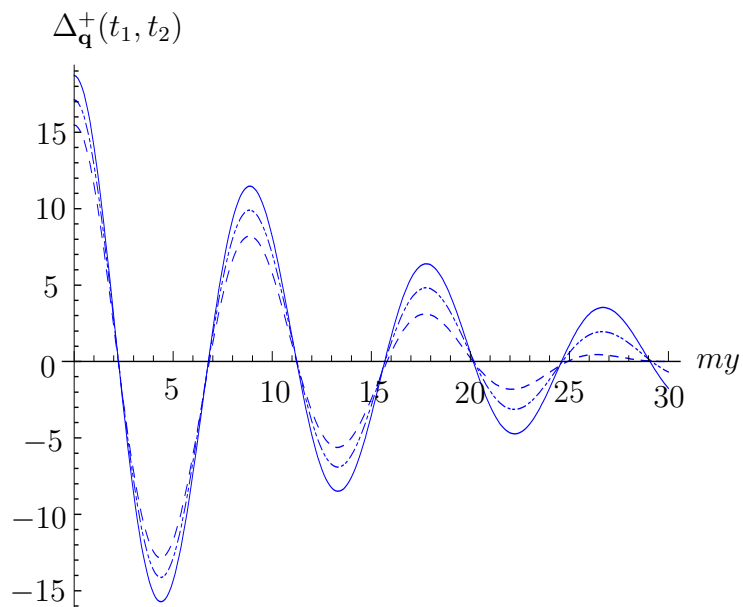


Figure 2.9: Statistical propagator $\Delta_{\mathbf{q}}^+(t_1, t_2)$ as function of $y = t_1 - t_2$ for $\mathbf{q} = 0$; case (b) with $m_1 = m$, $m_2 = 5m$, $T = 10m$ and three values of $t = (t_1 + t_2)/2$: $mt = 15$ (dashed line), $mt = 20$ (dotted-dashed), $mt = 60$ (solid).

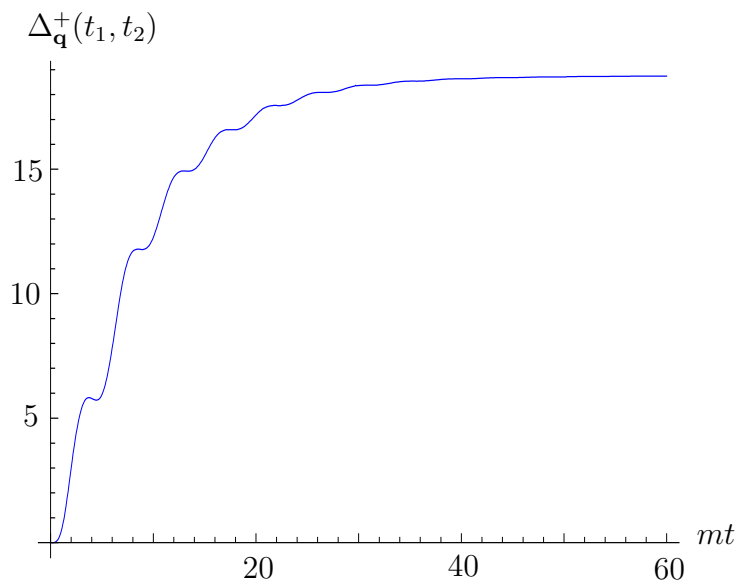


Figure 2.10: Statistical propagator $\Delta_{\mathbf{q}}^+(t_1, t_2)$ as function of $t = (t_1 + t_2)/2$ for $y = 0$, $\mathbf{q} = 0$; case (b) with masses $m_1 = m$, $m_2 = 5m$ and $T = 10m$.

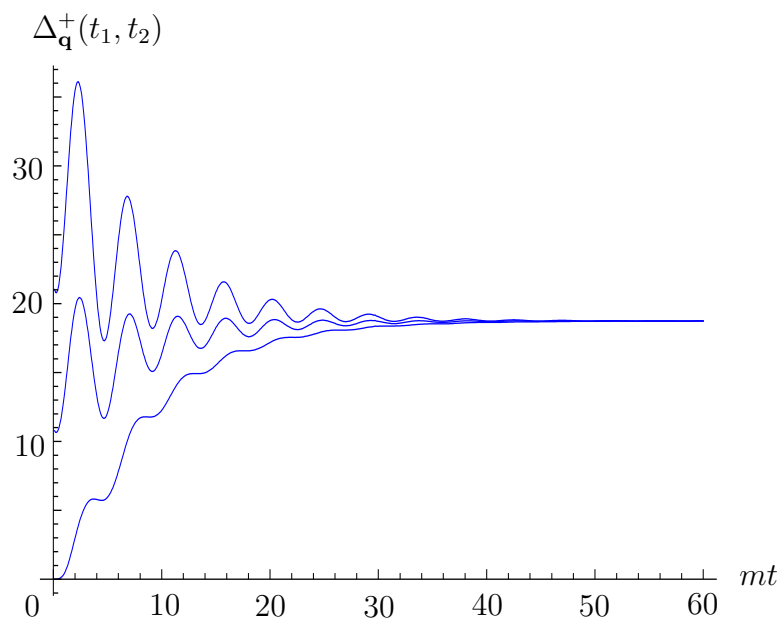


Figure 2.11: Statistical propagator $\Delta_{\mathbf{q}}^+(t_1, t_2)$ with $\mathbf{q} = 0$ as function of $t = (t_1 + t_2)/2$ for $y = 0$ and different initial conditions; case (b) with masses $\mathbf{q} = 0$, $m_1 = m$, $m_2 = 5m$ and $T = 10m$.

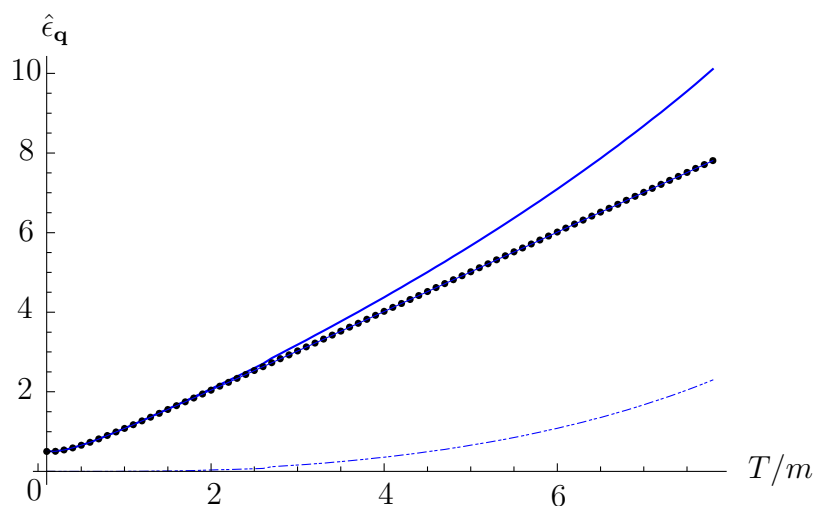


Figure 2.12: Energy density $\hat{\epsilon}_{\mathbf{q}} = \epsilon_{\mathbf{q}}/\omega_{\mathbf{q}}$ as function of temperature for $\mathbf{q} = 0$; case (b) with masses $m_1 = m$, $m_2 = 5m$: total energy density (solid), particle and quasi-particle energy densities (dotted), and 'vacuum' energy density (dashed).

guishable. The ‘vacuum contribution’ is positive, which means that the total energy is larger than the particle/quasi-particle one. The reason is that for the chosen parameters thermal corrections decrease the particle mass. For other parameter choices the ‘vacuum contribution’ can have opposite sign.

2.2 Keldysh-Schwinger formalism for Fermions

Analogue to the treatment of bosons in the previous section, we can apply the non-equilibrium formalism to interacting, weak coupled fermions, coupled to a thermal bath. For example, in the case of leptogenesis, a Majorana neutrino is coupled weakly to a bath of standard model particles of leptons and Higgs. Describing the non-equilibrium dynamics of fermions is a more complicated task than for scalars due to the fact of its Lorentz structure, which is reflected in a non-commutative algebra. In order to obtain a general solution of the Kadanoff-Baym equations, we will need to know two aspects of the bath. First, if the bath is strongly coupled, then back-reaction of the weakly interactive particle can be neglected, which means that the self-energy is composed only of equilibrium particles. This leads to a time translational invariant self-energy. Second, in order to compute the inverse of the self-energy, we need to know the Lorentz structure of the bath. If we assume that the temperature of our system is of the order of the lightest of the heavy Majorana neutrinos, then the electroweak symmetry is not broken, therefore the standard model particles in the bath are all massless. The self-energy will then have a purely 4-vector Lorentz structure. This will allow us to obtain a proper solution to the Kadanoff-Baym equations.

In the following we show how to describe the dynamics of a massive fermions. The later application to massless leptons is straightforward by taking the limit $M \rightarrow 0$. For standard model leptons, the projector P_L needs also to be taken into account. For Majorana fermions, the definition of the Green's functions has to be adjusted by taking into account that a Majorana particle is its own anti-particle. This will affect the symmetry properties. Qualitatively, the symmetry properties of non-equilibrium Majorana neutrinos will be given by the charge operator C .

Another difference with the calculation of the non-equilibrium fermion propagators $G(t)$ is that at $t = 0$ we have $G(t)|_{t=0} \neq 0$ but instead is equal to the free propagator at $t = 0$

$$G(t)|_{t=0} = G^{Free}(t)|_{t=0} . \quad (2.2.1)$$

This comes from the fact that we analyse the time-evolution of propagators instead of a ill-defined particle density quantity. We will see that introducing this propagator to the calculation of leptogenesis will guarantee that all the distribution functions of the particles involved are taken into account. Making the comparison with Boltzmann a possible.

2.2.1 Kadanoff-Baym equations for fermions

Let start by defining thermal averages of fermionic fields (Ψ) on a contour C given in Fig. 2.1

$$G_{\alpha\beta}^>(x_1, x_2) \equiv \langle \Psi_\alpha(x_1) \bar{\Psi}_\beta(x_2) \rangle = \text{Tr}(\rho \Psi_\alpha(x_1) \bar{\Psi}_\beta(x_2)) , \quad (2.2.2)$$

$$G_{\alpha\beta}^<(x_1, x_2) \equiv -\langle \Psi_\beta(x_2) \bar{\Psi}_\alpha(x_1) \rangle = -\text{Tr}(\rho \Psi_\beta(x_2) \bar{\Psi}_\alpha(x_1)) , \quad (2.2.3)$$

where α and β are spinor indices and the trace is taken in the thermal bath with a density matrix ρ . The sign difference from the scalar case in the above definition comes from the anti-commutation property of the fermions. The definition for the rest of the Green's functions in the contour is also straightforward (the spinor indices are omitted till they became relevant for calculations),

$$G_{++}(x_1, x_2) = \Theta(t_1 - t_2)G^>(x_1, x_2) + \Theta(t_2 - t_1)G^<(x_1, x_2) , \quad (2.2.4)$$

$$G_{--}(x_1, x_2) = \Theta(t_1 - t_2)G^<(x_1, x_2) + \Theta(t_2 - t_1)G^>(x_1, x_2) , \quad (2.2.5)$$

$$G_{+-}(x_1, x_2) = G^<(x_1, x_2) , \quad (2.2.6)$$

$$G_{-+}(x_1, x_2) = G^>(x_1, x_2) . \quad (2.2.7)$$

Let's remember that the subindices '+' and '-' refers to times on the upper and lower part of the contour respectively. Similar definitions will also be used for the self-energy Σ_{++} , Σ_{--} , Σ_{+-} and Σ_{-+} . The equation of motion for these propagators is given by the Dyson-Schwinger equation on the Schwinger-Keldysh contour,

$$(i\partial_1 - M)G_C(x_1, x_2) - i \int_C d^4x' \Sigma_C(x_1, x')G_C(x', x_2) = i\delta_C(x_1 - x_2) , \quad (2.2.8)$$

with ∂_1 referring to the partial derivative with respect to x_1 . Notice that this equation is a first order differential equation (see Appendix A.3). In order to obtain a solution for (2.2.8), we will only need one initial condition, as contrast to the scalar case where we needed only two. In a straightforward manner, we can write the Dyson-Schwinger equation on the contour (Figure 2.1) for the correlators $G^>$ and $G^<$,

$$(i\partial_1 - M)G^<(x_1, x_2) = -i \int d^4x' \left(\Sigma_{++}(x_1, x')G^<(x', x_2) - \Sigma^<(x_1, x')G_{--}(x', x_2) \right) , \quad (2.2.9)$$

$$(i\partial_1 - M)G^>(x_1, x_2) = -i \int d^4x' \left(\Sigma^>(x_1, x')G_{++}(x', x_2) - \Sigma_{--}(x_1, x')G^>(x', x_2) \right) . \quad (2.2.10)$$

Defining retarded and advanced Green's functions as usual,

$$G^R(x_1, x_2) = \Theta(t_1 - t_2)(G^>(x_1, x_2) - G^<(x_1, x_2)) , \quad (2.2.11)$$

$$G^A(x_1, x_2) = -\Theta(t_2 - t_1)(G^>(x_1, x_2) - G^<(x_1, x_2)) , \quad (2.2.12)$$

so we can use the following relations

$$G_{++}(x_1, x_2) = G^>(x_1, x_2) + G^A(x_1, x_2) , \quad (2.2.13)$$

$$G_{--}(x_1, x_2) = G^<(x_1, x_2) - G^A(x_1, x_2) , \quad (2.2.14)$$

$$\Sigma_{++}(x_1, x_2) = \Sigma^<(x_1, x_2) + \Sigma^R(x_1, x_2) , \quad (2.2.15)$$

$$\Sigma_{--}(x_1, x_2) = \Sigma^>(x_1, x_2) - \Sigma^R(x_1, x_2) , \quad (2.2.16)$$

to rewrite (2.2.9) and (2.2.10) in the form

$$(i\partial_1 - M)G^<(x_1, x_2) = -i \int d^4x' \left(\Sigma^R(x_1, x')G^<(x', x_2) + \Sigma^<(x_1, x')G^A(x', x_2) \right), \quad (2.2.17)$$

$$(i\partial_1 - M)G^>(x_1, x_2) = -i \int d^4x' \left(\Sigma^>(x_1, x')G^A(x', x_2) + \Sigma^R(x_1, x')G^>(x', x_2) \right). \quad (2.2.18)$$

The theta functions inside the advanced and retarded propagators in equations (2.2.11) and (2.2.12), respectively, will act as cut-off in the time coordinate, this will maintain causality and ensure that we do not double count. As a consequence, the solution of these equations will only depend on the initial conditions. Defining linear combinations of $G^>(x_1, x_2)$ and $G^<(x_1, x_2)$

$$G^-(x_1, x_2) \equiv i\langle\{\Psi(x_1), \bar{\Psi}(x_2)\}\rangle = i\left(G^>(x_1, x_2) - G^<(x_1, x_2)\right), \quad (2.2.19)$$

$$G^+(x_1, x_2) \equiv \frac{1}{2}\langle[\Psi(x_1), \bar{\Psi}(x_2)]\rangle = \frac{1}{2}\left(G^>(x_1, x_2) + G^<(x_1, x_2)\right), \quad (2.2.20)$$

we obtain the spectral function $G^-(x_1, x_2)$ and statistical propagator $G^+(x_1, x_2)$ respectively. For the self-energies we define similarly

$$\Sigma^-(x_1, x_2) \equiv i\left(\Sigma^>(x_1, x_2) - \Sigma^<(x_1, x_2)\right), \quad (2.2.21)$$

$$\Sigma^+(x_1, x_2) \equiv \frac{1}{2}\left(\Sigma^>(x_1, x_2) + \Sigma^<(x_1, x_2)\right). \quad (2.2.22)$$

Again we notice that with the conventions adopted (see Appendix A.3), the self-energies Σ^\pm are defined in the same way as the correlators G^\pm . After some straightforward calculation we can obtain the following set of equations

$$(i\partial_1 - M)G^-(x_1, x_2) = - \int_{t_1}^{t_2} dt' \int d^3x' \Sigma^-(x_1, x')G^-(x', x_2), \quad (2.2.23)$$

$$(i\partial_1 - M)G^+(x_1, x_2) = - \int_{t_i}^{t_2} dt' \int d^3x' \Sigma^+(x_1, x')G^-(x', x_2) + \int_{t_i}^{t_1} dt' \int d^3x' \Sigma^-(x_1, x')G^+(x', x_2). \quad (2.2.24)$$

Assuming spatial translation invariance, the above equations take the form after Fourier transformation,

$$(i\gamma^0 \frac{\partial}{\partial t_1} - \mathbf{k}\gamma - M)G_{\mathbf{k}}^-(t_1, t_2) = - \int_{t_1}^{t_2} dt' \Sigma_{\mathbf{k}}^-(t_1, t')G_{\mathbf{k}}^-(t', t_2), \quad (2.2.25)$$

$$(i\gamma^0 \frac{\partial}{\partial t_1} - \mathbf{k}\gamma - M)G_{\mathbf{k}}^+(t_1, t_2) = - \int_{t_i}^{t_2} dt' \Sigma_{\mathbf{k}}^+(t_1, t')G_{\mathbf{k}}^-(t', t_2) + \int_{t_i}^{t_1} dt' \Sigma_{\mathbf{k}}^-(t_1, t')G_{\mathbf{k}}^+(t', t_2). \quad (2.2.26)$$

If the self-energy has no particle out-of-equilibrium, then its dependance will only be on the difference of coordinates, i.e. $\Sigma_{\mathbf{k}}^{\pm eq}(t_1, t_2) = \Sigma_{\mathbf{k}}^{\pm}(t_1 - t_2)$. We also notice that the function $G_{\mathbf{k}}^-$ is time translational invariant when the self-energy $\Sigma_{\mathbf{k}}^-$ is time translation invariant (the proof from the scalar case also holds for the fermion case, see Appendix B.3). Therefore, the final form of the Kadanoff-Baym equations is

$$(i\gamma^0 \frac{\partial}{\partial t_1} - \mathbf{k}\gamma - M)G_{\mathbf{k}}^-(t_1 - t_2) = - \int_{t_1}^{t_2} dt' \Sigma_{\mathbf{k}}^-(t_1 - t')G_{\mathbf{k}}^-(t' - t_2) , \quad (2.2.27)$$

$$(i\gamma^0 \frac{\partial}{\partial t_1} - \mathbf{k}\gamma - M)G_{\mathbf{k}}^+(t_1, t_2) = - \int_{t_i}^{t_2} dt' \Sigma_{\mathbf{k}}^+(t_1 - t')G_{\mathbf{k}}^-(t' - t_2) \\ + \int_{t_i}^{t_1} dt' \Sigma_{\mathbf{k}}^-(t_1 - t')G_{\mathbf{k}}^+(t', t_2) . \quad (2.2.28)$$

The Kadanoff-Baym equations for fermions resemble the ones for scalars. Equation (2.2.27) is an homogeneous differential-integral equation, meanwhile equation (2.2.28) has a source term. The big difference comes from the Lorentz and flavour structure. Because the self-energies only depend on the difference of the arguments, we can solve both of them exactly with the use of the Laplace transform. We will see that the Lorentz and flavour structure of the self-energies is extremely important in order to obtain a solution of these equations.

2.2.2 Solutions for the KB equations

The solution of the Kadanoff-Baym equations for fermions is in principle similar as the case of scalar particles. The solution for G^- will only depend on the difference of coordinates but G^+ will have a dependency on the centre of mass coordinate as well. Both Green's functions have Lorentz and in principle flavour structure too. However, for our effective model, the flavour information is stored in the Yukawa effective coupling η . This coupling acts as constant when the inverse of the self-energy is needed. For a one hierarchal case, where two flavours needs to be taken into account in the self-energy one needs a more general solution (see Appendix C.1)

Solution of the first KB equation for fermions

Choosing a convenient change of variables $y = t_1 - t_2$ and $y' = t' - t_2$ we can rewrite the first KB equation (2.2.27) as

$$\left(i\gamma^0 \frac{\partial}{\partial y} - \mathbf{k}\gamma - M \right) G_{\mathbf{k}}^-(y) - \int_0^y dy' \Sigma_{\mathbf{k}}^-(y - y')G_{\mathbf{k}}^-(y') = 0 , \quad (2.2.29)$$

and applying Laplace transformation one obtains

$$\left(-i\gamma^0 \left(G_{\mathbf{k}}^-(0) - s\tilde{G}_{\mathbf{k}}^-(s) \right) - (\mathbf{k}\gamma + M)\tilde{G}_{\mathbf{k}}^-(s) \right) - \tilde{\Sigma}_{\mathbf{k}}^-(s)\tilde{G}_{\mathbf{k}}^-(s) = 0 , \quad (2.2.30)$$

where the *tilde* notation was introduced for the Laplace transformed quantities, e.g.

$$\tilde{G}_{\mathbf{k}}^-(s) = \int_0^\infty dt e^{-sy} G_{\mathbf{k}}^-(y) , \quad (2.2.31)$$

Again we emphasise that we are able to solve this equations via the Laplace transform, only because the self-energy is time translational invariant. Otherwise this method is not viable. The initial condition $G_{\mathbf{k}}^{-}(0)$ is obtained by using equal time commutation relation

$$G_{\mathbf{k}}^{-}(0) = i\gamma^0 , \quad (2.2.32)$$

then, one arrives at

$$(-is\gamma^0 + (\mathbf{k}\gamma + M)) \tilde{G}_{\mathbf{k}}^{-}(s) - \tilde{\Sigma}_{\mathbf{k}}^{-}(s)\tilde{G}_{\mathbf{k}}^{-}(s) = \mathbb{1} , \quad (2.2.33)$$

where $\mathbb{1}$ in the r.h.s. is a spinor four-by-four unit matrix. From the above equation we can easily find that

$$\tilde{G}_{\mathbf{k}}^{-}(s) = \frac{1}{-is\gamma^0 + (\mathbf{k}\gamma + M) - \tilde{\Sigma}_{\mathbf{k}}^{-}(s)} . \quad (2.2.34)$$

To obtain $G_{\mathbf{k}}^{-}(y)$ we must perform the inverse Laplace transform by integrating over the Bromwich contour Fig. 2.3

$$G_{\mathbf{k}}^{-}(y) = \frac{1}{2\pi i} \left(\int_{-i\infty+\epsilon}^{i\infty+\epsilon} \tilde{G}_{\mathbf{k}}^{-}(s)e^{sy} + \int_{i\infty-\epsilon}^{-i\infty-\epsilon} \tilde{G}_{\mathbf{k}}^{-}(s)e^{sy} \right) ds . \quad (2.2.35)$$

After introducing the integration variable $s = i\omega + \epsilon$ and $s = i\omega - \epsilon$ to equation (2.2.35) we obtain

$$G_{\mathbf{k}}^{-}(y) = \int_{-\infty}^{\infty} \frac{d\omega}{2\pi} e^{-i\omega y} \left(\frac{1}{\not{k} - M - \Sigma^R(\omega)} - \frac{1}{\not{k} - M - \Sigma^A(\omega)} \right) , \quad (2.2.36)$$

when using the identities

$$\Sigma^R(\omega) = \tilde{\Sigma}(-i\omega + \epsilon) , \quad (2.2.37)$$

$$\Sigma^A(\omega) = \tilde{\Sigma}(-i\omega - \epsilon) . \quad (2.2.38)$$

These identities comes from the fact that we can use spectral representation for the self-energies

$$\Sigma^R(\omega) = i \int_{-\infty}^{\infty} \frac{dp_0}{2\pi} \frac{\Sigma^{-}(p_0)}{\omega - p_0 + i\epsilon} , \quad (2.2.39)$$

$$\Sigma^A(\omega) = i \int_{-\infty}^{\infty} \frac{dp_0}{2\pi} \frac{\Sigma^{-}(p_0)}{\omega - p_0 - i\epsilon} , \quad (2.2.40)$$

$$\tilde{\Sigma}^{-}(s) = i \int_{-\infty}^{\infty} \frac{dp_0}{2\pi} \frac{\Sigma^{-}(p_0)}{is - p_0} . \quad (2.2.41)$$

In the high temperature case the fields constituting the thermal bath are massless. The self-energy Σ will be then a pure vector in Lorentz space, and is given by [109]

$$\Sigma_{\mathbf{k}}^R(\omega) = a_{\mathbf{k}}(\omega)\not{k} + b_{\mathbf{k}}(\omega)\not{y} , \quad (2.2.42)$$

where $a_{\mathbf{k}}$ and $b_{\mathbf{k}}$ are some functions whose symmetry properties with respect to ω are determined by the bath (for a complete calculation and comparison to the literature see Appendix C.2). The four-momentum \not{k} represents the momentum of external particle while the four-vector \not{v} represent the four-velocity of the thermal bath. In most cases one can perform all necessary computations in the bath reference frame where $u = (1, 0, 0, 0)$.

If the fields of the thermal bath have a mass, then there will be a scalar contribution to the self-energy. This scalar contribution $C^{-1}\Sigma_{scalar}$ can be incorporated into the mass M of the fermion field and define

$$\mathcal{M} = M + C^{-1}\Sigma_{scalar} . \quad (2.2.43)$$

For a high neutrino mass, the thermal contribution from the bath is small and can be neglected $\mathcal{M} \simeq M$. The solution for G^- can be rewritten as

$$G_{\mathbf{k}}^-(y) = \int_{-\infty}^{\infty} \frac{d\omega}{2\pi} e^{-i\omega y} \left(\frac{(1+a)\not{k} + b\not{v} + M}{D} - \frac{(1+a^*)\not{k} + b^*\not{v} + M}{D^*} \right) , \quad (2.2.44)$$

with

$$\begin{aligned} D &= (1+a)^2 k^2 + b^2 + 2(1+a)b k \cdot u - M^2 , \\ &\simeq (1+2a)k^2 + 2b\omega - M^2 , \end{aligned} \quad (2.2.45)$$

$a = a_{\mathbf{k}}(\omega)$ and $b = b_{\mathbf{k}}(\omega)$. For small a and b with respect to the mass of the fermion, the denominator can be taken up to first order in those variables, then we can rewrite

$$G_{\mathbf{k}}^-(y) = i \int_{-\infty}^{\infty} \frac{d\omega}{2\pi} e^{-i\omega y} \rho_{\mathbf{k}}(\omega) . \quad (2.2.46)$$

In the narrow width limit $\rho_{\mathbf{k}}(\omega)$ is given by

$$\rho_{\mathbf{k}}(\omega) = 2\text{sign}(\omega)(\not{k} + M) \frac{\omega_{\mathbf{k}}\Gamma_{\mathbf{k}}}{(k^2 - M^2)^2 + (\omega_{\mathbf{k}}\Gamma_{\mathbf{k}})^2} , \quad (2.2.47)$$

where $k^2 = \omega^2 - \mathbf{k}^2$ and

$$\Gamma_{\mathbf{k}} \equiv -2\text{Im} \left(a \frac{M^2}{\omega} + b \right)_{\omega=\omega_{\mathbf{k}}} , \quad (2.2.48)$$

The symmetry properties of a and b are described in the Appendix C.2. After performing the back Fourier transformation using residue theorem in ω we get

$$G_{\mathbf{k}}^-(y) = \left(i\gamma_0 \cos(\omega_{\mathbf{k}}y) + \left(\frac{M - \mathbf{k}\gamma}{\omega_{\mathbf{k}}} \right) \sin(\omega_{\mathbf{k}}y) \right) e^{-\Gamma_{\mathbf{k}}|y|/2} , \quad (2.2.49)$$

with y been a difference of two times. The solution of the first Kadanoff-Baym equation has the shape of a fermionic Breit-Wigner, where the oscillatory behaviour is exponentially suppressed by the width $\Gamma_{\mathbf{k}}$. Because of the equilibrium nature of the self-energy, the spectral function will also depend only on the difference of coordinates. One big difference between the fermionic and the scalar spectral functions is the fact that while the scalar spectral function has a definite symmetry in ω , the fermion spectral function has a symmetry depending on the Lorentz direction. This is no surprise because the fermion propagators must satisfy the properties in equation (A.3.14).

Solution of the second KB equation for fermions

We shall now proceed to solve the second Kadanoff-Baym equation (2.2.28), in which without loss of generality we can take $t_i = 0$

$$(i\gamma^0 \frac{\partial}{\partial t_1} - \mathbf{k}\gamma - M)G_{\mathbf{k}}^+(t_1, t_2) - \int_0^{t_1} dt' \Sigma_{\mathbf{k}}^-(t_1 - t')G_{\mathbf{k}}^+(t', t_2) = \zeta_{\mathbf{k}}(t_1 - t_2) , \quad (2.2.50)$$

with the source term $\zeta_{\mathbf{k}}(t_1 - t_2)$ given by

$$\zeta_{\mathbf{k}}(t_1 - t_2) = - \int_0^{t_2} dt' \Sigma_{\mathbf{k}}^+(t_1 - t')G_{\mathbf{k}}^-(t' - t_2) . \quad (2.2.51)$$

The general solution of (2.2.50) can be written as

$$G_{\mathbf{k}}^+(t_1, t_2) = \hat{G}_{\mathbf{k}}^+(t_1, t_2) + G_{\mathbf{k}, \text{mem}}^+(t_1, t_2) , \quad (2.2.52)$$

where $\hat{G}_{\mathbf{k}}^+(t_1, t_2)$ is the solution of the homogeneous equation

$$(i\gamma^0 \frac{\partial}{\partial t_1} - \mathbf{k}\gamma - M)\hat{G}_{\mathbf{k}}^+(t_1, t_2) - \int_0^{t_1} dt' \Sigma_{\mathbf{k}}^-(t_1 - t')\hat{G}_{\mathbf{k}}^+(t', t_2) = 0 , \quad (2.2.53)$$

and

$$G_{\mathbf{k}, \text{mem}}^+(t_1, t_2) = - \int_0^{t_1} dt' G_{\mathbf{k}}^-(t_1 - t')\zeta_{\mathbf{k}}(t' - t_2) , \quad (2.2.54)$$

is the solution to the memory integral. Let first concentrate on equation (2.2.54), which can be written after performing Fourier transformation on the variables $y_1 = t_1 - t'$ and $y_2 = t_2 - t'$ as

$$G_{\mathbf{k}, \text{mem}}^+(t_1, t_2) = \int \frac{d\omega}{2\pi} \mathcal{H}_{\mathbf{k}}(\omega, t_1) \Sigma_{\mathbf{k}}^+(\omega) \mathcal{H}_{\mathbf{k}}(\omega, t_2) e^{-i\omega y} , \quad (2.2.55)$$

with $y = t_1 - t_2$, and

$$\mathcal{H}_{\mathbf{k}}(\omega, t_1) = \int_0^{t_1} dy_1 G_{\mathbf{k}}^-(y_1) e^{i\omega y_1} , \quad (2.2.56)$$

$$\mathcal{H}_{\mathbf{k}}(\omega, t_2) = \int_0^{t_2} dy_2 G_{\mathbf{k}}^-(-y_2) e^{-i\omega y_2} . \quad (2.2.57)$$

The $y_{1,2}$ integrations can be performed analytically

$$\int_0^{t_1} dy_1 G_{\mathbf{k}}^-(y_1) e^{i\omega y_1} \approx \frac{1}{\omega_{\mathbf{k}}^2 - (\omega - i\Gamma_{\mathbf{k}}/2)^2} \left(i\gamma^0 (\omega_{\mathbf{k}} s_1 + i\omega c_1 - i\omega) + \frac{M - \mathbf{k}\gamma}{\omega_{\mathbf{k}}} (i\omega s_1 - \omega_{\mathbf{k}} c_1 + \omega_{\mathbf{k}}) \right) , \quad (2.2.58)$$

$$\int_0^{t_2} dy_1 G_{\mathbf{k}}^-(-y_2) e^{-i\omega y_2} \approx \frac{1}{\omega_{\mathbf{k}}^2 - (\omega + i\Gamma_{\mathbf{k}}/2)^2} \left(i\gamma^0 (\omega_{\mathbf{k}} s_2^* - i\omega c_2^* + i\omega) - \frac{M - \mathbf{k}\gamma}{\omega_{\mathbf{k}}} (-i\omega s_2^* - \omega_{\mathbf{k}} c_2^* + \omega_{\mathbf{k}}) \right), \quad (2.2.59)$$

where terms of order $\Gamma_{\mathbf{k}}$ in the numerator were neglected, and

$$s_i = \sin(\omega_{\mathbf{k}} t_i) e^{i(\omega + i\Gamma_{\mathbf{k}}/2)t_i}, \quad (2.2.60)$$

$$c_i = \cos(\omega_{\mathbf{k}} t_i) e^{i(\omega + i\Gamma_{\mathbf{k}}/2)t_i}. \quad (2.2.61)$$

Then

$$\begin{aligned} G_{\mathbf{k},mem}^+(t_1, t_2) &= \int \frac{d\omega}{2\pi} \frac{-i/2 \tanh(\beta\omega/2)}{|\omega_{\mathbf{k}}^2 - (\omega - i\Gamma_{\mathbf{k}}/2)^2|^2} \frac{M}{\omega_{\mathbf{k}}} e^{-i\omega(t_1-t_2)} \\ &\times \left(\gamma^0 \Sigma_{\mathbf{k}}^-(\omega) \gamma^0 (\omega_{\mathbf{k}} s_1 + i\omega c_1 - i\omega) (-\omega_{\mathbf{k}} s_2^* + i\omega c_2^* - i\omega) \right. \\ &+ \gamma^0 \Sigma_{\mathbf{k}}^-(\omega) \frac{M - \mathbf{k}\gamma}{\omega_{\mathbf{k}}} (i\omega_{\mathbf{k}} s_1 - \omega c_1 + \omega) (i\omega s_2^* + \omega_{\mathbf{k}} c_2^* - \omega_{\mathbf{k}}) \\ &+ \frac{M - \mathbf{k}\gamma}{\omega_{\mathbf{k}}} \Sigma_{\mathbf{k}}^-(\omega) \gamma^0 (i\omega s_1 - \omega_{\mathbf{k}} c_1 + \omega_{\mathbf{k}}) (i\omega_{\mathbf{k}} s_2^* + \omega c_2^* + i\omega) \\ &\left. + \frac{M - \mathbf{k}\gamma}{\omega_{\mathbf{k}}} \Sigma_{\mathbf{k}}^-(\omega) \frac{M - \mathbf{k}\gamma}{\omega_{\mathbf{k}}} (i\omega s_1 - \omega_{\mathbf{k}} c_1 + \omega_{\mathbf{k}}) (i\omega s_2^* + \omega_{\mathbf{k}} c_2^* - \omega_{\mathbf{k}}) \right). \end{aligned} \quad (2.2.62)$$

We can now proceed to simplify the above equation to be able to perform Cauchy's theorem on the ω integration with the poles $\pm\omega_{\mathbf{k}} \pm i\Gamma_{\mathbf{k}}/2$. If we again neglect corrections of order $\Gamma_{\mathbf{k}}$ in the numerator, we can then replace $\omega \leftrightarrow \omega_{\mathbf{k}} \text{sign}(\omega)$ and $\omega^2 \leftrightarrow \omega_{\mathbf{k}}^2$ under the integral. This, with $\text{sign}(\omega)^2 = 1$, allows to simplify the last expression to

$$\begin{aligned} G_{\mathbf{k},mem}^+(t_1, t_2) &= \int \frac{d\omega}{2\pi} \frac{-i/2 \tanh(\beta\omega/2)}{|\omega_{\mathbf{k}}^2 - (\omega - i\Gamma_{\mathbf{k}}/2)^2|^2} (\not{k} + M) \Sigma^-(\omega) (\not{k} + M) \\ &\times \left(-s_1 s_2^* - i\text{sign}(\omega) c_1 s_2^* + i\text{sign}(\omega) s_1 c_2^* - c_1 c_2^* \right. \\ &\left. - i\text{sign}(\omega) s_1 + c_1 + i\text{sign}(\omega) s_2^* + c_2^* - 1 \right) e^{-i\omega(t_1-t_2)}. \end{aligned} \quad (2.2.63)$$

Now, since $\Sigma_{\mathbf{k}}^-(\omega) = \text{Disc}\Sigma_{\mathbf{k}}^R(\omega)$ and, in our case for vanishing lepton and Higgs mass we have $\text{Disc}\Sigma_{\mathbf{k}}^R(\omega) = 2i(a_I \not{k} + b_I \not{t})$, we can write

$$\begin{aligned} G_{\mathbf{k},mem}^+(t_1, t_2) &= \int \frac{d\omega}{2\pi} \frac{\tanh(\beta\omega/2)}{|\omega_{\mathbf{k}}^2 - (\omega - i\Gamma_{\mathbf{k}}/2)^2|^2} e^{-i\omega(t_1-t_2)} \\ &\times \left(2M(a_I k^2 + b_I \omega) - \mathbf{k}\gamma ((a_I(k^2 + M^2) + 2b_I \omega)) \right. \\ &\left. + \gamma^0 (\omega (a_I(k^2 + M^2) + 2b_I \omega) + b_I(k^2 - M^2)) \right) \\ &\times \left(-s_1 s_2^* - i\text{sign}(\omega) c_1 s_2^* + i\text{sign}(\omega) s_1 c_2^* - c_1 c_2^* \right. \\ &\left. - i\text{sign}(\omega) s_1 + c_1 + i\text{sign}(\omega) s_2^* + c_2^* - 1 \right), \end{aligned} \quad (2.2.64)$$

where $a_I = \text{Im}[a]$ and $b_I = \text{Im}[b]$. Knowing that in fact the functions a_I and b_I are analytic, we can now apply Cauchy's theorem. The combination of exponentials coming

from the s_i and c_i with the $e^{-i\omega(t_1-t_2)}$ determine for each term individually whether one has to close the path in the upper or lower half of the imaginary plane. Due to the minus sign that comes if we take the direction of the path in the lower half plane, the denominator is always

$$\frac{1}{|\omega_{\mathbf{k}}^2 - (\omega - i\Gamma_{\mathbf{k}}/2)^2|^2} \rightarrow \frac{-i}{4\omega_{\mathbf{k}}^2\Gamma_{\mathbf{k}}},$$

while in the numerator, due to the antisymmetry of \tanh and a_I and the symmetry of b_I , the scalar and $\mathbf{k}\gamma$ part are symmetric while the γ^0 part is antisymmetric. Recalling the definition of $\Gamma_{\mathbf{k}}$ in equation (2.2.48)

$$\Gamma_{\mathbf{k}} = -2\frac{a_I(\omega_{\mathbf{k}})M^2 + b_I(\omega_{\mathbf{k}})\omega_{\mathbf{k}}}{\omega_{\mathbf{k}}}, \quad (2.2.65)$$

and the KMS relation

$$\Sigma_{\mathbf{k}}^+(\omega) = -i/2 \tanh(\beta\omega/2)\Sigma_{\mathbf{k}}^-(\omega). \quad (2.2.66)$$

one can further obtain by using the spectral function obtained in (2.2.49),

$$G_{\mathbf{k},\text{mem}}^+(y, t) = -\frac{\tanh\left(\frac{\beta\omega_{\mathbf{k}}}{2}\right)}{2} \left(e^{-\Gamma_{\mathbf{k}}|y|/2} - e^{-\Gamma_{\mathbf{k}}t} \right) \times \left(i\gamma_0 \sin(\omega_{\mathbf{k}}y) - \frac{M - \mathbf{k}\gamma}{\omega_{\mathbf{k}}} \cos(\omega_{\mathbf{k}}y) \right). \quad (2.2.67)$$

Note that when $t_1 = t_2 = 0$ this solution vanishes, which is absolutely trivial, because there are no memory effects at $t = 0$.

The homogeneous solution can be solved analogue to the first KB equation (2.2.27), the functional dependence on the first argument t_1 of the solution to the Eq. (2.2.28) can be easily obtained. Applying Laplace transform to (2.2.53) one finds

$$\tilde{G}_{\mathbf{k}}^+(s, t_2) = \frac{1}{i\gamma_0 s - \mathbf{k}\gamma - M + \tilde{\Sigma}_{\mathbf{k}}^-(s)} i\gamma_0 \hat{G}_{\mathbf{k}}^+(0, t_2). \quad (2.2.68)$$

Integrating further over Bromwich contour one obtains

$$\hat{G}_{\mathbf{k}}^+(t_1, t_2) = -G_{\mathbf{k}}^-(t_1) i\gamma_0 \hat{G}_{\mathbf{k}}^+(0, t_2), \quad (2.2.69)$$

where $\hat{G}_{\mathbf{k}}^+(0, t_2)$ can be found using the symmetry given in (A.3.15). Then

$$\hat{G}_{\mathbf{k}}^+(t_1, t_2) = G_{\mathbf{k}}^-(t_1) \gamma_0 G_{\mathbf{k}}^+(0, 0) \gamma_0 G_{\mathbf{k}}^-(-t_2). \quad (2.2.70)$$

We are interested in the case of zero initial abundance Majorana neutrinos, this corresponds to a vacuum Green function by choosing ⁴

$$G_{\mathbf{k}}^+(0, 0) = \frac{M - \mathbf{k}\gamma}{2\omega_{\mathbf{k}}}. \quad (2.2.71)$$

⁴We assume that the interaction is switched on when the system starts evolving in time to avoid problems related to the fact that the vacuum of the interactive theory can not be expressed by Gaussian initial conditions [111]

The full solution now reads

$$G_{\mathbf{k}}^+(t, y) = - \left(i\gamma_0 \sin(\omega_{\mathbf{k}}y) - \frac{M - \mathbf{k}\gamma}{\omega_{\mathbf{k}}} \cos(\omega_{\mathbf{k}}y) \right) \times \left[\frac{\tanh\left(\frac{\beta\omega_{\mathbf{k}}}{2}\right)}{2} e^{-\Gamma_{\mathbf{k}}|y|/2} + f^{eq}(\omega_{\mathbf{k}}) e^{-\Gamma_{\mathbf{k}}t} \right], \quad (2.2.72)$$

where the equilibrium distribution function for fermions $f^{eq}(\omega_{\mathbf{k}}) = 1/(e^{\beta\omega_{\mathbf{k}}-1})$ is explicitly shown. In order to verify that the solutions for $G_{\mathbf{k}}^-(y)$ and $G_{\mathbf{k}}^+(t, y)$ are correct, we need to check three conditions that these equations must satisfy: symmetries described in (A.3.14) and (A.3.15), initial conditions for $t \rightarrow 0$, and KMS condition for equilibrium when $t \rightarrow \infty$.

2.2.3 Properties of the solutions

Symmetries

Let us apply the symmetries conditions described in Eqs. (A.3.14) and (A.3.15) for our solution of the spectral function and the statistical propagator. Applying first the Hermitian conjugate to the spectral function

$$[G_{\mathbf{k}}^-(y)]^\dagger = \left(-i\gamma_0 \cos(\omega_{\mathbf{k}}y) + \left(\frac{M + \mathbf{k}\gamma}{\omega_{\mathbf{k}}} \right) \sin(\omega_{\mathbf{k}}y) \right) e^{-\Gamma_{\mathbf{k}}|y|/2}, \quad (2.2.73)$$

where we have used the Hermitian property of γ_0 and the anti-Hermitian of γ_i

$$(\gamma_0)^\dagger = \gamma_0, \quad (\gamma_i)^\dagger = -\gamma_i. \quad (2.2.74)$$

Applying γ_0 from the left and right

$$\gamma_0 [G_{\mathbf{k}}^-(y)]^\dagger \gamma_0 = \left(-i\gamma_0 \cos(\omega_{\mathbf{k}}y) + \left(\frac{M - \mathbf{k}\gamma}{\omega_{\mathbf{k}}} \right) \sin(\omega_{\mathbf{k}}y) \right) e^{-\Gamma_{\mathbf{k}}|y|/2}. \quad (2.2.75)$$

with $\{\gamma_0, \gamma_i\} = 0$ and $(\gamma_0)^2 = 1$. Finally

$$-\gamma_0 [G_{\mathbf{k}}^-(-y)]^\dagger \gamma_0 = \left(i\gamma_0 \cos(\omega_{\mathbf{k}}y) + \left(\frac{M - \mathbf{k}\gamma}{\omega_{\mathbf{k}}} \right) \sin(\omega_{\mathbf{k}}y) \right) e^{-\Gamma_{\mathbf{k}}|y|/2}, \quad (2.2.76)$$

$$= G_{\mathbf{k}}^-(y). \quad (2.2.77)$$

Now, for the case of the statistical propagator we can apply the same criteria. Because the exponentials depend on t and $|y|$, the exchange $t_1 \leftrightarrow t_2$ will no have any effect, so we can define

$$A_{\mathbf{k}}(t, |y|) = \frac{\tanh\left(\frac{\beta\omega_{\mathbf{k}}}{2}\right)}{2} e^{-\Gamma_{\mathbf{k}}|y|/2} + f^{eq}(\omega_{\mathbf{k}}) e^{-\Gamma_{\mathbf{k}}t}. \quad (2.2.78)$$

Then

$$[G_{\mathbf{k}}^+(t, y)]^\dagger = -A_{\mathbf{k}}(t, |y|) \left(-i\gamma_0 \sin(\omega_{\mathbf{k}}y) - \frac{M + \mathbf{k}\gamma}{\omega_{\mathbf{k}}} \cos(\omega_{\mathbf{k}}y) \right). \quad (2.2.79)$$

Finally

$$\gamma_0[G_{\mathbf{k}}^+(t, -y)]^\dagger \gamma_0 = -A_{\mathbf{k}}(t, |y|) \left(i\gamma_0 \sin(\omega_{\mathbf{k}}y) - \frac{M - \mathbf{k}\gamma}{\omega_{\mathbf{k}}} \cos(\omega_{\mathbf{k}}y) \right), \quad (2.2.80)$$

$$= G_{\mathbf{k}}^+(t, y). \quad (2.2.81)$$

We can conclude that our solution for the spectral function and the statistical propagator satisfy the required symmetry properties.

Initial conditions

At $t_1 = t_2 = 0$ the two correlation functions must become the free ones evaluated at $t = 0$, because at $t_1 = t_2 = 0$ there are no interactions. We can see that our solutions satisfy that condition

$$G_{\mathbf{k}}^-(y)|_{y=0} = i\gamma_0, \quad (2.2.82)$$

$$G_{\mathbf{k}}^+(y)|_{t=0, y=0} = \frac{M - \mathbf{k}\gamma}{2\omega_{\mathbf{k}}}, \quad (2.2.83)$$

where in the last equation we used the property

$$\tanh\left(\frac{\beta\omega_{\mathbf{k}}}{2}\right) = -2f^{eq}(\omega_{\mathbf{k}}) + 1. \quad (2.2.84)$$

The initial condition comes from the anti-commutation of the fermion field. Remember that the correlation functions are calculated in the mixed representation.

Equilibration and KMS condition

To look at the equilibration of the spectral and statistical propagators, we must set $\Gamma_{\mathbf{k}}t \rightarrow \infty$ but maintain the difference, i.e. $\Gamma_{\mathbf{k}}|y|$. We can see that because G^- does not depend on the sum of the coordinates, it maintains its form for large t times. But for G^+ we obtain

$$G_{\mathbf{k}}^+(t, y)|_{t \rightarrow \infty} = - \left(i\gamma_0 \sin(\omega_{\mathbf{k}}y) - \frac{M - \mathbf{k}\gamma}{\omega_{\mathbf{k}}} \cos(\omega_{\mathbf{k}}y) \right) \frac{\tanh\left(\frac{\beta\omega_{\mathbf{k}}}{2}\right)}{2} e^{-\Gamma_{\mathbf{k}}|y|/2}, \quad (2.2.85)$$

To check that this equation satisfies the KMS condition, thus is in equilibrium, we must perform a Fourier transformation from time-space to ω -space in order to satisfy

$$G_{\mathbf{k}}^+(\omega) = -\frac{i}{2} \tanh\left(\frac{\beta\omega}{2}\right) G_{\mathbf{k}}^-(\omega). \quad (2.2.86)$$

Let concentrate first on the scalar part of the above equation

$$G_{\mathbf{k}scalar}^+(y) = \frac{M}{2\omega_{\mathbf{k}}} \cos(\omega_{\mathbf{k}}y) \tanh\left(\frac{\beta\omega_{\mathbf{k}}}{2}\right) e^{-\Gamma_{\mathbf{k}}|y|/2}. \quad (2.2.87)$$

In ω -space we have

$$G_{\mathbf{k}scalar}^+(\omega) = \frac{M}{\omega_{\mathbf{k}}} \tanh\left(\frac{\beta\omega}{2}\right) \frac{\Gamma_{\mathbf{k}}\omega_{\mathbf{k}}\omega}{|\omega_{\mathbf{k}}^2 - (\omega - i\Gamma_{\mathbf{k}}/2)^2|}, \quad (2.2.88)$$

which has to be compared with the scalar part of $G_{\mathbf{k}}^-(y)$

$$G_{\mathbf{k}scalar}^-(y) = \frac{M}{\omega_{\mathbf{k}}} \sin(\omega_{\mathbf{k}}y) e^{-\Gamma_{\mathbf{k}}|y|}, \quad (2.2.89)$$

and in ω -space

$$G_{\mathbf{k}scalar}^-(\omega) \approx i \frac{M}{\omega_{\mathbf{k}}} \frac{\Gamma_{\mathbf{k}}(\omega_{\mathbf{k}}^2 + \omega^2)}{|\omega_{\mathbf{k}}^2 - (\omega - i\Gamma_{\mathbf{k}}/2)^2|}. \quad (2.2.90)$$

The \approx indicates that, again, we have neglected higher order of $\Gamma_{\mathbf{k}}$ in the numerator. We can see that equation (2.2.86) is satisfied in the narrow width approximation. It is straightforward to compare the vector parts of the statistical propagator with the spectral function to satisfy the KMS relation.

2.3 Keldysh-Schwinger formalism for standard model leptons

To get the non-equilibrium form for standard model leptons S^\pm , we can do the same procedure for the massive fermions and take the limit $M \rightarrow 0$. the corresponding KB equations read

$$(i\gamma^0 \frac{\partial}{\partial t_1} - \mathbf{k}\gamma) S_{\mathbf{k}}^-(t_1 - t_2) = - \int_{t_1}^{t_2} dt' \Sigma_{\mathbf{k}}^-(t_1 - t') S_{\mathbf{k}}^-(t' - t_2), \quad (2.3.1)$$

$$\begin{aligned} (i\gamma^0 \frac{\partial}{\partial t_1} - \mathbf{k}\gamma) S_{\mathbf{k}}^+(t_1, t_2) &= - \int_{t_i}^{t_2} dt' \Sigma_{\mathbf{k}}^+(t_1 - t') G_{\mathbf{k}}^-(t' - t_2) \\ &+ \int_{t_i}^{t_1} dt' \Sigma_{\mathbf{k}}^-(t_1 - t') G_{\mathbf{k}}^+(t', t_2) \end{aligned} \quad (2.3.2)$$

The solutions can be easily obtained with the following initial conditions

$$S_{\mathbf{k}}^-(0) = iP_L \gamma_0, \quad (2.3.3)$$

$$S_{\mathbf{k}}^+(0) = -P_L \frac{\mathbf{k}\gamma}{k}, \quad (2.3.4)$$

in order to get

$$S_{\mathbf{k}}^-(y) = P_L \left(i\gamma_0 \cos(ky) - \left(\frac{\mathbf{k}\gamma}{k} \right) \sin(ky) \right) e^{-\Gamma_{\mathbf{k}}|y|/2}, \quad (2.3.5)$$

$$S_{\mathbf{k}}^+(t, y) = - P_L \left(i\gamma_0 \sin(ky) + \frac{\mathbf{k}\gamma}{k} \cos(ky) \right) \times \left[\frac{\tanh\left(\frac{\beta k}{2}\right)}{2} e^{-\Gamma_{\mathbf{k}}|y|/2} + f^{eq}(k) e^{-\Gamma_{\mathbf{k}}t} \right], \quad (2.3.6)$$

where $k = |\mathbf{k}|$ is the energy of the massless lepton and the chirality is explicitly shown with the projector P_L .

2.4 Keldysh-Schwinger formalism for Majorana fermions

The Keldysh-Schwinger formalism for Majorana fermions is straightforward from the formalism for normal fermions. The differences comes naturally from the fact that a Majorana fermion is it's own anti-particle. This will give raise to different definitions, but same procedures. Let start with the Schwinger-Dyson equation on the contour

$$C(i\partial_1 - M)G_C(x_1, x_2) - i \int_C d^4z \Sigma_C(x_1, z)G_C(z, x_2) = i\delta_C(x_1 - x_2). \quad (2.4.1)$$

The spectral function and statistical propagators are defined right now as

$$G_{\alpha\beta}^-(x_1, x_2) = i\langle\{N_\alpha(x_1), N_\beta(x_2)\}\rangle, \quad (2.4.2)$$

$$G_{\alpha\beta}^+(x_1, x_2) = \frac{1}{2}\langle[N_\alpha(x_1), N_\beta(x_2)]\rangle, \quad (2.4.3)$$

which satisfies the following symmetries

$$G^-(x_1, x_2) = \gamma_0[G^-(x_2, x_1)]^\dagger\gamma_0 = G^-(x_2, x_1)^T, \quad (2.4.4)$$

$$G^+(x_1, x_2) = -\gamma_0[G^+(x_2, x_1)]^\dagger\gamma_0 = -G^+(x_2, x_1)^T. \quad (2.4.5)$$

Defining also the self energies

$$\Sigma^-(x_1, x_2) = i(\Sigma^>(x_1, x_2) - \Sigma^<(x_1, x_2)), \quad (2.4.6)$$

$$\Sigma^+(x_1, x_2) = \frac{1}{2}(\Sigma^>(x_1, x_2) + \Sigma^<(x_1, x_2)). \quad (2.4.7)$$

This will give us the Kadanoff-Baym equations

$$C(i\gamma^0\partial_{t_1} - \mathbf{p}\gamma - M)G_{\mathbf{p}}^-(t_1 - t_2) = - \int_{t_1}^{t_2} dt' \Sigma_{\mathbf{p}}^-(t_1 - t')G_{\mathbf{p}}^-(t' - t_2), \quad (2.4.8)$$

$$C(i\gamma^0\partial_{t_1} - \mathbf{p}\gamma - M)G_{\mathbf{p}}^+(t_1, t_2) = - \int_{t_i}^{t_2} dt' \Sigma_{\mathbf{p}}^+(t_1 - t')G_{\mathbf{p}}^-(t' - t_2) + \int_{t_i}^{t_1} dt' \Sigma_{\mathbf{p}}^-(t_1 - t')G_{\mathbf{p}}^+(t', t_2). \quad (2.4.9)$$

Without loss of generality in the following we will set $t_i = 0$. The solution of these equations can be found exactly as before with the following initial conditions

$$G_{\mathbf{p}}^-(0) = i\gamma_0 C^{-1}, \quad (2.4.10)$$

$$G_{\mathbf{p}}^+(0,0) = \frac{M - \mathbf{p}\gamma}{\omega_{\mathbf{p}}} C^{-1}. \quad (2.4.11)$$

With these we will get

$$G_{\mathbf{p}}^-(y) = \left(i\gamma_0 \cos(\omega_{\mathbf{p}}y) + \left(\frac{M - \mathbf{p}\gamma}{\omega_{\mathbf{p}}} \right) \sin(\omega_{\mathbf{p}}y) \right) e^{-\Gamma_{\mathbf{p}}|y|/2} C^{-1}. \quad (2.4.12)$$

and

$$G_{\mathbf{p}}^+(t,y) = - \left(i\gamma_0 \sin(\omega_{\mathbf{p}}y) - \frac{M - \mathbf{p}\gamma}{\omega_{\mathbf{p}}} \cos(\omega y) \right) \times \left[\frac{\tanh\left(\frac{\beta\omega_{\mathbf{p}}}{2}\right)}{2} e^{-\Gamma_{\mathbf{p}}|y|/2} + f_N^{eq}(\omega_{\mathbf{p}}) e^{-\Gamma_{\mathbf{p}}t} \right] C^{-1}, \quad (2.4.13)$$

As before, the equation for $G_{\mathbf{p}}^+(t,y)$ is the sum of the memory solution plus the homogeneous one. One difference between the above equations and the one for fermions, are the symmetries that these Green's functions need to satisfy. Let start with the spectral function and see the symmetry described in Appendix A. First we have

$$[G_{\mathbf{p}}^-(y)]^T = (C^{-1})^T \left(i\gamma_0^T \cos(\omega_{\mathbf{p}}y) + \left(\frac{M - \mathbf{p}\gamma^T}{\omega_{\mathbf{p}}} \right) \sin(\omega_{\mathbf{p}}y) \right) e^{-\Gamma_{\mathbf{p}}|y|/2}. \quad (2.4.14)$$

Using the fact that $(C^{-1}) = C^T$ and $C\gamma_{\mu}C^{-1} = -\gamma_{\mu}$ we get

$$[G_{\mathbf{p}}^-(y)]^T = \left(-i\gamma_0 \cos(\omega_{\mathbf{p}}y) + \left(\frac{M + \mathbf{p}\gamma}{\omega_{\mathbf{p}}} \right) \sin(\omega_{\mathbf{p}}y) \right) e^{-\Gamma_{\mathbf{p}}|y|/2} C. \quad (2.4.15)$$

Finally, using $C^{-1} = -C$ we obtain

$$[G_{-\mathbf{p}}^-(-y)]^T = \left(i\gamma_0 \cos(\omega_{\mathbf{p}}y) + \left(\frac{M - \mathbf{p}\gamma}{\omega_{\mathbf{p}}} \right) \sin(\omega_{\mathbf{p}}y) \right) e^{-\Gamma_{\mathbf{p}}|y|/2} C^{-1}, \quad (2.4.16)$$

$$= G_{\mathbf{p}}^-(y). \quad (2.4.17)$$

We can apply the same procedure for $G_{\mathbf{p}}^+(t,y)$, as before we introduce

$$B_{\mathbf{p}}(t,|y|) = \left[\frac{\tanh\left(\frac{\beta\omega_{\mathbf{p}}}{2}\right)}{2} e^{-\Gamma_{\mathbf{p}}|y|/2} + f_N^{eq}(\omega_{\mathbf{p}}) e^{-\Gamma_{\mathbf{p}}t} \right], \quad (2.4.18)$$

to get

$$[G_{\mathbf{p}}^+(t,y)]^T = -(C^{-1})^T B_{\mathbf{p}}(t,|y|) \left(i\gamma_0^T \sin(\omega_{\mathbf{p}}y) - \frac{M - \mathbf{p}\gamma^T}{\omega_{\mathbf{p}}} \cos(\omega y) \right). \quad (2.4.19)$$

We continue with the algebra

$$[G_{\mathbf{p}}^+(t, y)]^T = -B_{\mathbf{p}}(t, |y|) \left(-i\gamma_0^T \sin(\omega_{\mathbf{p}}y) - \frac{M + \mathbf{p}\gamma^T}{\omega_{\mathbf{p}}} \cos(\omega y) \right) C, \quad (2.4.20)$$

$$-[G_{-\mathbf{p}}^+(t, -y)]^T = -B_{\mathbf{p}}(t, |y|) \left(i\gamma_0^T \sin(\omega_{\mathbf{p}}y) - \frac{M - \mathbf{p}\gamma^T}{\omega_{\mathbf{p}}} \cos(\omega y) \right) C^{-1}, \quad (2.4.21)$$

$$= G_{\mathbf{p}}^+(t, y). \quad (2.4.22)$$

For completeness here is a list of the Majorana propagators which will be used in the next chapter.

$$G_{\mathbf{p}}^-(y) = \left(i\gamma_0 \cos(\omega_{\mathbf{p}}y) + \frac{M - \mathbf{p}\gamma}{\omega_{\mathbf{p}}} \sin(\omega_{\mathbf{p}}y) \right) e^{-\Gamma_{\mathbf{p}}|y|/2} C^{-1}, \quad (2.4.23)$$

$$G_{\mathbf{p}}^+(y, t) = - \left(i\gamma_0 \sin(\omega_{\mathbf{p}}y) - \frac{M - \mathbf{p}\gamma}{\omega_{\mathbf{p}}} \cos(\omega_{\mathbf{p}}y) \right) \\ \times \left(\frac{\tanh\left(\frac{\beta\omega_{\mathbf{p}}}{2}\right)}{2} e^{-\Gamma_{\mathbf{p}}|y|/2} + f_N^{eq}(\omega_{\mathbf{p}}) e^{-\Gamma_{\mathbf{p}}t} \right) C^{-1}, \quad (2.4.24)$$

$$G_{\mathbf{p}}^{11}(y, t) = - \frac{\gamma_0}{2} \left(2i \sin(\omega_{\mathbf{p}}y) \left(\frac{\tanh\left(\frac{\beta\omega_{\mathbf{p}}}{2}\right)}{2} e^{-\Gamma_{\mathbf{p}}|y|/2} + f_N^{eq}(\omega_{\mathbf{p}}) e^{-\Gamma_{\mathbf{p}}t} \right) \right. \\ \left. - \cos(\omega_{\mathbf{p}}y) \text{sign}(y) e^{-\Gamma_{\mathbf{p}}|y|/2} \right) C^{-1} \\ + \frac{M - \mathbf{p}\gamma}{2\omega_{\mathbf{p}}} \left(2 \cos(\omega_{\mathbf{p}}y) \left(\frac{\tanh\left(\frac{\beta\omega_{\mathbf{p}}}{2}\right)}{2} e^{-\Gamma_{\mathbf{p}}|y|/2} + f_N^{eq}(\omega_{\mathbf{p}}) e^{-\Gamma_{\mathbf{p}}t} \right) \right. \\ \left. - i \sin(\omega_{\mathbf{p}}|y|) e^{-\Gamma_{\mathbf{p}}|y|/2} \right) C^{-1}, \quad (2.4.25)$$

$$G_{\mathbf{p}}^{22}(y, t) = (G_{\mathbf{p}}^{11}(y, t))^*,$$

$$G_{\mathbf{p}}^>(y, t) = - \frac{\gamma_0}{2} \left(2i \sin(\omega_{\mathbf{p}}y) \left(\frac{\tanh\left(\frac{\beta\omega_{\mathbf{p}}}{2}\right)}{2} e^{-\Gamma_{\mathbf{p}}|y|/2} + f_N^{eq}(\omega_{\mathbf{p}}) e^{-\Gamma_{\mathbf{p}}t} \right) \right. \\ \left. - \cos(\omega_{\mathbf{p}}y) e^{-\Gamma_{\mathbf{p}}|y|/2} \right) C^{-1} \\ + \frac{M - \mathbf{p}\gamma}{2\omega_{\mathbf{p}}} \left(2 \cos(\omega_{\mathbf{p}}y) \left(\frac{\tanh\left(\frac{\beta\omega_{\mathbf{p}}}{2}\right)}{2} e^{-\Gamma_{\mathbf{p}}|y|/2} + f_N^{eq}(\omega_{\mathbf{p}}) e^{-\Gamma_{\mathbf{p}}t} \right) \right. \\ \left. - i \sin(\omega_{\mathbf{p}}y) e^{-\Gamma_{\mathbf{p}}|y|/2} \right) C^{-1}, \quad (2.4.26)$$

$$\begin{aligned}
G_{\mathbf{p}}^{\leq}(y, t) = & - \frac{\gamma_0}{2} \left(2i \sin(\omega_{\mathbf{p}} y) \left(\frac{\tanh\left(\frac{\beta\omega_{\mathbf{p}}}{2}\right)}{2} e^{-\Gamma_{\mathbf{p}}|y|/2} + f_N^{eq}(\omega_{\mathbf{p}}) e^{-\Gamma_{\mathbf{p}} t} \right) \right. \\
& \left. + \cos(\omega_{\mathbf{p}} y) e^{-\Gamma_{\mathbf{p}}|y|/2} \right) C^{-1} \\
& + \frac{M - \mathbf{p}\gamma}{2\omega_{\mathbf{p}}} \left(2 \cos(\omega_{\mathbf{p}} y) \left(\frac{\tanh\left(\frac{\beta\omega_{\mathbf{p}}}{2}\right)}{2} e^{-\Gamma_{\mathbf{p}}|y|/2} + f_N^{eq}(\omega_{\mathbf{p}}) e^{-\Gamma_{\mathbf{p}} t} \right) \right. \\
& \left. + i \sin(\omega_{\mathbf{p}} y) e^{-\Gamma_{\mathbf{p}}|y|/2} \right) C^{-1} . \tag{2.4.27}
\end{aligned}$$

For a full list of propagators see appendix D.

Chapter 3

Thermal leptogenesis

In this chapter we present a realistic model for leptogenesis. We show first the semi-classical approach for the asymmetry calculation via the Boltzmann equations. We then apply the quantum formalism developed in the previous chapter for the creation of Green's functions for Majorana neutrinos, and finally use it to compute the time evolution of dressed lepton Green's functions. In terms of the lepton charge operator computed from the dressed lepton statistical propagator we are able to study the production of the desired lepton asymmetry. In order to compare both methods, we neglect wash-out terms and concentrate only on the generation of the asymmetry.

3.1 Boltzmann formalism

Leptogenesis is normally studied in terms of coupled Boltzmann equations. Those describe the evolution of the distribution function of the Majorana neutrino and the generated asymmetry via the decay of the heavy Majorana neutrino. As shown in the previous chapters, one of the most important parameter that comes into play is the CP violating parameter ϵ (coming from flavour mixing in the Yukawa sector). In what follows we will concentrate on the comparison between the Boltzmann equation and the Kadanoff-Baym formalism. In order to do that, we can neglect the wash-out and focus only on the generation of an asymmetry by studying the decay of the heavy Majorana neutrino.

3.1.1 Boltzmann equation for the production of Majorana fermions

Following the definition of the Boltzmann equation, we can write the evolution of the Majorana distribution function $f_N(t, \omega)$ in a thermal bath composed by leptons and Higgs, with distribution functions $f_l(t, k)$ and $f_\phi(t, q)$ respectively. If the bath is strongly coupled and its temperature varies slowly in comparison to the expansion of the universe, we can assume that the distribution function of particles in this bath are not time-dependent and they will remain in equilibrium, i.e. $f_l(k) = (e^{\beta k} + 1)^{-1}$ and $f_\phi(q) =$

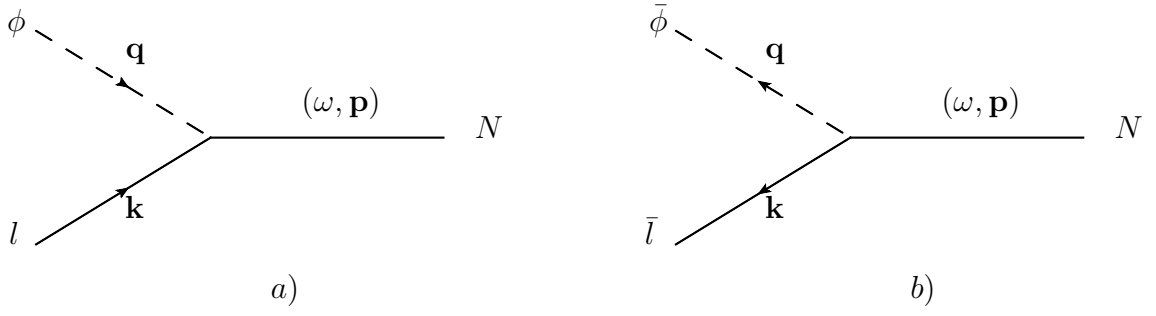


Figure 3.1: Processes involved in the matrix elements of the Boltzmann equation. a) $\mathcal{M}(N \rightarrow l\phi)$ and b) $\mathcal{M}(N(p) \rightarrow \bar{l}(k)\bar{\phi}(q))$. The inverse processes can be derived easily from these two.

$(e^{\beta k} - 1)^{-1}$. Hence

$$\begin{aligned} \frac{\partial}{\partial t} f_N(t, \omega) = & -\frac{1}{2\omega} \int_{\mathbf{k}, \mathbf{q}} (2\pi)^4 \delta^4(k + q - p) \\ & \times \left[f_N(t, \omega) (1 - f_l(k)) (1 + f_\phi(q)) \left(|\mathcal{M}(N \rightarrow l\phi)|^2 + |\mathcal{M}(N \rightarrow \bar{l}\bar{\phi})|^2 \right) \right. \\ & \left. - f_l(k) f_\phi(q) (1 - f_N(t, \omega)) \left(|\mathcal{M}(l\phi \rightarrow N)|^2 + |\mathcal{M}(\bar{l}\bar{\phi} \rightarrow N)|^2 \right) \right], \end{aligned} \quad (3.1.1)$$

where $\mathcal{M}(N \rightarrow l\phi)$ and $\mathcal{M}(N \rightarrow \bar{l}\bar{\phi})$ are the matrix elements of the decay of the Majorana neutrino into a lepton-higgs and anti-lepton-anti-higgs respectively, and $\mathcal{M}(l\phi \rightarrow N)$, $\mathcal{M}(\bar{l}\bar{\phi} \rightarrow N)$ are matrix elements of the inverse processes. Using CPT invariance we see that

$$|\mathcal{M}(l\phi \rightarrow N)|^2 = |\mathcal{M}(N \rightarrow \bar{l}\bar{\phi})|^2, \quad (3.1.2)$$

so the Boltzmann equation for the Majorana neutrinos can be rewritten as

$$\begin{aligned} \frac{\partial}{\partial t} f_N(t, \omega) = & -\frac{1}{2\omega} \int_{\mathbf{k}, \mathbf{q}} (2\pi)^4 \delta^4(k + q - p) \\ & \times \left(|\mathcal{M}(N \rightarrow l\phi)|^2 + |\mathcal{M}(N \rightarrow \bar{l}\bar{\phi})|^2 \right) \\ & \times [f_N(t, \omega) (1 - f_l(k)) (1 + f_\phi(q)) - f_l(k) f_\phi(q) (1 - f_N(t, \omega))], \end{aligned} \quad (3.1.3)$$

where we defined $\omega = \sqrt{M^2 + \mathbf{p}^2}$, k and q as the energies of N , l and ϕ with equilibrium distribution functions f_i and f_ϕ^1 , respectively; the averaged decay matrix element is (cf. [73])

$$|\mathcal{M}(N(p) \rightarrow l(k)\phi(q))|^2 = 2 (\lambda^\dagger \lambda)_{11} p \cdot k. \quad (3.1.4)$$

¹In the absence of chemical potential the distribution functions for a certain particle is equal to the one for its anti-particle.

The sign in front on the distribution functions in the r.h.s. corresponds to a bosonic enhancement (+) or Pauli blocking (-). The momentum integrations was conveniently written with the notation

$$\int_{\mathbf{p}} \cdots = \int \frac{d^3 p}{(2\pi)^3 2\omega} \cdots \quad (3.1.5)$$

The sum of decay and inverse decay widths, which determines the rate for the approach to equilibrium, is given by

$$\Gamma_\beta(\omega) = (\lambda^\dagger \lambda)_{11} \frac{2}{\omega} \int_{\mathbf{k}, \mathbf{q}} (2\pi)^4 \delta^4(k + q - p) p \cdot k f_{l\phi}(k, q), \quad (3.1.6)$$

where we have introduced the function

$$\begin{aligned} f_{l\phi}(k, q) &= f_l(k) f_\phi(q) + (1 - f_l(k))(1 + f_\phi(q)) \\ &= 1 - f_l(k) + f_\phi(q), \\ &= \frac{f_l(k) f_\phi(q)}{f_N^{eq}(\omega)}, \end{aligned} \quad (3.1.7)$$

and in the last line of (3.1.7) the 4-momentum conservation $p = k + q$ has been used and $f_N^{eq}(\omega) = 1/(e^{\beta\omega} + 1)$. Using the optical theorem one can see that the decay width obtained in (3.1.6) is exactly the same as the decay width that one obtains from the one loop diagram [108]. The Boltzmann equation can be then written as

$$\frac{\partial}{\partial t} f_N(t, \omega) = -(f_N(t, \omega) - f_N^{eq}(\omega)) \Gamma_\beta(\omega) \quad (3.1.8)$$

For the solution of the Boltzmann equation (3.1.8) with vacuum initial condition, $f_N(0, \omega) = 0$, one easily obtains ($\Gamma_\beta(\omega) \equiv \Gamma$)

$$f_N(t, \omega) = f_N^{eq}(\omega) (1 - e^{-\Gamma t}), \quad (3.1.9)$$

We can see that when $t \rightarrow \infty$ the distribution of the Majorana neutrinos approaches the equilibrium one and all quantum corrections disappear. For $t \rightarrow 0$ there is no Majorana particles.

3.1.2 Boltzmann equations for the production of a the lepton asymmetry

The solution (3.1.9) needs to be introduced in the Boltzmann equation for the lepton distribution function (see Figure 3.2), which reads

$$\begin{aligned} \frac{\partial}{\partial t} f_l(t, k) &= - \frac{1}{2k} \int_{\mathbf{q}, \mathbf{p}} (2\pi)^4 \delta^4(k + q - p) \\ &\times \left[f_l(k) f_\phi(q) (1 - f_N(t, \omega)) |\mathcal{M}(l\phi \rightarrow N)|^2 \right. \\ &\quad \left. - f_N(t, \omega) (1 - f_l(k)) (1 + f_\phi(q)) |\mathcal{M}(N \rightarrow l\phi)|^2 \right], \end{aligned} \quad (3.1.10)$$

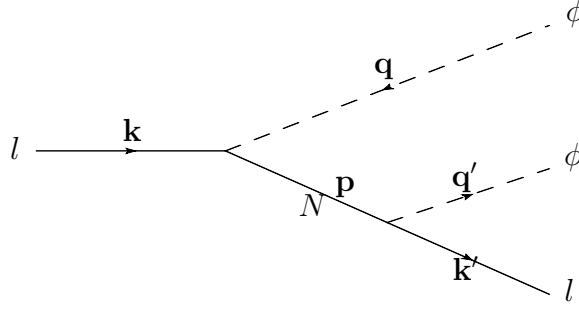


Figure 3.2: Diagram contributing to the matrix elements of the Boltzmann equation for leptons.

and for the anti-lepton

$$\begin{aligned} \frac{\partial}{\partial t} f_{\bar{l}}(t, k) = & - \frac{1}{2k} \int_{\mathbf{q}, \mathbf{p}} (2\pi)^4 \delta^4(k + q - p) \\ & \times \left[f_{\bar{l}}(k) f_{\bar{\phi}}(q) (1 - f_N(t, \omega)) |\mathcal{M}(\bar{l}\bar{\phi} \rightarrow N)|^2 \right. \\ & \left. - f_N(t, \omega) (1 - f_{\bar{l}}(k)) (1 + f_{\bar{\phi}}(q)) |\mathcal{M}(N \rightarrow \bar{l}\bar{\phi})|^2 \right], \end{aligned} \quad (3.1.11)$$

where now $\mathcal{O}(\lambda^4)$ corrections to the matrix elements have to be kept. In order to compare with the quantum formalism, we have dropped the *wash-out* terms. These will not contribute to the production of lepton asymmetry, but they will be important if one wants to obtain a quantitative result on the lepton asymmetry, which is not the goal of this thesis.²

If chemical potential can be neglected, one can see that the equilibrium distribution functions of l and ϕ are the same as for their anti-particles ($f_l \simeq f_{\bar{l}}$ and $f_\phi \simeq f_{\bar{\phi}}$). Defining the lepton asymmetry as the difference between the out-of-equilibrium lepton distribution function and the one for its anti-particle, i.e. $f_{Li}(t, k) = f_{li}(t, k) - f_{\bar{l}i}(t, k)$ and using equation (3.1.2) we get

$$\begin{aligned} \frac{\partial}{\partial t} f_{Li}(t, k) = & \frac{1}{2k} \int_{\mathbf{q}, \mathbf{p}} (2\pi)^4 \delta^4(k + q - p) \epsilon_{ii} \left(|\mathcal{M}(N \rightarrow l\phi)|^2 + |\mathcal{M}(N \rightarrow \bar{l}\bar{\phi})|^2 \right) \\ & \times \left(f_N(t, \omega) (1 - f_l(k)) (1 + f_\phi(q)) + f_l(k) f_\phi(q) (1 - f_N(t, \omega)) \right). \end{aligned} \quad (3.1.12)$$

Considering the effects of scattering processes we get finally the Boltzmann equation for the lepton asymmetry

$$\begin{aligned} \frac{\partial}{\partial t} f_{Li}(t, k) = & \frac{1}{2k} \int_{\mathbf{q}, \mathbf{p}} (2\pi)^4 \delta^4(k + q - p) \epsilon_{ii} \left(|\mathcal{M}(N \rightarrow l\phi)|^2 + |\mathcal{M}(N \rightarrow \bar{l}\bar{\phi})|^2 \right) \\ & \times \left(f_N(t, \omega) (1 - f_l(k)) (1 + f_\phi(q)) - f_l(k) f_\phi(q) (1 - f_N(t, \omega)) \right). \end{aligned} \quad (3.1.13)$$

²See [27] and references therein for a detailed discussion of the wash-out processes.

notice the minus sign difference between equations (3.1.12) and (3.1.13). In both equations we defined the CP violating parameter ϵ

$$\epsilon_{ii} \left(|\mathcal{M}(N \rightarrow l\phi)|^2 + |\mathcal{M}(N \rightarrow \bar{l}\bar{\phi})|^2 \right) = |\mathcal{M}(N \rightarrow l\phi)|^2 - |\mathcal{M}(N \rightarrow \bar{l}\bar{\phi})|^2 . \quad (3.1.14)$$

The CP-violating parameter comes from the difference from the off-diagonal terms of the coupling. There is no asymmetry at initial times, hence we have the initial condition

$$f_{Li}(0, k) = 0 . \quad (3.1.15)$$

Since the Boltzmann equation is a first order differential equation, only one initial condition is required. Using equation (3.1.9) and (3.1.15), one obtains for the lepton asymmetry

$$f_{Li}(t, k) = -\epsilon_{ii} \frac{1}{k} \int_{\mathbf{q}, \mathbf{p}} (2\pi)^4 \delta^4(k + q - p) p \cdot k f_{l\phi}(k, q) f_N^{eq}(\omega) \frac{1}{\Gamma} (1 - e^{-\Gamma t}) , \quad (3.1.16)$$

where

$$\epsilon_{ij} = \frac{3\text{Im}\{\lambda_{i1}^*(\eta\lambda^*)_{j1}\}M}{16\pi} . \quad (3.1.17)$$

Summing over all flavours, the generated asymmetry is proportional to the familiar CP-asymmetry: $\epsilon = \sum_i \epsilon_{ii} / (\lambda^\dagger \lambda)_{11} = 3\text{Im}(\lambda^\dagger \eta \lambda) M / (16\pi (\lambda^\dagger \lambda)_{11})$ [73]. For later comparison with the solutions of the Kadanoff-Baym equations, it is convenient to rewrite (3.1.16) in the form

$$f_{Li}(t, k) = -\epsilon_{ii} \frac{16\pi}{k} \int_{\mathbf{q}, \mathbf{p}, \mathbf{q}', \mathbf{k}'} k \cdot k' \times (2\pi)^4 \delta^4(k + q - p) (2\pi)^4 \delta^4(k' + q' - p) \\ \times f_{l\phi}(k, q) f_N^{eq}(\omega) \frac{1}{\Gamma} (1 - e^{-\Gamma t}) . \quad (3.1.18)$$

Note that the integrand is now proportional to the averaged matrix element $|\mathcal{M}(l\phi \rightarrow \bar{l}\bar{\phi})|^2 = 2k \cdot k' (\lambda^\dagger \lambda)_{11} / M^2$ (cf. [73]), which involves the product of the 4-vectors k and k' . At low temperatures, $T \ll M$, the integrand falls off like $e^{-\beta\omega} < e^{-\beta M}$, i.e., the generated lepton asymmetry is strongly suppressed.

3.2 Quantum formalism

A full quantum description of leptogenesis can be obtained from the Kadanoff-Baym equations. Performing an analogous procedure as in the Boltzmann case, we need to describe the production of Majorana particle, whose decay produces the lepton asymmetry. In order to do that, we need to insert the solution of the non-equilibrium Majorana neutrino already obtained in (2.4.23) to (2.4.27) in the Kadanoff-Baym equations for leptons. This is analogous to the Boltzmann formalism, where we insert the time-dependent distribution function of the Majorana to the differential equation for the asymmetry. In the Kadanoff-Baym case, the out-of-equilibrium Majorana propagators are inserted into the CP violating self-energy, and interference with the bath will cause the generation of the asymmetry. The SM bath remains in equilibrium, but the CP violating part of the lepton self-energy is not. In this case the methods from the previous chapter cannot be applied directly. However, we are only interested in the CP violating part ‘ δS ’ and we can solve the quantum equations to leading order of δS . In order to obtain a solution to the equation, we need to explicitly calculate the self-energy, concentrating on the out-of-equilibrium part described by the Majorana propagator.

To compare our result with (3.1.18), we will not consider wash-out terms (scattering processes) and concentrate purely on the generation of the asymmetry. In a quantum approach, we will not have to subtract real intermediate states as it is commonly done in a normal Boltzmann mechanism [110]. The optical theorem gives us the advantage that we do not over-count processes. We will also see that if we consider naively only the on-shell effects, the result will suffer from the same problems as the ones obtained from Boltzmann equations.

3.2.1 Simple exemplary case

In order to know how to compare the classical Boltzmann approach and a quantum one, we need to know the functions that describe the lepton asymmetry. Let start with a simple exemplary model consisted of charged leptons with chemical potential. The number density will be then given by

$$n_L = n_l - n_{\bar{l}} = \int d^3k f_L(k) = \int d^3k (f_l(k) - f_{\bar{l}}(k)) , \quad (3.2.1)$$

where n_L is the asymmetry, n_l and $n_{\bar{l}}$ are the number densities for the leptons and anti-lepton respectively with f_l and $f_{\bar{l}}$ their distribution functions. In equilibrium, with chemical potential, the distribution functions are given by

$$f_l(k) = \frac{1}{e^{\beta(k-\mu)} + 1} , \quad (3.2.2)$$

$$f_{\bar{l}}(k) = \frac{1}{e^{\beta(k+\mu)} - 1} . \quad (3.2.3)$$

For large temperatures ($\beta\mu \ll 1$) we can expand the last equations

$$f_l(k) \simeq \frac{1}{e^{\beta k} + 1} + \frac{1}{(e^{\beta k} + 1)^2} \beta\mu + \dots, \quad (3.2.4)$$

$$\simeq f_0 + f_0^2 \beta\mu + \dots, \quad (3.2.5)$$

$$f_{\bar{l}}(k) \simeq \frac{1}{e^{\beta k} + 1} - \frac{1}{(e^{\beta k} + 1)^2} \beta\mu + \dots, \quad (3.2.6)$$

$$\simeq f_0 - f_0^2 \beta\mu + \dots, \quad (3.2.7)$$

where f_0 is the equilibrium distribution function without chemical potential. The asymmetry will be given by

$$f_L^{eq} = f_l(k) - f_{\bar{l}}(k) \simeq 2f_0^2 \beta\mu, \quad (3.2.8)$$

which will vanish in the absence of chemical potential. In order to compare this result with the one obtained from thermal field theory, we need to consider the definition of the propagators in a thermal bath [79]. Let start with the equilibrium thermal-propagator in momentum space $S^>(k)$

$$iS^>(k) = 2\pi(1 - f_l(k))\epsilon(k_0)\not{P}_L\delta(k^2), \quad (3.2.9)$$

$$= 2\pi(\theta(k_0)(1 - f_l(k)) - \theta(-k_0)(1 - f_l(-k)))\not{P}_L\delta(k^2), \quad (3.2.10)$$

where $\delta(k^2) = \frac{1}{2k}(\delta(k_0 - k) + \delta(k_0 + k))$. Equation (3.2.9) can be rewritten by using the fact that $1 - f(-k) \equiv \bar{f}(k)$

$$iS^>(k) = 2\pi(\theta(k_0) - \theta(k_0)f(k) - \theta(-k_0)\bar{f}(k))\not{P}_L\delta(k^2). \quad (3.2.11)$$

The same can be applied to $S^<(k)$

$$iS^<(k) = 2\pi(\theta(-k_0) - \theta(k_0)f(k) - \theta(-k_0)\bar{f}(k))\not{P}_L\delta(k^2). \quad (3.2.12)$$

Lets calculate $S_{\mathbf{k}}^+(t)$, by definition we have

$$S^+(k) = \frac{1}{2}(S^>(k) + S^<(k)), \quad (3.2.13)$$

or in mix-representation

$$\begin{aligned} S_{\mathbf{k}}^+(t) &= \frac{1}{2} \int dk_0 e^{-ik_0 t} (S^>(k) + S^<(k)), \quad (3.2.14) \\ &= \int dk_0 \left(\frac{1}{2}(\theta(k_0) + \theta(-k_0)) - \theta(k_0)f(k) - \theta(-k_0)\bar{f}(k) \right) \not{P}_L\delta(k^2). \end{aligned}$$

After some algebra we obtain

$$\begin{aligned}
S_{\mathbf{k}}^+(t) = & \left(-\frac{i}{2}\gamma^0 \sin(kt) - \frac{1}{2k}\mathbf{k}\gamma \cos(kt) \right. \\
& + \frac{i}{2}\gamma^0 \sin(kt)(f(k) + \bar{f}(k)) - \frac{1}{2}\gamma^0 \cos(kt)(f(k) - \bar{f}(k)) \\
& \left. + \frac{1}{2}\mathbf{k}\gamma \cos(kt)(f(k) + \bar{f}(k)) - \frac{i}{2}\mathbf{k}\gamma \sin(kt)(f(k) - \bar{f}(k)) \right) P_L . \quad (3.2.15)
\end{aligned}$$

We can expand the above result for large temperatures in order to get

$$\begin{aligned}
S_{\mathbf{k}}^+(t) \approx & \left(-\frac{i}{2}\sin(kt) - \frac{1}{2k}\mathbf{k}\gamma \cos(kt) \right) (1 - 2f_0(k)) P_L \\
& - (\gamma^0 \cos(kt) + \frac{i}{k}\mathbf{k}\gamma \sin(kt)) f_0^2 \beta \mu P_L + \mathcal{O}((\beta\mu)^2) , \quad (3.2.16)
\end{aligned}$$

again $f_0(k) = (e^{\beta k} + 1)^{-1}$. If we take a equilibrium bath, i.e. time independent, we can set $t \rightarrow 0$. Multiplying by γ_0 and taking the trace gives

$$tr(\gamma^0 S_{\mathbf{k}}^+(0)) = -2f_0^2 \beta \mu + \mathcal{O}((\beta\mu)^2) , \quad (3.2.17)$$

which is the same result as the one in (3.2.8) only differing by a global minus sign. For a time dependent bath, we get an asymmetry

$$L_{\mathbf{k}}(t) = -tr(\gamma^0 S_{\mathbf{k}}^+(t)) , \quad (3.2.18)$$

$$= i \sin(kt)(1 - f(k) - \bar{f}(k)) - \cos(kt)(f(k) - \bar{f}(k)) . \quad (3.2.19)$$

In this simple model, for vanishing chemical potential the $k = 0$ mode also vanishes.

3.2.2 Kadanoff-Baym equations for leptons

After the identification of the proper quantity that describes the asymmetry in quantum field theory, we are able now to proceed to a real leptogenesis model. In order to do so, we need to write the Kadanoff-Baym equations for leptons with a CP violating self-energy. The introduction of the non-equilibrium Majorana neutrino inside the two-loop Feynman diagram leads to a non-equilibrium self-energy with no time-translational invariance. In order to solve this equations, a decomposition of the equilibrium and non-equilibrium parts of the self-energies and propagators is needed. As a difference with respect to Chapter 2, where the kinetics of non-equilibrium particles were described by the decay width, and no further knowledge of the self energy was needed (only its Lorentz structure)³, the exact calculation of the self energy is required. The results will be compare to the Boltzmann formalism.

Solution for the spectral function for leptons

In order to calculate the asymmetry generated in a quantum formalism, solving the first equation is not necessary, but an analysis is made for completeness. Let us now start

³In this case the bath is always time-translational invariant.

with the first Kadanoff-Baym equation for the a massless lepton

$$(i\gamma_0\partial_1 - \mathbf{k}\gamma) S_{\mathbf{k}}^-(t_1, t_2)P_L + \int_{t_2}^{t_1} \Pi_{\mathbf{k}}^-(t_1, t')S_{\mathbf{k}}^-(t', t_2)P_L = 0 , \quad (3.2.20)$$

here P_L is the left handed chiral projector, which we can be drop for the rest of the section. In the following we will also drop the index ‘ \mathbf{k} ’ for convenience. Since Π is not time translation invariant, S^- is not either. However, one can decompose Π into a part that comes from standard model interactions and a part from the interaction with the heavy Majorana neutrinos.

$$\Pi^-(t_1, t_2) = \Pi_{SM}^-(t_1 - t_2) + \Pi_N^-(t_1, t_2) . \quad (3.2.21)$$

The standard model part is in equilibrium, therefore it is time translation invariant and obeys the KMS condition. We can define S_{eq}^- as the solution to (3.2.20) for $\Pi_N^-(t_1, t_2) = 0$. As proven in the scalar case, for a time translational self-energy also S^- is time translation invariant, therefore $S_{eq}^-(t_1, t_2) = S_{eq}^-(t_1 - t_2)$. One can then define δS^- by

$$S^-(t_1, t_2) = S_{eq}^-(t_1 - t_2) + \delta S^-(t_1, t_2) . \quad (3.2.22)$$

Inserting the decompositions for Π^- and S^- into (3.2.20) and using the fact that S_{eq}^- fulfills (3.2.20) with Π_{SM}^- , one can write an equation for δS^- :

$$(i\gamma_0\partial_1 - \mathbf{k}\gamma) \delta S^-(t_1, t_2) = - \int_{t_2}^{t_1} dt' (\Pi_{SM}^-(t_1 - t')\delta S^-(t', t_2) + \Pi_N^-(t_1, t')S_{eq}^-(t' - t_2) + \Pi_N^-(t_1, t')\delta S^-(t', t_2)) , \quad (3.2.23)$$

S_{eq}^- can be computed in the same way as G^- in Sec. 2 and is given by

$$S_{eq}^-(y) = \int_{-\infty}^{\infty} \frac{d\omega}{2\pi} e^{-i\omega y} \left(\frac{1}{\not{k} - \Pi_{SM}^R(\omega)} - \frac{1}{\not{k} - \Pi_{SM}^A(\omega)} \right) , \quad (3.2.24)$$

where the 4-momentum $k_\mu = (\omega, \mathbf{k})$. Due to the smallness of the neutrino Yukawa coupling λ , one has

$$\Pi_{SM} \gg \Pi_N . \quad (3.2.25)$$

and consequently

$$S_{eq} \gg \delta S , \quad (3.2.26)$$

which allows to drop the $\Pi_N^-(t_1, t')\delta S^-(t', t_2)$ term. One can then rewrite (3.2.23) as

$$(i\gamma_0\partial_1 - \mathbf{k}\gamma) \delta S^-(t_1, t_2) + \int_{t_2}^{t_1} dt' \Pi_{SM}^-(t_1 - t')\delta S^-(t', t_2) = \zeta(t_1, t_2) . \quad (3.2.27)$$

The source term ζ does not depend on δS^- and is given by the known functions

$$\zeta(t_1, t_2) = - \int_{t_2}^{t_1} \Pi_N(t_1, t')S_{eq}^-(t' - t_2) . \quad (3.2.28)$$

The solution of this equation is given

$$\delta S^- = \delta \hat{S}^- + \delta S_{mem}^- , \quad (3.2.29)$$

where $\delta \hat{S}^-$ is the solution to the homogenous equation that can be obtained from (3.2.27) by setting $\zeta = 0$. $\delta \hat{S}^-$ is time translation invariant because the self-energy is time translation invariant (see scalar case). The equation to be solved is the same as for S_{eq}^- so we easily get $\delta \hat{S}^- = S_{eq}^-$. Then the complete solution for S^- is given by

$$S^-(t_1, t_2) = c_L S_{eq}^-(t_1 - t_2) + \delta S_{mem}^-(t_1, t_2) , \quad (3.2.30)$$

with

$$S_{mem}^-(t_1, t_2) = \int_{t_2}^{t_1} dt' \delta S_{eq}^-(t_1 - t') \zeta(t', t_2) , \quad (3.2.31)$$

as can be proven by insertion. Here c_L is a coefficient that is fixed to $c_L = 1$ by the initial conditions which follow from the anti-commutation relations for fermions. The standard model part to the lepton self-energy Π_{SM} , has to be computed at finite temperature. Since the temperatures during leptogenesis are far above the electroweak scale this computation cannot be done perturbatively due to the known breakdown of perturbation theory at high temperatures. An estimate could be made by using a hard thermal loop resummation or an exact result for given temperature could be found using lattice gauge theory. For the moment we will keep it as a function that is in principle known.

Solution for the statistical propagator for leptons

From Sec. 3.2.1 we know that the statistical propagator give us the desired asymmetry. The Kadanoff-Baym equation for the statistical propagator is given by

$$(i\gamma^0 \partial_{t_1} - \mathbf{k}\gamma) S_{\mathbf{k}ij}^+(t_1, t_2) = - \int_0^{t_2} dt' \Pi_{\mathbf{k}ij}^+(t_1, t') S_{\mathbf{k}ij}^-(t', t_2) + \int_0^{t_1} dt' \Pi_{\mathbf{k}ij}^-(t_1, t') S_{\mathbf{k}ij}^+(t', t_2) , \quad (3.2.32)$$

Where again we can see that the self-energies are non time translational invariant. If the initial correlations are non-Gaussian, an additional term $\mathcal{O}[S_{in}, \Pi_{in}]$ should be added to eq. (3.2.32) [111]. This term will vanish when we calculate the asymmetry of the system, due to the fact that we assume no asymmetry as an initial condition, i.e. from the deviation of the equilibrium propagator. This deviation is always Gaussian. Following the procedure from the last section, we can decompose the self-energy and the propagator in an equilibrium and non-equilibrium part

$$S_{\mathbf{k}ij}^\pm(t_1, t_2) = S_{\mathbf{k}ij}^{\pm,eq}(t_1 - t_2) + \delta S_{\mathbf{k}ij}^\pm(t_1, t_2) , \quad (3.2.33)$$

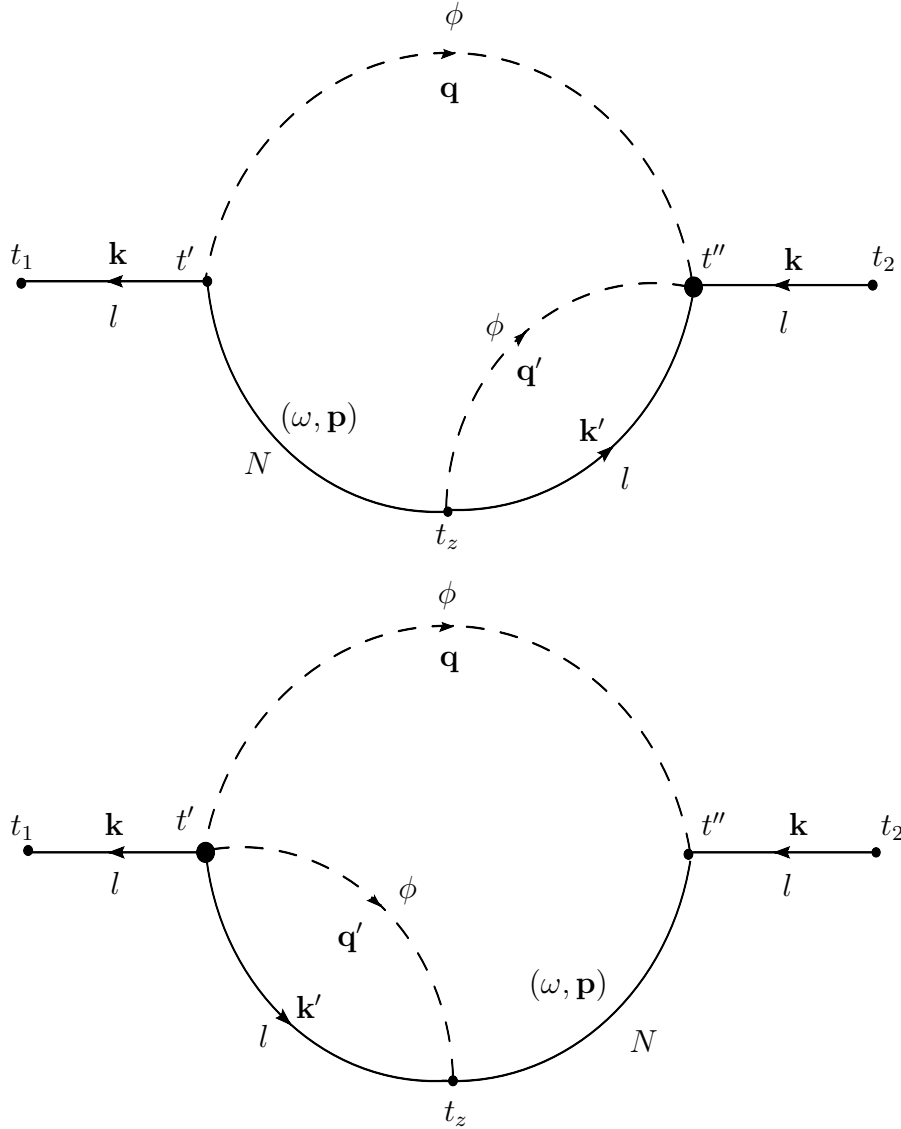


Figure 3.3: Two-loop contributions to the lepton self-energies $\Pi_{\mathbf{k}}^{\pm}$, which leads to a non-zero lepton number asymmetry.

as well as the decomposition of the self-energy between the SM and the Majorana contribution

$$\Pi_{\mathbf{k}ij}^{\pm}(t_1, t_2) = \Pi_{\mathbf{k}ij}^{\pm, \text{SM}}(t_1 - t_2) + \delta\Pi_{\mathbf{k}ij}^{\pm}(t_1, t_2). \quad (3.2.34)$$

In this way we get

$$\begin{aligned} (i\gamma_0\partial_{t_1} - \mathbf{k}\gamma) \delta S_{\mathbf{k}ij}^+(t_1, t_2) &= \int_0^{t_1} dt' \Pi_{\mathbf{k}ij}^-, \text{SM}(t_1 - t') \delta S_{\mathbf{k}ij}^+(t', t_2) \\ &= \zeta_{\mathbf{k}ij}^1(t_1, t_2) + \zeta_{\mathbf{k}ij}^2(t_1, t_2) + \zeta_{\mathbf{k}ij}^3(t_1, t_2), \end{aligned} \quad (3.2.35)$$

where the term $\delta S^+ \delta \Pi^-$ was dropped. This can be understood by assuming that the leptons are close to equilibrium. This fact does not imply that the Majorana neutrinos

are close to equilibrium too. The l.h.s. of equation (3.2.35) is the homogenous solution for $\delta S_{\mathbf{k}ij}^+$, and the sources are given by

$$\zeta_{\mathbf{k}ij}^1(t_1, t_2) = \int_0^{t_1} dt' \delta \Pi_{\mathbf{k}ij}^-(t_1, t') S_{\mathbf{k}ij}^{+,eq}(t' - t_2), \quad (3.2.36)$$

$$\zeta_{\mathbf{k}ij}^2(t_1, t_2) = - \int_0^{t_2} dt' \delta \Pi_{\mathbf{k}ij}^+(t_1, t') S_{\mathbf{k}ij}^{-,eq}(t' - t_2), \quad (3.2.37)$$

and

$$\zeta_{\mathbf{k}ij}^3(t_1, t_2) = - \int_0^{t_2} dt' \Pi_{\mathbf{k}ij}^{+,SM}(t_1 - t') \delta S_{\mathbf{k}ij}^-(t', t_2). \quad (3.2.38)$$

Standard model corrections should not be neglected. However, the determination of these corrections at high temperatures is a non-trivial task. At high T perturbation theory breaks down and the quasi-particle spectrum cannot be determined. In order to compare with the Boltzmann equation and the literature (where also SM correction are neglected) we drop the terms Π_{SM} , this will make all the equilibrium propagators besides the Majorana propagator in (3.2.35) and inside the self-energy Π to become the free propagator ($S^{eq} \rightarrow \hat{S}$, $\Delta^{eq} \rightarrow \Delta^F$). Therefore the source term ζ^3 will drop out. The solution to (3.2.35) is then

$$\begin{aligned} \delta S_{\mathbf{k}ij}^+(t_1, t_2) = & + \int_0^{t_1} dt' \int_0^{t_2} dt'' S_{\mathbf{k}ij}^{-,F}(t_1 - t') \delta \Pi_{\mathbf{k}ij}^+(t', t'') S_{\mathbf{k}ij}^{-,F}(t'' - t_2) \\ & - \int_0^{t_1} dt' \int_0^{t'} dt'' S_{\mathbf{k}ij}^{-,F}(t_1 - t') \delta \Pi_{\mathbf{k}ij}^-(t', t'') S_{\mathbf{k}ij}^{+,F}(t'' - t_2) \\ & + C_{\mathbf{k}}(t_1, t_2), \end{aligned} \quad (3.2.39)$$

where $C_{\mathbf{k}}(t_1, t_2)$ is a function that only depends on t_2 and vanishes when the differential operator is applied⁴

$$(i\gamma_0 \partial_{t_1} - \mathbf{k}\gamma) C_{\mathbf{k}}(t_1, t_2) = 0. \quad (3.2.40)$$

One big difference with Chapter 2, is that we now have two source terms ζ_1 and ζ_2 . The source ζ_2 can be treated in the same way as in Chapter 2, giving us the first line of (3.2.39), meanwhile ζ_1 needs to be treated differently. This difference comes from the fact that the limits of integration of the source η_1 goes from 0 to t_1 , which will give us the second line in (3.2.39). In order to this solution to have the right symmetries described in Appendix A.3, the function $C_{\mathbf{k}}(t_1, t_2)$ must be

$$C_{\mathbf{k}}(t_1, t_2) = - \int_0^{t_2} dt'' \int_0^{t''} dt' S_{\mathbf{k}ij}^{+,F}(t_1 - t'') \delta \Pi_{\mathbf{k}ij}^-(t'', t') S_{\mathbf{k}ij}^{-,F}(t' - t_2). \quad (3.2.41)$$

⁴Remember that $(i\gamma_0 \partial_{t_1} - \mathbf{k}\gamma) S_{\mathbf{k}ij}^{\pm,F}(t_1 - t_2) = 0$.

A final decomposition can be made, since the asymmetry is generated from the non-equilibrium part of the Majorana propagator only. Therefore we can separate one more time the self energy $\delta\Pi$

$$\delta\Pi_{\mathbf{k}ij}^-(t'', t') = \delta\Pi_{\mathbf{k}ij}^{-,eq}(t'' - t') + \delta\tilde{\Pi}_{\mathbf{k}ij}^-(t'', t') , \quad (3.2.42)$$

where $\delta\Pi_{\mathbf{k}ij}^{-,eq}(t'' - t')$ comes from the equilibrium part of the Majorana propagator, and $\delta\tilde{\Pi}_{\mathbf{k}ij}^-(t'', t')$ from the non-equilibrium part. This decomposition will allow us to define the departure of equilibrium of δS^+

$$\delta\tilde{S}_{\mathbf{k}ij}^+(t_1, t_2) = \delta S_{\mathbf{k}ij}^+(t_1, t_2) - \delta S_{\mathbf{k}ij}^{+,eq}(t_1 - t_2) , \quad (3.2.43)$$

which will finally give us the solution for the asymmetry to be

$$\begin{aligned} \delta\tilde{S}_{\mathbf{k}ij}^+(t_1, t_2) = & + \int_0^{t_1} dt' \int_0^{t_2} dt'' S_{\mathbf{k}ij}^{-,F}(t_1 - t') \delta\tilde{\Pi}_{\mathbf{k}ij}^+(t', t'') S_{\mathbf{k}ij}^{-,F}(t'' - t_2) \\ & - \int_0^{t_1} dt' \int_0^{t'} dt'' S_{\mathbf{k}ij}^{-,F}(t_1 - t') \delta\tilde{\Pi}_{\mathbf{k}ij}^-(t', t'') S_{\mathbf{k}ij}^{+,F}(t'' - t_2) \\ & - \int_0^{t_2} dt'' \int_0^{t''} dt' S_{\mathbf{k}ij}^{+,F}(t_1 - t'') \delta\tilde{\Pi}_{\mathbf{k}ij}^-(t'', t') S_{\mathbf{k}ij}^{-,F}(t' - t_2) . \end{aligned} \quad (3.2.44)$$

The self-energy $\tilde{\Pi}$ will be only computed with the non-equilibrium part of the Majorana propagator, i.e. the term which depends on the center of mass coordinate.

3.2.3 Asymmetry from the quantum formalism

According to equation (3.2.18), the correlator S^+ is proportional to the asymmetry. We can define a ‘lepton number matrix’ from the statistical propagator of the lepton fields,

$$L_{\mathbf{k}ij}(t_1, t_2) = -\text{tr}[\gamma^0 \tilde{S}_{\mathbf{k}ij}^+(t_1, t_2)] . \quad (3.2.45)$$

For free fields in equilibrium we have seen that this is proportional to $L_{\mathbf{k}ii}|_{t_1=t_2} = f_{li}(k) - \bar{f}_{li}(k)$, which vanishes for zero chemical potential. To leading order in λ , a flavour non-diagonal asymmetry is generated by the two-loop self-energies shown in Fig. 3.3 (cf. [73]). Using the solution of the Kadanoff-Baym equation for $\tilde{S}_{\mathbf{k}}^+$ in (3.2.44) to first order in the self-energy $\tilde{\Pi}_{\mathbf{k}}^\pm$, one finds after some algebra

$$\begin{aligned} L_{\mathbf{k}ij}(t, t) = & -i \int_0^t dt' \int_0^t dt'' \text{tr} [S_{\mathbf{k}}^{F,+}(t'' - t') \delta\tilde{\Pi}_{\mathbf{k}ij}^-(t', t'') \\ & - S_{\mathbf{k}}^{F,-}(t'' - t') \delta\tilde{\Pi}_{\mathbf{k}ij}^+(t', t'')] . \end{aligned} \quad (3.2.46)$$

Let start by looking at $\delta\tilde{\Pi}_{\mathbf{k}}^+$, which is defined by

$$\delta\tilde{\Pi}_{\mathbf{k}ij}^+(t', t'') = \frac{1}{2} [\delta\tilde{\Pi}_{\mathbf{k}ij}^>(t', t'') + \delta\tilde{\Pi}_{\mathbf{k}ij}^<(t', t'')] , \quad (3.2.47)$$

with

$$\delta\tilde{\Pi}_{\mathbf{k}ij}^>(t', t'') = i\tilde{\lambda}_{ij}\tilde{\Pi}_{\mathbf{k}(1)}^>(t', t'') + i\tilde{\lambda}_{ij}^*\tilde{\Pi}_{\mathbf{k}(2)}^>(t', t'') , \quad (3.2.48)$$

$$\delta\tilde{\Pi}_{\mathbf{k}ij}^<(t', t'') = i\tilde{\lambda}_{ij}\tilde{\Pi}_{\mathbf{k}(1)}^<(t', t'') + i\tilde{\lambda}_{ij}^*\tilde{\Pi}_{\mathbf{k}(2)}^<(t', t'') . \quad (3.2.49)$$

The subindices (1) and (2) represents each 2-loop diagram from Figure 3.3. Notice that we extracted the coupling λ and the imaginary number from the self-energies (see Appendix C.4). Expanding the self-energies showing explicitly the Lorentz structure gives

$$\tilde{\Pi}_{\mathbf{k}(1,2)}^{\geq}(t', t'') = \tilde{\Pi}_{\mathbf{k}(1,2)}^{\geq 0}(t', t'')\gamma_0 + \tilde{\Pi}_{\mathbf{k}(1,2)}^{\geq j}(t', t'')\gamma_j . \quad (3.2.50)$$

We can use the following properties for the propagators

$$S_{\mathbf{k}}^{F,11}(y) = (S_{\mathbf{k}}^{F,22}(-y))^* , \quad (3.2.51)$$

$$S_{\mathbf{k}}^{F,>}(y) = (S_{\mathbf{k}}^{F,<,0}(-y))^*\gamma_0 - (S_{\mathbf{k}}^{F,<,i}(-y))^*\gamma_i , \quad (3.2.52)$$

$$\Delta_{\mathbf{q}}^{F,11}(y) = (\Delta_{\mathbf{q}}^{F,22}(-y))^* , \quad (3.2.53)$$

$$\Delta_{\mathbf{q}}^{F,>}(y) = (\Delta_{\mathbf{q}}^{F,<}(y))^* , \quad (3.2.54)$$

and using also the following property for the scalar part of the Majorana propagator

$$G_{S\mathbf{p}}(y) = (G_{S\mathbf{p}}(-y))^* , \quad (3.2.55)$$

we get a relation between $\tilde{\Pi}_{\mathbf{k}(1,2)}^>$ with $\tilde{\Pi}_{\mathbf{k}(1,2)}^<$:

$$\tilde{\Pi}_{\mathbf{k}(1,2)}^<(t', t'') = [\tilde{\Pi}_{\mathbf{k}(1,2)}^>0(t', t'')]^*\gamma_0 - [\tilde{\Pi}_{\mathbf{k}(1,2)}^>j(t', t'')]^*\gamma_j . \quad (3.2.56)$$

Using the above properties we can also obtain a relation between the first diagram $\tilde{\Pi}_{(1)}$ and the second one $\tilde{\Pi}_{(2)}$

$$\tilde{\Pi}_{\mathbf{k}(2)}^>(t', t'') = -[\tilde{\Pi}_{\mathbf{k}(1)}^>(t'', t')]^* . \quad (3.2.57)$$

Introducing Eqs. (3.2.56) and (3.2.57) in (3.2.47), we obtain an expression for $\delta\tilde{\Pi}^+$ that only depends on the first diagram of figure 3.3.

$$\begin{aligned} \delta\tilde{\Pi}_{\mathbf{k}ij}^+(t', t'') = & - \tilde{\lambda}_{ij}[\text{Re}\tilde{\Pi}_{\mathbf{k}(1)}^>0(t', t'')\gamma_0 + i\text{Im}\tilde{\Pi}_{\mathbf{k}(1)}^>j(t', t'')\gamma_j] \\ & + \tilde{\lambda}_{ij}^*[\text{Re}\tilde{\Pi}_{\mathbf{k}(1)}^>0(t'', t')\gamma_0 - i\text{Im}\tilde{\Pi}_{\mathbf{k}(1)}^>j(t'', t')\gamma_j] . \end{aligned} \quad (3.2.58)$$

In the same way we obtain for $\delta\tilde{\Pi}_{\mathbf{k}ij}^- (t', t'') = i[\delta\tilde{\Pi}_{\mathbf{k}ij}^>(t', t'') - \delta\tilde{\Pi}_{\mathbf{k}ij}^<(t', t'')]$

$$\begin{aligned} \delta\tilde{\Pi}_{\mathbf{k}ij}^-(t', t'') = & - 2\tilde{\lambda}_{ij}[i\text{Im}\tilde{\Pi}_{\mathbf{k}(1)}^>0(t', t'')\gamma_0 + \text{Re}\tilde{\Pi}_{\mathbf{k}(1)}^>j(t', t'')\gamma_j] \\ & + 2\tilde{\lambda}_{ij}^*[i\text{Im}\tilde{\Pi}_{\mathbf{k}(1)}^>0(t'', t')\gamma_0 - \text{Re}\tilde{\Pi}_{\mathbf{k}(1)}^>j(t'', t')\gamma_j] . \end{aligned} \quad (3.2.59)$$

Inserting $\delta\tilde{\Pi}^\pm$ to (3.2.46), and remembering that

$$S_{\mathbf{k}}^{F,-}(y) = \left(i\gamma_0 \cos(ky) - \left(\frac{\mathbf{k}\gamma}{k} \right) \sin(ky) \right) P_L , \quad (3.2.60)$$

$$S_{\mathbf{k}}^{F,+}(y) = -\frac{\tanh\left(\frac{\beta k}{2}\right)}{2} \left(i\gamma_0 \sin(ky) + \left(\frac{\mathbf{k}\gamma}{k}\right) \cos(ky) \right) P_L, \quad (3.2.61)$$

we can rewrite the lepton number matrix at equal times

$$\begin{aligned} L_{\mathbf{k}ij}(t) = & 2\text{Im}[\tilde{\lambda}_{ij}] \text{tr} \int_0^t dt' \int_0^t dt'' \left\{ \cos(k(t'' - t')) \text{Re}\tilde{\Pi}_{\mathbf{k}(1)}^{>0}(t', t'') \right. \\ & + \tanh\left(\frac{\beta k}{2}\right) \sin(k(t'' - t')) \text{Im}\tilde{\Pi}_{\mathbf{k}(1)}^{>0}(t', t'') \\ & - \frac{\mathbf{k}\gamma}{k} \gamma_j \left(\sin(k(t'' - t')) \text{Im}\tilde{\Pi}_{\mathbf{k}(1)}^{>j}(t', t'') \right. \\ & \left. \left. + \tanh\left(\frac{\beta k}{2}\right) \cos(k(t'' - t')) \text{Re}\tilde{\Pi}_{\mathbf{k}(1)}^{>j}(t', t'') \right) \right\}. \end{aligned} \quad (3.2.62)$$

Notice that the symmetric part of the self-energy which are multiplied by cosine survives the integration, meanwhile the anti-symmetric part survives for those terms multiplied by sine. Inserting the exact form of the self energies in the above equation

$$\begin{aligned} L_{\mathbf{k}ij}(t) = & -\text{Im}[\tilde{\lambda}_{ij}] \int_0^t dt' \int_0^t dt'' \int_0^{t''} dt_z \int_{\mathbf{q}, \mathbf{q}'} \frac{M}{\omega} f_N^{eq}(\omega) e^{-\frac{\Gamma}{2}(t'+t_z)} \cos[\omega(t_z - t')] \\ & \times \left\{ \left(\frac{\coth\left(\frac{\beta q}{2}\right)}{2} \left(\cos[(k+q)(t'' - t')] + \cos[(k-q)(t'' - t')] \right) \right. \right. \\ & \left. \left. + \frac{\tanh\left(\frac{\beta k}{2}\right)}{2} \left(\cos[(k+q)(t'' - t')] - \cos[(k-q)(t'' - t')] \right) \right) \right. \\ & \times \left(\frac{\coth\left(\frac{\beta q'}{2}\right)}{2} \left(\cos[(k'+q')(t'' - t_z)] + \cos[(k'-q')(t'' - t_z)] \right) \right. \\ & \left. \left. + \frac{\tanh\left(\frac{\beta k'}{2}\right)}{2} \left(\cos[(k'+q')(t'' - t_z)] - \cos[(k'-q')(t'' - t_z)] \right) \right) \right. \\ & + \frac{\mathbf{k} \cdot \mathbf{k}'}{kk'} \left(\frac{\coth\left(\frac{\beta q}{2}\right)}{2} \left(\sin[(k+q)(t'' - t')] - \sin[(k-q)(t'' - t')] \right) \right. \\ & \left. \left. + \frac{\tanh\left(\frac{\beta k}{2}\right)}{2} \left(\sin[(k+q)(t'' - t')] + \sin[(k-q)(t'' - t')] \right) \right) \right. \\ & \times \left(\frac{\coth\left(\frac{\beta q'}{2}\right)}{2} \left(\sin[(k'+q')(t'' - t_z)] - \sin[(k'-q')(t'' - t_z)] \right) \right. \\ & \left. \left. + \frac{\tanh\left(\frac{\beta k'}{2}\right)}{2} \left(\sin[(k'+q')(t'' - t_z)] + \sin[(k'-q')(t'' - t_z)] \right) \right) \right\}. \end{aligned} \quad (3.2.63)$$

The time integration can be performed, and after taking small Γ we obtain

$$\begin{aligned}
L_{\mathbf{k}ij}(t, t) = & -\epsilon_{ij} 8\pi \int_{\mathbf{q}, \mathbf{q}'} \frac{k \cdot k'}{k k' \omega} f_{l\phi}(k, q) f_{l\phi}(k', q') f_N^{eq}(\omega) \\
& \times \frac{\frac{1}{2}\Gamma}{((\omega - k - q)^2 + \frac{\Gamma^2}{4})(\omega - k' - q')^2 + \frac{\Gamma^2}{4})} \\
& \times \left(\cos[(k + q - k' - q')t] + e^{-\Gamma t} \right. \\
& \quad \left. - e^{-\frac{\Gamma t}{2}} (\cos[(\omega - k - q)t] + \cos[(\omega - k' - q')t]) \right) \\
& + \text{combinations ,} \tag{3.2.64}
\end{aligned}$$

where $\mathbf{p} = \mathbf{q} + \mathbf{k} = \mathbf{q}' + \mathbf{k}'$. The combinations mentioned in the above equation refer to all the possible energy sign change, e.g. $\omega \rightarrow -\omega$. However, we are only interested in terms of order $1/\Gamma$, which can only be obtained in the case when $\omega \rightarrow k + q$ and $\omega \rightarrow k' + q'$, this will remove the last line of (3.2.64). This equation shows the total asymmetry as a function of time and it is the most important result of this work. Equation (3.2.64) shows the oscillatory behaviour of the off-shell contributions. For late times, the exponential will suppress part of the integral, meanwhile the one without suppression will oscillate to zero due to its fast oscillatory behaviour at late times. This fact shows that there is no asymmetry created in equilibrium. This is well known to be a problem that can appear in the naive Boltzmann approach, and needs to be cured by the ‘real intermediate state subtraction’.

Performing the integral over the momenta is not an easy task, although for short times some of the momenta can be performed analytically (by making a narrow width approximation), there is still to perform a numerical analysis. For late times, the narrow width approximation cannot be performed analytically due to fast oscillation. This oscillatory behaviour is a key issue in the difference between our full quantum treatment and the classical Boltzmann approach.

3.2.4 Comparison with Boltzmann

It is interesting to compare the diagonal elements of the lepton number matrix $L_{\mathbf{k}ij}(t, t)$ with the distribution functions $f_{Li}(t, k)$ given in (3.1.18).

As expected, the same CP asymmetries ϵ_{ii} appear, whereas the dependence of the integrands on time and temperature is different. The reason for the different temperature dependence is the fact that the matrix elements in the Boltzmann equations were calculated at zero temperature. Hence, the factor $f_{l\phi}(k', q')$ is missing in (3.1.18). Since Boltzmann equations are local in time whereas Kadanoff-Baym equations contain ‘memory effects’, the different time dependence of the asymmetries is also expected. One consequence is that $\partial_t f_{Li}(t, k)|_{t=0} \neq 0$, whereas $\partial_t L_{\mathbf{k}ij}(t, t)|_{t=0} = 0$. Particularly important are off-shell effects in (3.2.64), which lead to terms oscillating in time.

It is instructive to consider the approximations, even if they might not be justified, which lead from (3.2.64) to the result of the Boltzmann equations. Neglecting off-shell effects, i.e., imposing $\omega = k + q = k' + q'$, the cosines are replaced by one; performing then the zero-width approximation $\Gamma \rightarrow 0$, with Γt fixed, the integral (3.2.64) becomes

$$\begin{aligned}
L_{\mathbf{k}ij}^{os}(t, t) &= -\epsilon_{ij} \frac{16\pi}{k} \int_{\mathbf{q}, \mathbf{q}', \mathbf{p}, \mathbf{k}'} k \cdot k' \\
&\times (2\pi)^4 \delta^4(k + q - p) (2\pi)^4 \delta^4(k' + q' - p) \\
&\times f_{l\phi}(k, q) f_{l\phi}(k', q') f_N^{eq}(\omega) \\
&\times \frac{1}{\Gamma} \left(1 - e^{-\frac{\Gamma t}{2}}\right)^2.
\end{aligned} \tag{3.2.65}$$

Except for the factor $f_{l\phi}(k', q')$, the only difference compared to the solution (3.1.18) of the Boltzmann equations is the time dependence. It is obvious from Figure 2 and equation (3.2.46) that in the quantum theory the generation of the lepton asymmetry is nonlocal in time. This leads to the square of the exponential fall-off in (3.2.65). On the contrary, in the Boltzmann equations the asymmetry is generated locally in time yielding a simple exponential behaviour. The difference can be numerically important at cosmologically relevant times $t_L \sim 1/\Gamma$.

3.3 Introducing SM widths

The calculations leading to equation (3.2.64) also demonstrate that the result for the lepton asymmetry will be significantly modified by the thermal damping rates for lepton and Higgs fields in the plasma. These thermal widths (cf. [112]) are known to be much larger than the decay width of the Majorana neutrino: $\Gamma_l \sim \Gamma_\phi \sim g^4 T \gg \lambda^2 M$ for $M \lesssim T$. For quantum interferences the thermal damping rates are qualitatively more important than thermal masses which, for simplicity, we ignore in the following. Including naively thermal widths for lepton and Higgs fields in the propagators⁵

$$\begin{aligned}
\Delta_{\mathbf{q}}^-(y) &= \frac{1}{q} \sin(qy) e^{-\frac{\Gamma_\phi |y|}{2}}, \\
\Delta_{\mathbf{q}}^+(y) &= \frac{1}{2q} \coth\left(\frac{\beta q}{2}\right) \cos(qy) e^{-\frac{\Gamma_\phi |y|}{2}}, \\
S_{\mathbf{k}}^-(y) &= \left(i\gamma_0 \cos(ky) + \frac{M - \mathbf{k}\gamma}{k} \sin(\omega_{\mathbf{k}} y)\right) e^{-\frac{\Gamma_l |y|}{2}}, \\
S_{\mathbf{k}}^+(y) &= -\frac{\tanh\left(\frac{\beta k}{2}\right)}{2} \left(i\gamma_0 \sin(ky) - \frac{M - \mathbf{k}\gamma}{k} \cos(ky)\right) e^{-\frac{\Gamma_l |y|}{2}},
\end{aligned}$$

and then insert them into the self-energy $\Pi_{\mathbf{k}}^+$, one obtains instead of (3.2.64) to leading order in these widths ($\Gamma_{l\phi} = \Gamma_l + \Gamma_\phi$)

⁵For a full list see Appendix D.

$$\begin{aligned}
\tilde{L}_{\mathbf{k}ij}(t, t) &= -\epsilon_{ij} 16\pi \int_{\mathbf{q}, \mathbf{q}'} \frac{k \cdot k'}{k k' \omega} \\
&\times \frac{\frac{1}{4}\Gamma_l \Gamma_\phi}{((\omega - k - q)^2 + \frac{1}{4}\Gamma_l^2)((\omega - k' - q')^2 + \frac{1}{4}\Gamma_\phi^2)} \\
&\times f_{l\phi}(k, q) f_{l\phi}(k', q') f_N^{eq}(\omega) \\
&\times \frac{1}{\Gamma} (1 - e^{-\Gamma t}). \tag{3.3.1}
\end{aligned}$$

Note that the factors oscillating in time have disappeared. The thermal widths of lepton and Higgs fields have led to a behaviour which is local in time. In the zero-width limit one now obtains the result (3.1.18) of the Boltzmann equations except for the thermal correction factor $f_{l\phi}(k', q')$. The locality of the result is obtained as a consequence of the the strong SM widths inserted in the internal lines of the self-energy (see Figure 3.4). The contributions from the Higgs and lepton propagators that are not strongly suppressed, comes when the times between these two propagators are close to each other. The only contribution that is not suppressed comes from the Majorana propagator. Figure 3.4 shows diagrammatically how the two-loop process becomes local after the insertion of SM widths, leading to a normal Boltzmann behaviour.

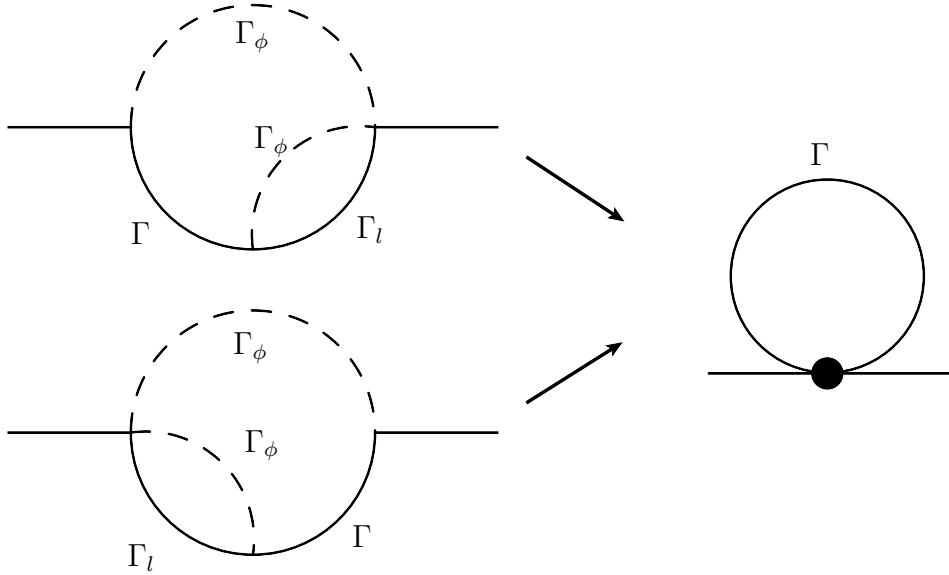


Figure 3.4: Regain of locality after the insertion of SM widths

We need to emphasize that (3.3.1) is speculative at present, and it remains to be seen whether it follows from a solid calculation which includes gauge interactions at high temperatures in a systematic way.

Chapter 4

Future work

4.1 Including expansion of the universe

The inclusion of an expanding universe must be performed in order to obtain a full theory of leptogenesis. Solving the Kadanoff-Baym equations in this scenario is a complicated task. For the production of a non-equilibrium particle there is no guarantee that the self-energy will be time-translational invariant. Moreover, a Lorentz invariant integrand will include expansion rate terms that will have severe consequences for the applicability of a Laplace transform. For example a Lorentz invariant Kadanoff-Baym equation for the spectral propagator of scalar particles in phase space can be written as [113]

$$\square\Delta^-(x_1, x_2) - \int \sqrt{-g}d^4z\Pi^R(x_1, z)\Delta^A(z, x_2) = 0, \quad (4.1.1)$$

going to momentum space

$$(\partial_{t_1}^2 + 3H(t_1)\partial_{t_1} + \frac{\mathbf{q}^2}{a^2(t_1)} + M^2)\Delta_{\mathbf{q}}^-(t_1, t_2) = - \int_{t_2}^{t_1} dt_z \frac{a^3(t_z)}{a^3(t_1)} \Pi_{\mathbf{q}}^-(t_1, t_x) \Delta_{\mathbf{q}}^-(t_z, t_2), \quad (4.1.2)$$

where $H(t)$ is the Hubble expansion rate and $a(t)$ is the scale factor. A way to proceed in order to obtain a solution of this equation is to introduce a conformal time $ad\eta = dt$ and assume quasi-equilibrium for the particles in the thermal bath. If the scale factor varies slowly in comparison to the rapid change of Π as well as Δ in the integrand, then one can assume $a^3(\eta_z)$ to behave as a constant within the integration. This will help us to solve the Kadanoff-Baym equation for the spectral function. However, developing a way to obtain the solution for the statistical propagator in such a manner can prove to be difficult. Moreover, using then this new spectral and statistical propagators to obtain a generated asymmetry will be even harder.

4.2 Wash-out terms

A second task is to include wash-out terms. This type of terms only break CP when a chemical potential is included. They are responsible for the wash-out or dilution of

the asymmetry in the thermal bath and they do not contribute to the generation of the asymmetry. As seen in the introductory Section 1.8. Wash-out terms enter the Boltzmann equations in the asymmetry differential equation

$$\frac{dN_{B-L}}{dt} = -\epsilon D(N_N - N_N^{eq}) - W N_{B-L}, \quad (4.2.1)$$

where now W must include inverse decays and scattering processes. The inclusion of the wash-out terms must be performed in the Kadanoff-Baym formalism in order to have an exact final asymmetry. A final quantitative calculation should be performed with the inclusion of these terms.

4.3 Non-perturbative regime

As we saw in Section 3.3, standard model corrections to the particles that constituted the bath have a big impact on the generated asymmetry. Due to the large coupling of the SM compared to λ , quantum interference vanishes and all off-shell effects are erased. Leading the result for the asymmetry to have a typical Boltzmann form.

However this type of thermal width inclusion is not fully justified, at high temperatures when the Imaginary part of the self energy is large enough compared to the energy of the particle, perturbation theory is broken and particles will not behave as quasi-particles. SM corrections will have then a huge impact on the equations when the temperature is of the order of the Majorana mass ($T \sim M$). There is still no knowledge about the impact of the high temperature regime for behaviour of the standard models corrections. One approach that can be performed is a hard thermal loop resummation to obtain an exact solution for the propagators. The use of Lattice techniques can also help to understand the problem [114,115], although lattice models are still being developed to simulate low temperatures observables, and the high temperature regime is still far away.

4.4 Resonant leptogenesis

Another important issue that we need to take into account is resonant leptogenesis. Here two or more of the heavy Majorana neutrinos have a degeneracy or quasi-degeneracy on the mass, for example we can consider the case where two masses are much lower than the mass of the third neutrino ($M_1, M_2 \ll M_3$) and with a degeneracy $|M_1 - M_2| \lesssim \Gamma$. We can integrate out the mass of the third massive neutrino and obtain a different effective Lagrangian. One problem comes from the fact that now the self energy has a matrix flavour 2×2 matrix structure (consequently the solution for the propagators will have a matrix structure too), so its inverse generates a more complicated solution. Although a general inverse can be found (see Appendix C.1) for the non-equilibrium Majorana propagators, it is easier to see that when we include this propagators on the leptonic Kadanoff-Baym equations, the asymmetry generated will only depend on the mixture between the diagonal part of the non-equilibrium Majorana propagators. The

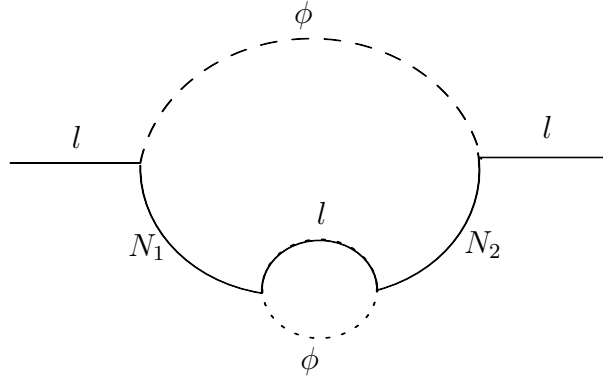


Figure 4.1: Self-energy for the production of the lepton asymmetry.

shape of the diagonal propagators have the same form as those in (2.4.23) but with different masses and decay widths. For example, the statistical propagator for both diagonal terms will be

$$G_{11\mathbf{p}}^+(y, t) = - \left(i\gamma_0 \sin(\omega_{\mathbf{p}}y) - \frac{M_1 - \mathbf{p}\gamma}{\omega_{\mathbf{p}}} \cos(\omega_{\mathbf{p}}y) \right) \times \left(\frac{\tanh\left(\frac{\beta\omega_{\mathbf{p}}}{2}\right)}{2} e^{-\Gamma_1|y|/2} + f_N^{eq}(\omega_{\mathbf{p}}) e^{-\Gamma_1 t} \right) C^{-1}, \quad (4.4.1)$$

$$G_{22\mathbf{q}}^+(y, t) = - \left(i\gamma_0 \sin(\omega_{\mathbf{q}}y) - \frac{M_2 - \mathbf{q}\gamma}{\omega_{\mathbf{q}}} \cos(\omega_{\mathbf{q}}y) \right) \times \left(\frac{\tanh\left(\frac{\beta\omega_{\mathbf{q}}}{2}\right)}{2} e^{-\Gamma_2|y|/2} + f_N^{eq}(\omega_{\mathbf{q}}) e^{-\Gamma_2 t} \right) C^{-1}, \quad (4.4.2)$$

where $\omega_{\mathbf{p}} = (\mathbf{p}^2 + M_1^2)^{1/2}$ and $\omega_{\mathbf{q}} = (\mathbf{q}^2 + M_2^2)^{1/2}$ are the energies of the Majorana neutrinos respectively. Here Γ_1 and Γ_2 are the corresponding widths. Although these widths are in principle different, we can assume that in comparison to the masses of the Majorana neutrinos, one can always assume $\Gamma_1 = \Gamma_2$.

The asymmetry will now be calculated with the insertion of these propagators to the two-loop graphs in Fig. 4.1. This diagram has the peculiarity that it is the only one that will be inverse proportional to the resonant parameter $\Delta M = |M_1 - M_2|$ that enhances the asymmetry production. Other graphs will either not contribute to a CP asymmetry or they are not proportional to $1/\Delta M$.

Previously, resonant case has been treated at zero and finite temperature where a big emphasis on the real intermediate state subtraction is performed. One advantage from the quantum treatment, is that we do not over-count processes and no subtraction is required. One can start by looking only at the Yukawa sector of the theory, and then incorporate other interactions, in order to compare with [68–71].

Chapter 5

Conclusions

In this work we presented a systematic approach towards a quantum theory of leptogenesis, by solving the Kadanoff-Baym equations (KBEs) of motion for the Green's functions describing excitations in a plasma. The KBEs are the thermal equivalent to the Schwinger-Dyson equations, i.e. they carry all the information necessary to describe the thermal bath. The KBEs can only be solved analytically under certain conditions: either when the thermal bath is time-translational invariant or by taking a first order solution in terms of the self-energy. In the case of leptogenesis, we showed how to obtain the solution of the proper KBEs by describing the generation of excitations in a plasma and its contribution to the creation of a lepton asymmetry.

The standard description of the dynamics of leptogenesis is performed via Boltzmann equations. However, these equations suffer from the absence of quantum phenomena, such as off-shell-, memory-effects and quantum coherence. Commonly in the literature an expansion of the KBEs around equilibrium is performed in order to address this issue and to include such quantum effects. The result is a set of Boltzmann equations with improved S-matrix elements. Although it appears to be a plausible approach, a first order expansion close to equilibrium of the KBEs has a fundamental problem; it assumes a slow variation of the center of mass coordinate of the solution, and thus it ignores important quantum interference effects that arise from the created particles.

In order to fully understand the mechanics of an out-of equilibrium system, we started by studying the behaviour of a non-equilibrium toy-model composed only of scalar fields. These fields interact weakly with a strongly coupled thermal bath. We focused on the computation of the time-evolution of quantities such as the spectral and statistical propagators instead of the evolution of an ill-defined 'number density'. The solution of the KBEs for the spectral and statistical Green's functions could be found analytically because the particles contributing to the self-energy of the bath are in thermal equilibrium, i.e. the back-reaction of the generated particles can be neglected. We found an important feature in this scenario: the spectral function depends only on the relative difference of space-time coordinates, which is granted by the time-invariance of the self-energy, and thus can be described with a normal Breit-Wigner spectral representation. The statistical propagator depends on the difference of coordinates

as well as on the center of mass. Therefore, it carries all the non-equilibrium information.

The fact that at $t = 0$ there are no out-of-equilibrium particles, and that the value of the statistical propagator is zero are purely coincidental. The initial condition for the statistical propagator is that of a free field propagator, which will be zero in the case of scalar fields. This fact becomes clear when non-equilibrium fermions are taken into account. Another important aspect to mention is the thermalisation and quasi-particle representation. A system that is out-of-equilibrium does not have a well defined particle number density. We showed that even in equilibrium after thermalisation, a vacuum energy contribution to the total energy of the system appears when a quasi-particle picture is performed.

The study of non-equilibrium fermions was performed in a similar way as for scalars. When the thermal bath is in equilibrium, i.e. time-translational invariant, the spectral fermionic Green's function has a standard Breit-Wigner representation, and the statistical propagator shows all the non-equilibrium properties of the created fermionic particle. In this case, the statistical propagator at $t = 0$ is equal to the free propagator at $t = 0$, which is non-zero even in the absence of out-of-equilibrium particles.

In the semi-classical leptogenesis, the asymmetry is created via CP violating processes that originates from the mixture between one-loop and tree level diagrams. However, the Boltzmann equations fail to describe quantum interference and off-shell effects between these two diagrams, since they rely on taking on-shell particles in the external lines of the one-loop and tree level diagrams. In the KBEs the S-matrix elements are all incorporated in the self-energy, where off-shell effects are also taken into account. In this way we were able to formulate a systematic approach to the quantum mechanics effects that are important for leptogenesis. For this, we introduced a non-equilibrium Majorana neutrino into the self-energy of a thermal bath of SM particles. The out-of-equilibrium dynamics are then described by the Majorana propagator and its decay width Γ . It is important that even if asymmetry creation is a processes close to equilibrium, the Majorana neutrino particle can be far out-of-equilibrium, making its non-local quantum interference very important. We were able to obtain an analytical solution for the creation of an asymmetry shown in eq. (3.2.64), where we defined a two-time flavour dependent matrix (lepton number matrix). A big qualitative difference that comes from the off-shell effects is the oscillatory behaviour which vanishes if one takes only on-shell contributions into account. This effect cannot be described by semi-classical approaches. Another qualitative difference comes from the behaviour of the asymmetry at $t = 0$. While the time derivative of the semi-classical asymmetry at $t = 0$ is zero, the same derivative over the quantum asymmetry is non-zero.

A comparison with respect to the Boltzmann equations was also performed. We neglect off-shell effects from the lepton number matrix in (3.2.64) in order to understand the necessary steps to regain back the Boltzmann result. This leads to an asymmetry that behaves (for small times) as t^2 instead of being linear in t . The integrands can have an order of magnitude difference. This shows us that even neglecting off-shell effects,

non-locality in the quantum processes have a big consequence on the final asymmetry.

The SM effects on the thermal bath were introduced as a first approximation. Here we consider the decay widths in the Breit-Wigner propagators as decay widths of the SM particles in the plasma. The widths of the SM particles are much larger than the width of the Majorana field, i.e. $\Gamma_l, \Gamma_\phi \gg \Gamma_N$, thus suppressing the integral for large separation of times exponentially. The propagators inside the loop will contribute only when the time-separation between both vertices is small, $\Delta t_{vertices} \rightarrow 0$ (see figure 3.4). The locality is then regained and all quantum interferences are suppressed. However, this type of insertion of the SM widths is not yet a systematic way to describe this problem. At high temperatures and strong couplings, the Breit-Wigner representation breaks down, and fields have no longer a quasi-particle representation. Therefore a proper study of SM particles at high temperatures is required in order to have a complete theory.

A complete ‘quantum theory of leptogenesis’ is not yet obtained, as many factors need to be taken into account, such as expansion of the universe and wash-out terms. A numerical analysis of the final asymmetry needs also to be performed. This is work in progress.

As a final remark, the understanding of the quantum mechanics behind leptogenesis, can be used to expand the model to other cosmological problems. For example, applying our result to a resonant case, where we have degeneracy or quasi-degeneracy in Majorana masses, can in principle lower the scale where leptogenesis is efficient and in this way relax the constraints for gravitino production.

Appendix A

Notation and conventions

In this section we will describe the definitions used to describe full Green's functions as for the self-energy for scalar and fermion particles.

A.1 Conventions

Throughout this thesis we use natural units $\hbar = c = k_B = 1$. The metric is chosen in a flat Minkowski space as

$$\eta_{\mu\nu} = \text{diag}(1, -1, -1, -1) . \quad (\text{A.1.1})$$

List of notation for the propagators

- $\Delta(x_1, x_2)$: scalar propagator
- $S(x_1, x_2)$: massless lepton propagator
- $G(x_1, x_2)$: massive fermionic propagator

List of self-energies

- $\Pi(x_1, x_2)$: scalar
- $\Pi(x_1, x_2)$: massless lepton
- $\Sigma(x_1, x_2)$: massive fermion

List of used energies and momenta

- $q = |\mathbf{q}|$: massless scalar
- $\omega_{\mathbf{q}} = \sqrt{\mathbf{q}^2 + m^2}$: massive scalar
- $\Omega_{\mathbf{q}} = \sqrt{\mathbf{q}^2 + m(T)^2}$: pseudo-scalar
- $k = |\mathbf{k}|$: massless lepton
- $\omega_{\mathbf{k}} = \sqrt{\mathbf{k}^2 + M^2}$: massive fermion
- $\omega_{\mathbf{p}} = \sqrt{\mathbf{p}^2 + M^2}$: massive Majorana fermion

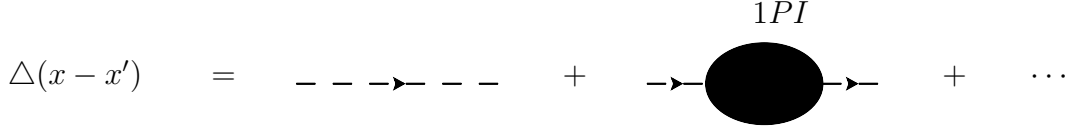
$$\Delta(x-x') = \text{---} \text{---} \text{---} \text{---} + \text{---} \text{---} \text{---} \text{---} \text{---} \text{---} + \dots$$


Figure A.1: Diagrammatic view of the scalar full-propagator.

A.2 Scalars Green's functions

Definitions

The free scalar Green's function Δ_F is defined in order that the equation of motion applied to it is

$$(\square_x + m_\phi^2)\Delta_F(x-x') = -i\delta^4(x-x'), \quad (\text{A.2.1})$$

where we assume the same criteria as in [85]. This Green's function can be written as

$$\Delta_F(x-x') = \int \frac{d^3q}{(2\pi)^3 2\omega_{\mathbf{q}}} \left[\theta(t-t')e^{-i\mathbf{q}(\mathbf{x}-\mathbf{x}')} + \theta(t'-t)e^{i\mathbf{q}(\mathbf{x}-\mathbf{x}')} \right], \quad (\text{A.2.2})$$

$$= \int \frac{d^4q}{(2\pi)^4} \frac{i}{q^2 - m_\phi^2 + i\epsilon}, \quad (\text{A.2.3})$$

$$= \theta(t-t')\langle 0|\phi(x)\phi(x')|0\rangle + \theta(t'-t)\langle 0|\phi(x')\phi(x)|0\rangle. \quad (\text{A.2.4})$$

The free propagator in momentum space is then given by

$$\Delta_F(q) = \frac{i}{q^2 - m_\phi^2}. \quad (\text{A.2.5})$$

After having a good definition of the free propagator we can define the full-propagator $\Delta(x-x')$, which diagrammatically can be seen in figure A.1, by solving

$$\Delta(x,x') = \Delta_F(x-x') + \int d^4y \int d^4y' \Delta_F(x-y)\Pi(y,y')\Delta(y',x'), \quad (\text{A.2.6})$$

where Π is now defined as the sum of all one-particle-irreducible (1PI) diagrams. Applying the differential operator and using eq. (A.2.1) we obtain the Schwinger-Dyson equation for scalars

$$(\square_x + m^2)\Delta(x,x') = -i\delta^4(x-x') - i \int d^4y' \Pi(x,y')\Delta(y',x'). \quad (\text{A.2.7})$$

The biggest difference with the most common notation, is the fact that we define the self energy as the sum of all IPI diagrams $\Pi = \sum_i \Pi_{i(1PI)}$ (the same notation is used in [80]), meanwhile in the literature such as [85], the self energy is defined as $\Pi = -i \sum_i \Pi_{i(1PI)}$. With this type of definition we can obtain that in the contour of Figure 2.1 we can now define consistently

$$\Delta^-(x,x') = i(\Delta^>(x,x') - \Delta^<(x,x')), \quad (\text{A.2.8})$$

$$\Delta^+(x, x') = \frac{1}{2}(\Delta^>(x, x') + \Delta^<(x, x')) , \quad (\text{A.2.9})$$

and

$$\Pi^-(x, x') = i(\Pi^>(x, x') - \Pi^<(x, x')) , \quad (\text{A.2.10})$$

$$\Pi^+(x, x') = \frac{1}{2}(\Pi^>(x, x') + \Pi^<(x, x')) . \quad (\text{A.2.11})$$

Symmetries

With the definition of Δ^- and Δ^+ it is easy to check some symmetry properties of this functions

$$\Delta^-(x, x') = -\Delta^-(x', x) , \quad (\text{A.2.12})$$

$$\Delta^+(x, x') = \Delta^+(x', x) . \quad (\text{A.2.13})$$

or in momentum space

$$\Delta_{\mathbf{q}}^-(t, t') = -\Delta_{-\mathbf{q}}^-(t', t) , \quad (\text{A.2.14})$$

$$\Delta_{\mathbf{q}}^+(t, t') = \Delta_{-\mathbf{q}}^+(t', t) . \quad (\text{A.2.15})$$

Here the symmetry properties are the same for space-phase as for momentum-space. This can be think as something trivial, but we will see that symmetries properties for fermions need to be taken carefully.

A.3 Fermionic Green's functions

Definitions

The same definition procedure as the last section can be performed for fermions, let start by talking the equation of motion that the free fermion propagator S_F satisfies (defined in the same way as [85])

$$(i\partial_x - m_\psi)S_F(x - x') = i\delta^4(x - x') . \quad (\text{A.3.1})$$

The Green's function has the form

$$S_F(x - x') = \int \frac{d^3k}{(2\pi)^3 2\omega_{\mathbf{k}}} \left[\theta(t - t') (\not{k} + m_\psi) e^{-i\mathbf{k}(\mathbf{x} - \mathbf{x}')} + \theta(t' - t) (\not{k} - m_\psi) e^{i\mathbf{k}(\mathbf{x} - \mathbf{x}')} \right] , \quad (\text{A.3.2})$$

$$= \int \frac{d^4k}{(2\pi)^4} \frac{i}{\not{k} - m_\psi + i\epsilon} , \quad (\text{A.3.3})$$

$$= \theta(t - t') \langle 0 | \psi(x) \bar{\psi}(x') | 0 \rangle - \theta(t' - t) \langle 0 | \bar{\psi}(x') \psi(x) | 0 \rangle , \quad (\text{A.3.4})$$

$$S(x-x') = \longrightarrow + \begin{array}{c} 1PI \\ \bullet \end{array} \longrightarrow + \dots$$

Figure A.2: Diagrammatic view of the fermionic full-propagator.

and in momentum space given by

$$S_F(k) = \frac{i}{\not{k} - m_\psi} . \quad (\text{A.3.5})$$

The full propagator is given by (see Figure A.2)

$$S(x, x') = S_F(x-x') + \int d^4y \int d^4y' S_F(x-y) \Sigma(y, y') S(y', x') , \quad (\text{A.3.6})$$

Applying the differential operator and using equation (A.3.1) we get the Schwinger-Dyson equation for fermions

$$(i\partial_x - m_\psi)S(x, x') = -i\delta^4(x-x') - i \int d^4y' \Sigma(x, y') S(y', x') . \quad (\text{A.3.7})$$

As before, we define the self-energy as the sum of all 1PI diagrams, which will allow us to define in the same way

$$S^-(x, x') = i(S^>(x, x') - S^<(x, x')) , \quad (\text{A.3.8})$$

$$S^+(x, x') = \frac{1}{2}(S^>(x, x') + S^<(x, x')) , \quad (\text{A.3.9})$$

and

$$\Sigma^-(x, x') = i(\Sigma^>(x, x') - \Sigma^<(x, x')) , \quad (\text{A.3.10})$$

$$\Sigma^+(x, x') = \frac{1}{2}(\Sigma^>(x, x') + \Sigma^<(x, x')) . \quad (\text{A.3.11})$$

Symmetries

Because of the Lorentz structure of fermions, symmetry properties will vary if one takes into account the scalar part or the vector part of the propagators. Let see first the symmetries of the Dirac fermion propagator, which we will denote by S . These symmetries are given by

$$\gamma_0[S^-(x, x')]^\dagger \gamma_0 = -S^-(x', x) , \quad (\text{A.3.12})$$

$$\gamma_0[S^+(x, x')]^\dagger \gamma_0 = S^+(x', x) . \quad (\text{A.3.13})$$

To go to momentum space, we must be careful, the Hermitian conjugate transforms $i \rightarrow -i$ which will affect in the exponent of the Fourier transformation. Thats why

taking the Hermitian conjugation will have the same repercussion as taking $k \rightarrow -k$. Now the symmetries in momentum space are

$$\gamma_0[S^-(t, t')_{\mathbf{k}}]^\dagger \gamma_0 = -S_{\mathbf{k}}^-(t', t) , \quad (\text{A.3.14})$$

$$\gamma_0[S_{\mathbf{k}}^+(t, t')]^\dagger \gamma_0 = S_{\mathbf{k}}^+(t', t) . \quad (\text{A.3.15})$$

As explained above, there is no need to take $k \rightarrow -k$.

If we now consider Majorana fermions (which we will denote as G), Eqs. (A.3.12) and (A.3.13) are modified by the definition of the Green's function, basically the difference comes from the fact that the anti-particle of a Majorana particle is its own particle, this will be translated in the following symmetry properties

$$G^-(x, x')^T = G^-(x', x) , \quad (\text{A.3.16})$$

$$G^+(x, x')^T = -G^+(x', x) , \quad (\text{A.3.17})$$

and for the ones in momentum space

$$G_{\mathbf{p}}^-(t, t')^T = G_{-\mathbf{p}}^-(t', t) , \quad (\text{A.3.18})$$

$$G_{\mathbf{p}}^+(t, t')^T = -G_{-\mathbf{p}}^+(t', t) . \quad (\text{A.3.19})$$

In the last equations, we can see that it is necessary the change $p \rightarrow -p$.

Appendix B

Scalar theory

B.1 Self Energy

The interaction with the thermal bath changes the spectral function of a free scalar particle,

$$\rho_{\mathbf{q}}(\omega) = 2\pi \text{sign}(\omega) \delta(\omega^2 - \omega_{\mathbf{q}}^2) , \quad (\text{B.1.1})$$

to the expression (2.1.53) which depends on real and imaginary part of the self-energy,

$$\rho_{\mathbf{q}}(\omega) = \frac{-2\text{Im}\Pi_{\mathbf{q}}^R(\omega) + 2\omega\epsilon}{[\omega^2 - \omega_{\mathbf{q}}^2 - \text{Re}\Pi_{\mathbf{q}}^R(\omega)]^2 + [\text{Im}\Pi_{\mathbf{q}}^R(\omega) + \omega\epsilon]^2} . \quad (\text{B.1.2})$$

We have computed the imaginary part of the self-energy in the scalar field model defined in Section 2.1.4, assuming free thermal propagators for the fields χ_1 and χ_2 . The result agrees with [84]. One obtains ($q = (\omega_{\mathbf{q}}, \mathbf{q})$):

$$-\text{Im}\Pi_{\mathbf{q}}^R(\omega) = \sigma_0(q) + \sigma_{\beta}^{(a)}(q) + \sigma_{\beta}^{(b)}(q) . \quad (\text{B.1.3})$$

Here σ_0 is the zero-temperature contribution due to the decay process $\Phi \rightarrow \chi_1\chi_2$,

$$\begin{aligned} \sigma_0(q) &= \frac{g^2}{16\pi q^2} \text{sign}(\omega) \Theta(q^2 - (m_1 + m_2)^2) \\ &\quad \times \left((q^2)^2 - 2q^2(m_1^2 + m_2^2) + (m_1^2 - m_2^2)^2 \right)^{\frac{1}{2}} , \end{aligned} \quad (\text{B.1.4})$$

$\sigma_{\beta}^{(a)}$ is the finite-temperature contribution from this process,

$$\begin{aligned} \sigma_{\beta}^{(a)}(q) &= \frac{g^2}{16\pi|\mathbf{q}|\beta} \text{sign}(\omega) \Theta(q^2 - (m_1 + m_2)^2) \\ &\quad \times \left(\ln \left(\frac{1 - e^{-\beta\omega_+}}{1 - e^{-\beta\omega_-}} \right) + (m_1 \leftrightarrow m_2) \right) , \end{aligned} \quad (\text{B.1.5})$$

and $\sigma_\beta^{(b)}(\mathbf{q})$ is the finite-temperature contribution from processes $\chi_i \rightarrow \chi_j \phi$,¹

$$\begin{aligned} \sigma_\beta^{(b)}(q) &= \frac{g^2}{16\pi|\mathbf{q}|\beta} \text{sign}(\omega) \Theta((m_1 - m_2)^2 - q^2) \\ &\quad \times \left(\ln \left(\frac{1 - e^{-\beta|\omega_-|}}{1 - e^{-\beta|\omega_+|}} \right) + (m_1 \leftrightarrow m_2) \right), \end{aligned} \quad (\text{B.1.6})$$

where we have used the abbreviations

$$\omega_\pm = \frac{|\omega|}{2q^2} (q^2 + m_1^2 - m_2^2) \pm \frac{|\mathbf{q}|}{2|q^2|} \left((q^2 + m_1^2 - m_2^2)^2 - 4q^2 m_1^2 \right)^{\frac{1}{2}}. \quad (\text{B.1.7})$$

The real part of the self-energy can be computed using the dispersion relation relation,

$$\text{Re}\Pi_{\mathbf{q}}^R(\omega) = \frac{1}{\pi} \mathcal{P} \int_{-\infty}^{\infty} d\omega' \frac{\text{Im}\Pi_{\mathbf{q}}^R(\omega')}{\omega' - \omega}. \quad (\text{B.1.8})$$

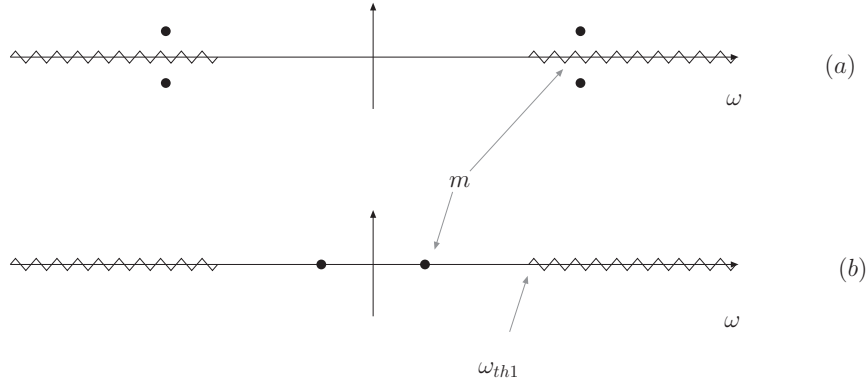


Figure B.1: Poles and cuts of the spectral function $\rho(\omega)$ for $\mathbf{q} = 0$ at $T = 0$: (a) $m > m_1 + m_2$, and (b) $m < m_1 + m_2$.

Based on these expressions we can discuss the analytic structure of the spectral function. For a free field $\rho_{\mathbf{q}}(\omega)$ is given by (B.1.1) which has two poles at $\omega = \pm\omega_q$ in the complex ω -plane. The interaction of Φ with χ_1 and χ_2 does not modify these poles for $m < m_1 + m_2$, where Φ is stable at zero temperature. In addition there are branch cuts at the two-particle thresholds $|\omega| > \omega_{th1} = \sqrt{\mathbf{q}^2 + (m_1 + m_2)^2}$ (see Fig. B.1b). They correspond to virtual decays and inverse decays, $\Phi \leftrightarrow \chi\chi$. In the case $m > m_1 + m_2$ these processes can happen on-shell since $m > \omega_{th1}$, and Φ becomes unstable. Now the spectral function has four poles in the complex ω -plane, whose real parts lie in the region of the branch cuts (see Fig. B.1a). The imaginary parts of the poles correspond to the decay width of Φ .

The analytic structure of the spectral function at finite temperature is displayed in Fig. B.2. The position of ω_{th1} is shifted due to thermal corrections from $\text{Re}\Pi_{\mathbf{q}}^R$.

¹Note that we disagree with the discussion in [108] which implies the additional factor $\Theta(|m_1^2 - m_2^2| - q^2)$.

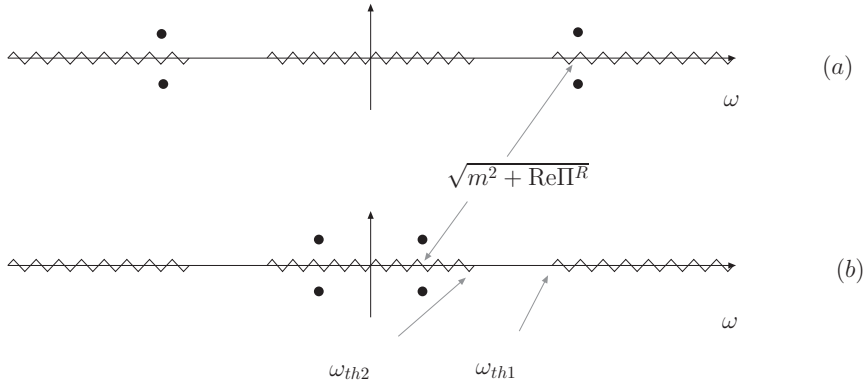


Figure B.2: Poles and cuts of the spectral function $\rho(\omega)$ for $\mathbf{q} = 0$ at $T \neq 0$: (a) $m > m_1 + m_2$, and (b) $m < m_1 + m_2$.

Furthermore, a new branch cut appears in the region where $\sigma_b \neq 0$, i.e. for $|\omega| < \omega_{th2} = \sqrt{\mathbf{q}^2 + (m_1 - m_2)^2}$. This is due to processes $\chi \leftrightarrow \phi\chi$ and corresponds to Landau damping of quasi-particles in the plasma. If the real part of the poles falls into the regions of one of the branch cuts, i.e. $|\omega| < \omega_{th2}$ or $|\omega| > \omega_{th1}$, they acquire an imaginary part which corresponds to the quasi-particle decay width (see Fig. B.2).

Qualitatively, this analytic structure is typical for interacting quantum field theories at finite temperature. In general, the spectral function can have additional singular contributions for $m < |\omega| < \omega_{th1}$ corresponding to bound states. At finite temperature they are also dressed to quasi-particles.

B.2 Breit-Wigner

In the regime of couplings and temperatures where $|\text{Im}\Pi_{\mathbf{q}}^R(\Omega_{\mathbf{q}})| \ll \Omega_{\mathbf{q}}^2$, so that the quasi-particle picture holds, one can approximate the spectral function $\rho_{\mathbf{q}}(\omega)$ by a Breit-Wigner function. From the expression (2.1.53) one easily obtains

$$\rho_{\mathbf{q}}(\omega) \simeq \frac{Z_{\mathbf{q}}}{2\Omega_{\mathbf{q}}} \frac{\text{sign}(\omega)\Gamma_{\mathbf{q}}}{(|\omega| - \Omega_{\mathbf{q}})^2 + \frac{1}{4}\Gamma_{\mathbf{q}}^2}, \quad (\text{B.2.1})$$

where $\Gamma_{\mathbf{q}}$ is the quasi-particle width

$$\Gamma_{\mathbf{q}} = -Z_{\mathbf{q}} \frac{\text{Im}\Pi_{\mathbf{q}}^R(\Omega_{\mathbf{q}})}{\Omega_{\mathbf{q}}}, \quad (\text{B.2.2})$$

with

$$Z_{\mathbf{q}} = \left(1 - \frac{1}{2\Omega_{\mathbf{q}}} \frac{\partial \text{Re}\Pi_{\mathbf{q}}^R(\omega)}{\partial \omega} \Big|_{\omega=\Omega_{\mathbf{q}}} \right)^{-1}. \quad (\text{B.2.3})$$

Contrary to the exact spectral function (2.1.53), the Breit-Wigner approximation (B.2.1) has no branch cuts. The integrals over ω are dominated by the regions around the

quasi-particle poles where the two functions are very similar. For the Fourier transform, the spectral function in real time, one obtains

$$\Delta_{\mathbf{q}}^{-}(y) \simeq Z_{\mathbf{q}} \frac{\sin(\Omega_{\mathbf{q}} y)}{\Omega_{\mathbf{q}}} e^{-\Gamma_{\mathbf{q}} y/2} . \quad (\text{B.2.4})$$

B.3 Time translational invariance

In this section we shall prove that the most general solution of the first Kadanoff-Baym equation is time-translation invariant. The starting point is Eq. (2.1.29) with the boundary conditions (2.1.31) - (2.1.33). Performing the change of variables $t_1 = t + y/2$, $t_2 = t - y/2$, Eq. (2.1.29) becomes

$$\left(\frac{1}{4} \partial_t^2 + \partial_t \partial_y + \partial_y^2 + \omega_{\mathbf{q}}^2 \right) \Delta_{\mathbf{q}}^{-}(t; y) + \int_0^y dy' \Pi_{\mathbf{q}}^{-}(y - y') \Delta_{\mathbf{q}}^{-}(t'; y') = 0 , \quad (\text{B.3.1})$$

where $t' = t - (y - y')/2$ and $\omega_{\mathbf{q}}^2 = \mathbf{q}^2 + m^2$. Note that $\Delta_{\mathbf{q}}^{-}$ and $\Pi_{\mathbf{q}}^{-}$ only depend on $|\mathbf{q}|$ because of rotational invariance. Both functions are antisymmetric in y . The boundary conditions (2.1.31) - (2.1.33) read

$$\Delta_{\mathbf{q}}^{-}(t; 0) = 0 , \quad (\text{B.3.2})$$

$$\partial_t \Delta_{\mathbf{q}}^{-}(t; 0) = 0 , \quad (\text{B.3.3})$$

$$\partial_y \Delta_{\mathbf{q}}^{-}(t; y)|_{y=0} = 1 , \quad (\text{B.3.4})$$

$$\left(\frac{1}{4} \partial_t^2 - \partial_y^2 \right) \Delta_{\mathbf{q}}^{-}(t; y)|_{y=0} = 0 . \quad (\text{B.3.5})$$

The condition (B.3.2) is automatically fulfilled because of the antisymmetry in y .

To prove that Δ^{-} is time-translation invariant we now perform an expansion in powers of Π^{-} ,

$$\Delta_{\mathbf{q}}^{-} = \sum_{n=0}^{\infty} \Delta_{\mathbf{q}}^{(n)} , \quad \Delta_{\mathbf{q}}^{(n)} = \mathcal{O}(\Pi_{\mathbf{q}}^{(n)}) . \quad (\text{B.3.6})$$

For $n = 0$ one has

$$\left(\frac{1}{4} \partial_t^2 + \partial_t \partial_y + \partial_y^2 + \omega_{\mathbf{q}}^2 \right) \Delta_{\mathbf{q}}^{(0)}(t; y) = 0 . \quad (\text{B.3.7})$$

Using the antisymmetry of $\Delta_{\mathbf{q}}^{-}$ in y , one obtains

$$\partial_t \partial_y \Delta_{\mathbf{q}}^{(0)}(t; y) = 0 , \quad (\text{B.3.8})$$

which has the general solution

$$\Delta_{\mathbf{q}}^{(0)} = a_{\mathbf{q}}^{(0)}(t) + b_{\mathbf{q}}^{(0)}(y) . \quad (\text{B.3.9})$$

Every solution of Eqs. (B.3.7) and (B.3.8) satisfies the boundary condition (B.3.5). The condition (B.3.3) implies

$$\partial_t \Delta_{\mathbf{q}}^{(0)}(t; 0) = \partial_t a_{\mathbf{q}}^{(0)}(t) = 0 . \quad (\text{B.3.10})$$

Hence, $a_{\mathbf{q}}^{(0)}$ is constant and $\Delta_{\mathbf{q}}^{(0)}$ only depends on y . Eq. (B.3.7) now becomes

$$(\partial_y^2 + \omega_{\mathbf{q}}^2) \Delta_{\mathbf{q}}^{(0)}(y) = 0 , \quad (\text{B.3.11})$$

which has the antisymmetric solution

$$\Delta_{\mathbf{q}}^{(0)}(y) = c_{\mathbf{q}}^{(0)} \sin(\omega_{\mathbf{q}} y) . \quad (\text{B.3.12})$$

For $n \neq 0$ one can use the recurrence relation

$$\left(\frac{1}{4} \partial_t^2 + \partial_t \partial_y + \partial_y^2 + \omega_{\mathbf{q}}^2 \right) \Delta_{\mathbf{q}}^{(n+1)}(t; y) + \int_0^y dy' \Pi_{\mathbf{q}}^-(y - y') \Delta_{\mathbf{q}}^{(n)}(y') = 0 . \quad (\text{B.3.13})$$

Using the antisymmetry of $\Pi_{\mathbf{q}}^-$ and $\Delta_{\mathbf{q}}^-$ in y , one again finds

$$\partial_t \partial_y \Delta_{\mathbf{q}}^{(n+1)}(t; y) = 0 . \quad (\text{B.3.14})$$

Repeating the same steps as for $\Delta_{\mathbf{q}}^{(0)}$ yields the result that also $\Delta_{\mathbf{q}}^{(n+1)}$ is independent of t .

We conclude that the spectral function is the antisymmetric solution of the equation

$$(\partial_y^2 + \omega_{\mathbf{q}}^2) \Delta_{\mathbf{q}}^-(y) + \int_0^y dy' \Pi_{\mathbf{q}}^-(y - y') \Delta_{\mathbf{q}}^-(y') = 0 , \quad (\text{B.3.15})$$

with the boundary condition

$$\partial_y \Delta_{\mathbf{q}}^-(y)|_{y=0} = 1 . \quad (\text{B.3.16})$$

Appendix C

Fermion theory

C.1 2 flavour structure matrix Inverse

2x2 case suppose that we have a matrix of the form

$$\begin{pmatrix} A_{11} & A_{12} \\ A_{21} & A_{22} \end{pmatrix} \begin{pmatrix} B_{11} & B_{12} \\ B_{21} & B_{22} \end{pmatrix} = \begin{pmatrix} 1 & 0 \\ 0 & 1 \end{pmatrix}. \quad (\text{C.1.1})$$

with $B_{ij} = \not{k}_{ijL}P_L + \not{k}_{ijR}P_R$, where $\not{k}_{ijL} = a_{ijL}\not{k} + b_{ijL}\not{y}$ for $i \neq j$ and $B_{ii} = \not{k}_{ii} - M_{ii}$ with

$$M = \begin{pmatrix} M_1 & 0 \\ 0 & M_2 \end{pmatrix}. \quad (\text{C.1.2})$$

with $\not{k}_{ii} = (1 + a_{ii})\not{k} + b_{ii}\not{y}$. Then, the components A_{ij} are given by

$$A_{11} = (B_{11} - B_{12}B_{22}^{-1}B_{21})^{-1} \quad (\text{C.1.3})$$

$$A_{12} = (B_{21} - B_{22}B_{12}^{-1}B_{11})^{-1}. \quad (\text{C.1.4})$$

Let start with A_{12} . we need to compute first

$$B_{12}^{-1} = (\not{k}_{12L}P_L + \not{k}_{12R}P_R)^{-1} \quad (\text{C.1.5})$$

which will give us

$$B_{12}^{-1} = P_L \frac{\not{k}_{12L}}{q_{12L}^2} + P_R \frac{\not{k}_{12R}}{q_{12R}^2}. \quad (\text{C.1.6})$$

then

$$A_{12} = \left(\not{k}_{21L}P_L + \not{k}_{21R}P_R - (\not{k}_{22} - M_2) \left(P_L \frac{\not{k}_{12L}}{q_{12L}^2} + P_R \frac{\not{k}_{12R}}{q_{12R}^2} \right) (\not{k}_{11} - M_1) \right) \quad (\text{C.1.7})$$

with a little bit of algebra we get

$$A_{12} = \{ [\mathbf{k}_{21L} - (\mathbf{k}_{22} - M_2)(\mathbf{k}_{12L}^{-1}\mathbf{k}_{11} - \mathbf{k}_{12R}^{-1}M)]P_L + [\mathbf{k}_{21R} - (\mathbf{k}_{22} - M_2)(\mathbf{k}_{12R}^{-1}\mathbf{k}_{11} - \mathbf{k}_{12L}^{-1}M)]P_R \}^{-1} \quad (\text{C.1.8})$$

we finally obtain

$$A_{12} = P_L B_L + P_R B_R, \quad (\text{C.1.9})$$

where B_L and B_R are solutions of the following equation

$$aB_L + bB_R = 1, \quad (\text{C.1.10})$$

$$cB_L + dB_R = 1. \quad (\text{C.1.11})$$

and

$$a = \mathbf{k}_{12L}^{-1}\mathbf{k}_{11}M_2 + \mathbf{k}_{12R}\mathbf{k}_{22}M_1, \quad (\text{C.1.12})$$

$$b = \mathbf{k}_{21R} - \mathbf{k}_{22}\mathbf{k}_{12R}^{-1}\mathbf{k}_{11} - M_1\mathbf{k}_{12L}^{-1}M_2, \quad (\text{C.1.13})$$

$$c = \mathbf{k}_{21L} - \mathbf{k}_{22}\mathbf{k}_{12L}^{-1}\mathbf{k}_{11} - M_1\mathbf{k}_{12R}^{-1}M_2, \quad (\text{C.1.14})$$

$$d = \mathbf{k}_{12R}^{-1}\mathbf{k}_{11}M_2 + \mathbf{k}_{12L}\mathbf{k}_{22}M_1 \quad (\text{C.1.15})$$

we get that

$$B_R = (d - ca^{-1}b)^{-1}(1 - ca^{-1}), \quad (\text{C.1.16})$$

$$= (b - ac^{-1}d)^{-1}(1 - ac^{-1}), \quad (\text{C.1.17})$$

$$B_L = (c - db^{-1}a)^{-1}(1 - db^{-1}), \quad (\text{C.1.18})$$

$$= (a - bd^{-1}c)^{-1}(1 - bd^{-1}). \quad (\text{C.1.19})$$

Let us see now A_{11} , for this case we need first

$$B_{22}^{-1} = \frac{\mathbf{k}_{22} + M_2}{D_2}, \quad (\text{C.1.20})$$

with $D_2 = q_{22}^2 - M_2^2$. With a little bit of algebra we get

$$A_{11} = \left([\mathbf{k}_{11} - M_1 - \frac{\mathbf{k}_{12L}\mathbf{k}_{22}\mathbf{k}_{21L}}{D_2} - \frac{\mathbf{k}_{12R}M_2\mathbf{k}_{21L}}{D_2}]P_L + [\mathbf{k}_{11} - M_1 - \frac{\mathbf{k}_{12R}\mathbf{k}_{22}\mathbf{k}_{21R}}{D_2} - \frac{\mathbf{k}_{12L}M_2\mathbf{k}_{21R}}{D_2}]P_R \right)^{-1} \quad (\text{C.1.21})$$

The result will be given by

$$A_{11} = P_L C_L + P_R C_R. \quad (\text{C.1.22})$$

where C_L and C_R are solutions of the following equation

$$a'C_L + b'C_R = 1, \quad (\text{C.1.23})$$

$$c' C_L + d' C_R = 1. \quad (\text{C.1.24})$$

with

$$a' = -M_1 - \frac{1}{D_2} \mathbf{k}_{12R} M_2 \mathbf{k}_{21L}, \quad (\text{C.1.25})$$

$$b' = \mathbf{k}_{11} - \frac{1}{D_2} \mathbf{k}_{12R} \mathbf{k}_{22} \mathbf{k}_{21R}, \quad (\text{C.1.26})$$

$$c' = \mathbf{k}_{11} - \frac{1}{D_2} \mathbf{k}_{12L} \mathbf{k}_{22} \mathbf{k}_{21L}, \quad (\text{C.1.27})$$

$$d' = -M_1 - \frac{1}{D_2} \mathbf{k}_{12L} M_2 \mathbf{k}_{21R}. \quad (\text{C.1.28})$$

and

$$C_R = (d' - c' a'^{-1} b')^{-1} (1 - c' a'^{-1}), \quad (\text{C.1.29})$$

$$= (b' - a' c'^{-1} d')^{-1} (1 - a' c'^{-1}), \quad (\text{C.1.30})$$

$$C_L = (c' - d' b'^{-1} a')^{-1} (1 - d' b'^{-1}), \quad (\text{C.1.31})$$

$$= (a' - b' d'^{-1} c')^{-1} (1 - b' d'^{-1}). \quad (\text{C.1.32})$$

For A_{21} and A_{22} , just take the solutions for above and interchange the indices $1 \rightarrow 2$ and $2 \rightarrow 1$

C.2 Calculation of the 1-loop self-energy

a) First diagram

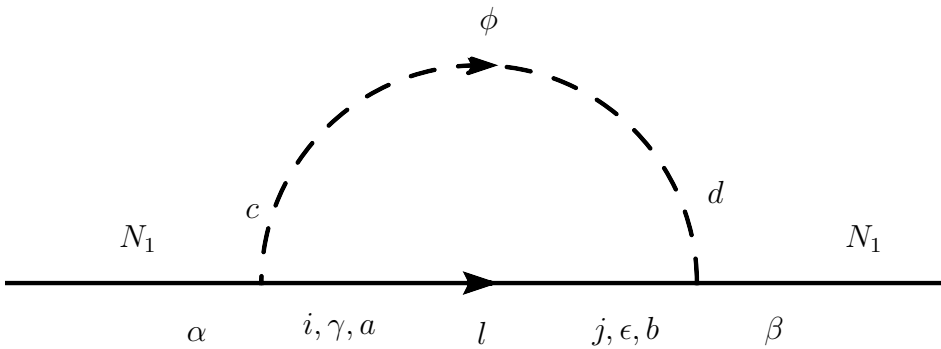


Figure C.1: 1-loop graph a)

the Feynman rules will give us

$$\begin{aligned} \Sigma_a(q) = \frac{1}{2} \int \frac{d^4 p}{(2\pi)^4} & [i\lambda_{i1}^* \epsilon_{ac} (P_R)_{\gamma\alpha}] [i\delta_{ij} \delta_{ab} S_{\epsilon\gamma}(p)] \\ & \times [i\lambda_{i1} (C P_L)_{\beta\epsilon} \epsilon_{bd}] [i\delta_{dc} \Delta(q-p)]. \end{aligned} \quad (\text{C.2.1})$$

The sum over the isospin index will give us a factor of 2. Now, using the fact that S is massless, so $P_R S = S P_L$ and $S^T C = C S$, we obtain

$$\Sigma_a(q) = C^{-1} \int \frac{d^4 p}{(2\pi)^4} (\lambda \lambda^\dagger)_{11}^2 S(q) \Delta(q-p) P_L . \quad (\text{C.2.2})$$

b) Second diagram

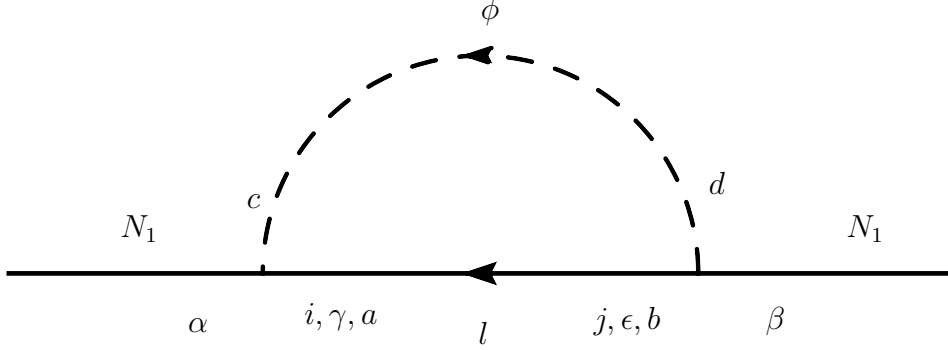


Figure C.2: 1-loop graph b)

the Feynman rules will give us

$$\begin{aligned} \Sigma_b(q) = & -\frac{1}{2} \int \frac{d^4 p}{(2\pi)^4} [i\lambda_{i1}\epsilon_{ac}(C P_L)_{\alpha\gamma}] [i\delta_{ij}\delta_{ab}S_{\epsilon\gamma}(p)] \\ & \times [i\lambda_{i1}^*(P_R)_{\epsilon\beta}\epsilon_{bd}] [i\delta_{dc}\Delta(q-p)] . \end{aligned} \quad (\text{C.2.3})$$

The isospin sum will give us a factor of 2. The negative sign comes from the momentum inversion? Now, using $C^{-1} = -C$ and the same procedure as above we obtain

$$\Sigma_b(q) = C^{-1} \int \frac{d^4 p}{(2\pi)^4} (\lambda \lambda^\dagger)_{11}^2 S(p) \Delta(q-p) P_R . \quad (\text{C.2.4})$$

Note that $\Sigma_a(q) + \Sigma_b(q) = \Sigma(q)$, which does not depend on a specific chirality. This is not surprising because at 1-loop level, there is no CP violation.

The Lorentz structure of $\Sigma^> \propto \int S^> \Delta^>$ comes only from the thermal fermion propagator $S^>$ which has a scalar piece $\Sigma_{(S)}$ proportional to the fermion mass m_ψ and a vector piece $\Sigma_{(V)}^\mu$ proportional to q . In a homogenous and isotropic bath the only two vectors are the external momentum q_μ and the four velocity of the bath u_μ . This allows to parametrize

$$\Sigma = aq + bu + c\mathbb{1} . \quad (\text{C.2.5})$$

Obviously $\hat{\Sigma}_{(S)} = c$, $\hat{\Sigma}_{(V)}^\mu = aq^\mu + bu^\mu$. For computational simplicity it is useful to introduce the quantities

$$A = \left(\frac{1}{4} \text{tr} \left(q \hat{\Sigma}_{\mathbf{q}}^R(\omega) \right) \right) , \quad (\text{C.2.6})$$

$$B = \left(\frac{1}{4} \text{tr} \left(\psi \hat{\Sigma}_{\mathbf{q}}^R(\omega) \right) \right), \quad (\text{C.2.7})$$

$$C = \left(\frac{1}{4} \text{tr} \left(\hat{\Sigma}_{\mathbf{q}}^R(\omega) \right) \right), \quad (\text{C.2.8})$$

from which one can obtain a , b and c via

$$a = \frac{Bq \cdot u - Au^2}{(q \cdot u)^2 - q^2 u^2}, \quad (\text{C.2.9})$$

$$b = \frac{-Bq^2 + Aq \cdot u}{(q \cdot u)^2 - q^2 u^2}, \quad (\text{C.2.10})$$

$$c = C, \quad (\text{C.2.11})$$

where $q \cdot u = q_\mu u^\mu$. The quantities defined above are generally complex scalars that can be always decomposed as $a = a_R + ia_I$ where a_I is defined via the discontinuity.

$$a_I = \frac{1}{2i} (a(\omega + i\epsilon, \mathbf{q}) - a(\omega - i\epsilon, \mathbf{q})). \quad (\text{C.2.12})$$

Going to the rest frame of the bath where $u = (1, 0, 0, 0)$ we can introduce the free propagator for the Higgs and lepton

$$S^>(p) = (1 - f_F(p_0))\rho_\Psi(p), \quad (\text{C.2.13})$$

$$\Delta^>(p) = (1 + f_B(p_0))\rho_\phi(p), \quad (\text{C.2.14})$$

with

$$\rho_\Psi(p) = 2\pi \text{sign}(p_0) (\not{p} + m_\Psi) \delta(p^2 - m_\Psi^2), \quad (\text{C.2.15})$$

$$\rho_\phi(p) = 2\pi \text{sign}(p_0) \delta(p^2 - m_\phi^2), \quad (\text{C.2.16})$$

and

$$f_B(\omega) = \frac{1}{e^{\beta\omega} - 1}, \quad (\text{C.2.17})$$

$$f_F(\omega) = \frac{1}{e^{\beta\omega} + 1}, \quad (\text{C.2.18})$$

into (??) and obtain

$$\text{Disc}\Sigma_{\mathbf{q}}^R(\omega) = -i\lambda^2 (e^{-\beta\omega} + 1) \int \frac{d^4p}{(2\pi)^4} S^>(p) \Delta^>(q-p) \quad (\text{C.2.19})$$

$$\begin{aligned} &= -i\lambda^2 f_F(\omega)^{-1} \int \frac{d^4p}{(2\pi)^2} (1 - f_F(p_0))(1 + f_B(\omega - p_0)) \text{sign}(p_0) \text{sign}(\omega - p_0) \\ &\quad \times (\not{p} + m_\Psi) \delta(p^2 - m_\Psi^2) \delta((q-p)^2 - m_\phi^2), \end{aligned} \quad (\text{C.2.20})$$

$$\begin{aligned} &= -i\lambda^2 f_F(-\omega)^{-1} \int \frac{d^4p}{(2\pi)^2} \frac{1}{2\omega_1 2\omega_2} (1 - f_F(p_0))(1 + f_B(\omega - p_0)) \\ &\quad \times \text{sign}(p_0) \text{sign}(\omega - p_0) (\not{p} + m_\Psi) \end{aligned} \quad (\text{C.2.21})$$

$$\times \left(\delta(p_0 - \omega_1) + \delta(p_0 + \omega_1) \right) \left(\delta(\omega - p_0 - \omega_2) + \delta(\omega - p_0 + \omega_2) \right),$$

with $\omega_1 = \sqrt{\mathbf{p}^2 + m_\phi^2}$ and $\omega_2 = \sqrt{(\mathbf{q} - \mathbf{p})^2 + m_\Psi^2}$. Performing the p_0 integration leads to

$$\begin{aligned} \text{Disc}\Sigma_{\mathbf{q}}^R(\omega) = & \\ & - i\lambda^2 f_F(-\omega)^{-1} \int \frac{d^3p}{(2\pi)^2} \frac{1}{2\omega_1 2\omega_2} \left(\right. \\ & (1 - f_F(\omega_1))(1 + f_B(\omega - \omega_1)) \text{sign}(\omega - \omega_1) (\omega_1 \gamma^0 - \mathbf{p}\boldsymbol{\gamma} + m_\Psi) \\ & \quad \times \left(\delta(\omega - \omega_1 - \omega_2) + \delta(\omega - \omega_1 + \omega_2) \right) \\ & - (1 - f_F(-\omega_1))(1 + f_B(\omega + \omega_1)) \text{sign}(\omega + \omega_1) (-\omega_1 \gamma^0 - \mathbf{p}\boldsymbol{\gamma} + m_\Psi) \\ & \quad \left. \times \left(\delta(\omega + \omega_1 - \omega_2) + \delta(\omega + \omega_1 + \omega_2) \right) \right). \end{aligned} \quad (\text{C.2.22})$$

Each δ -function can only be nonzero for one sign of $\omega - \omega_1$. Now we define

$$n_B(\omega) = \frac{1}{e^{\beta|\omega|} - 1}, \quad (\text{C.2.23})$$

$$n_F(\omega) = \frac{1}{e^{\beta|\omega|} + 1}. \quad (\text{C.2.24})$$

We notice that $n_{B,F}(w) = f_{B,F}(w)$ for $w > 0$ and use

$$f_B(-w) + f_B(w) = -1, \quad (\text{C.2.25})$$

$$f_F(-w) + f_F(w) = 1, \quad (\text{C.2.26})$$

and relations as $\text{sign}(\omega - \omega_1) f(\omega - \omega_1) \delta(\omega - \omega_1 - \omega_2) = f(\omega_2) \delta(\omega - \omega_1 - \omega_2)$ to rewrite

$$\begin{aligned} \text{Disc}\Sigma_{\mathbf{q}}^R(\omega) = & \quad (\text{C.2.27}) \\ & - i\lambda^2 \int \frac{d^3p}{(2\pi)^2} \frac{1}{2\omega_1 2\omega_2} \left((1 - n_F(\omega_1) + n_B(\omega_2)) \left((\omega_1 \gamma^0 - \mathbf{p}\boldsymbol{\gamma} + m_\Psi) \delta(\omega - \omega_1 - \omega_2) \right. \right. \\ & \quad \left. \left. + (\omega_1 \gamma^0 + \mathbf{p}\boldsymbol{\gamma} - m_\Psi) \delta(\omega + \omega_1 + \omega_2) \right) \right. \\ & \quad \left. + (n_F(\omega_1) + n_B(\omega_2)) \left((\omega_1 \gamma^0 - \mathbf{p}\boldsymbol{\gamma} + m_\Psi) \delta(\omega - \omega_1 + \omega_2) \right. \right. \\ & \quad \left. \left. + (\omega_1 \gamma^0 + \mathbf{p}\boldsymbol{\gamma} - m_\Psi) \delta(\omega + \omega_1 - \omega_2) \right) \right). \end{aligned}$$

Note that this expression agrees with (3.6) in [116] while it differs from (2.22) in [108]. We are finally interested in leptogenesis which happens at temperatures above the electroweak phase transition, so we can set all fermion masses except the Majorana mass of the right handed neutrino to zero. This immediately means

$$c_I = C_I = \left(\hat{\Sigma}_{(S)} \right)_I = 0. \quad (\text{C.2.28})$$

Now we introduce $n_1 = n_F(\omega_1)$ and $n_2 = n_B(\omega_2)$ to compute A_I and B_I .

$$A_I = \lambda^2 \int \frac{d^3\mathbf{p}}{(2\pi)^3} \frac{2\pi}{8\omega_1 \omega_2} \left((1 - n_1 + n_2) ((\omega\omega_1 - \mathbf{q}\mathbf{p}) \delta(\omega - \omega_1 - \omega_2)) \right.$$

$$\begin{aligned}
& + (\omega\omega_1 + \mathbf{q}\mathbf{p})\delta(\omega + \omega_1 + \omega_2)) \\
& + (n_1 + n_2)((\omega\omega_1 - \mathbf{q}\mathbf{p})\delta(\omega - \omega_1 + \omega_2) \\
& + (\omega\omega_1 + \mathbf{q}\mathbf{p})\delta(\omega + \omega_1 - \omega_2)) .
\end{aligned} \tag{C.2.29}$$

This expression is as a whole antisymmetric in ω which allows to rewrite

$$\begin{aligned}
A_I = \lambda^2 \int \frac{d^3\mathbf{p}}{(2\pi)^3} \frac{2\pi}{8\omega_1\omega_2} & \left(\omega\omega_1((1 - n_1 + n_2)(\delta_1 + \delta_2) + (n_1 + n_2)(\delta_3 + \delta_4)) \right. \\
& \left. - \text{sign}(\omega)\mathbf{q}\mathbf{p}((1 - n_1 + n_2)(\delta_1 - \delta_2) + (n_1 + n_2)(\delta_4 - \delta_3)) \right) ,
\end{aligned} \tag{C.2.30}$$

where

$$\delta_1 = \delta(|\omega| - \omega_1 - \omega_2) , \tag{C.2.31}$$

$$\delta_2 = \delta(|\omega| + \omega_1 + \omega_2) , \tag{C.2.32}$$

$$\delta_3 = \delta(|\omega| + \omega_1 - \omega_2) , \tag{C.2.33}$$

$$\delta_4 = \delta(|\omega| - \omega_1 + \omega_2) . \tag{C.2.34}$$

At this point it is already clear that δ_2 does not contribute. Changing to spherical coordinates $\varphi, \vartheta, |\mathbf{p}|$. The φ integration is trivial and due to $m_\Psi = 0$ one has $|\mathbf{p}| = \omega_1$. Introducing $x = |\mathbf{p}||\mathbf{q}| \cos(\vartheta) = \mathbf{p}\mathbf{q}$ one then has

$$\begin{aligned}
A_I = & \\
& \frac{\lambda^2}{16\pi|\mathbf{q}|} \int_0^\infty d\omega_1 \int_{-\omega_1|\mathbf{q}|}^{\omega_1|\mathbf{q}|} dx \left(\delta(x - x_{01})(\omega\omega_1(1 - n_1 + n_2) - \text{sign}(\omega)x(1 - n_1 + n_2)) \right. \\
& + \delta(x - x_{03})(\omega\omega_1(n_1 + n_2) + \text{sign}(\omega)x(n_1 + n_2)) \\
& \left. + \delta(x - x_{04})(\omega\omega_1(n_1 + n_2) - \text{sign}(\omega)x(n_1 + n_2)) \right) ,
\end{aligned} \tag{C.2.35}$$

where we used $\delta_i = \omega_2\delta(x - x_{0i})$. The x_{0i} can easily be determined as

$$x_{01} = \frac{1}{2}(\mathbf{q}^2 - \omega^2 + m_\phi^2) + \omega_1|\omega| , \tag{C.2.36}$$

$$x_{03} = \frac{1}{2}(\mathbf{q}^2 - \omega^2 + m_\phi^2) - \omega_1|\omega| , \tag{C.2.37}$$

$$x_{04} = x_{01} . \tag{C.2.38}$$

This allows to perform the x integration and to write

$$A_I = \frac{\lambda^2}{16\pi|\mathbf{q}|} \left(\int_1 d\omega_1 (\omega f_1 + g_1) + \int_3 d\omega_1 (\omega f_3 - g_3) + \int_4 d\omega_1 (\omega f_4 + g_4) \right) , \tag{C.2.39}$$

where the subscript in the integral \int_i indicates by which δ_i the integration limits for the ω_1 integration are determined. The f_i and g_i are given by

$$f_1 = \omega_1(1 - n_F(\omega_1) + n_B(|\omega| - \omega_1)) , \tag{C.2.40}$$

$$f_3 = \omega_1 (n_F(\omega_1) + n_B(|\omega| + \omega_1)) , \quad (\text{C.2.41})$$

$$f_4 = \omega_1 (n_F(\omega_1) + n_B(\omega_1 - |\omega|)) , \quad (\text{C.2.42})$$

$$g_1 = \text{sign}(\omega) \left(\frac{1}{2}(\omega^2 - \mathbf{q}^2 - m_\phi^2) - \omega_1 |\omega| \right) (1 - n_F(\omega_1) + n_B(|\omega| - \omega_1)) , \quad (\text{C.2.43})$$

$$g_3 = \text{sign}(\omega) \left(\frac{1}{2}(\omega^2 - \mathbf{q}^2 - m_\phi^2) + \omega_1 |\omega| \right) (n_F(\omega_1) + n_B(|\omega| + \omega_1)) , \quad (\text{C.2.44})$$

$$g_4 = \text{sign}(\omega) \left(\frac{1}{2}(\omega^2 - \mathbf{q}^2 - m_\phi^2) - \omega_1 |\omega| \right) (n_F(\omega_1) + n_B(\omega_1 - |\omega|)) . \quad (\text{C.2.45})$$

$$(\text{C.2.46})$$

It is easy to see from (C.2.6), (C.2.7) and (C.2.35) that

$$B_I = \frac{\lambda^2}{16\pi|\mathbf{q}|} \left(\int_1 d\omega_1 f_1 + \int_3 d\omega_1 f_3 + \int_4 d\omega_1 f_4 \right) , \quad (\text{C.2.47})$$

f_1 and g_1 are contributinos from decay and inverse decay of the external fermion and can lead to a zero temperature part if kinematically allowed while f_3 , f_4 , g_3 and g_4 come from scatterings in the plasma (Landau damping). It is interesting to note that

$$f_1 = f_4 , \quad (\text{C.2.48})$$

$$g_1 = g_4 , \quad (\text{C.2.49})$$

despite the fact that they originate from different processes¹. The f_i are symmetric in ω , the g_i antisymmetric. In the rest frame of the bath (C.2.9) can be written as

$$a = \frac{B\omega - A}{\mathbf{q}^2} , \quad (\text{C.2.50})$$

$$b = \frac{\omega(A - B\omega)}{\mathbf{q}^2} + B , \quad (\text{C.2.51})$$

$$c = C , \quad (\text{C.2.52})$$

B_I is obviously symmetric in ω while A_I is antisymmetric. As a consequence, a_I is antisymmetric while b_I is symmetric which seems consistent with [109]. The stem functions of all f_i , g_i are known analytically, so the only remaining difficult task is the determination of the proper integration limits.

Limits for $\delta_1 = \delta(|\omega| - \omega_1 - \omega_2)$

In order for x_{01} to actually really be a zero point, the condition

$$|\omega| - \omega_1 > 0 , \quad (\text{C.2.53})$$

has to be fulfilled. In any case,

$$\omega_1 > m_\Psi = 0 . \quad (\text{C.2.54})$$

¹Note that despite (C.2.48,C.2.49) the Landau damping terms f_4 , g_4 never lead to a contribution to Σ at zero temperature while the decay and inverse decay parts f_1 and g_1 can contribute as expected. The reason lies in the different integration limits, see (C.2.53) and (C.2.62)

In order for the x -integral to be nonzero it requires

$$|x_{01}| < \omega_1 |\mathbf{q}|. \quad (\text{C.2.55})$$

The solutions to $|x_{01}| = \omega_1 |\mathbf{q}|$ are

$$\omega_{\pm} = \frac{1}{2} \frac{q^2 - m_{\phi}^2}{q^2} (|\omega| \pm |\mathbf{q}|), \quad (\text{C.2.56})$$

with $q^2 = \omega^2 - \mathbf{q}^2$. One has three different regimes:

a) For $0 < |\omega| < |\mathbf{q}|$ and $\omega_1 > 0$ only ω_+ is a solution, and it puts a lower bound on ω_1 in order for the inequality (C.2.55) to be fulfilled, leading to $\omega_1 > \omega_+$. On the other hand one has the condition (C.2.53), and since for $|\omega| < |\mathbf{q}|$ always $\omega_+ > |\omega|$, there is no contribution to the integral from this region.

b) For $|\mathbf{q}| < |\omega| < \sqrt{\mathbf{q}^2 + m_{\phi}^2}$ one has $\omega_{\pm} < 0$ and none of them makes (C.2.60) an equality.

c) For $|\omega| > \sqrt{\mathbf{q}^2 + m_{\phi}^2}$ both ω_{\pm} are always smaller than $|\omega|$ and (C.2.60) leads to $\omega_- < |\omega| < \omega_+$. Therefore

$$\int_1 d\omega_1 = \theta(q^2 - m_{\phi}^2) \int_{\omega_-}^{\omega_+} d\omega_1 \quad (\text{C.2.57})$$

Limits for $\delta_3 = \delta(|\omega| + \omega_1 - \omega_2)$

Here one has the three conditions

$$|\omega| + \omega_1 > 0, \quad (\text{C.2.58})$$

$$\omega_1 > m_{\Psi} = 0, \quad (\text{C.2.59})$$

$$|x_{03}| < \omega_1 |\mathbf{q}|. \quad (\text{C.2.60})$$

This time (C.2.60) has made an equality for $\omega_1 = -\omega_{\pm}$. Again the same regimes have to be distinguished.

a) For $|\omega| < |\mathbf{q}|$ only $-\omega_-$ makes (C.2.60) an equality while $-\omega_+$ is negative and not a solution. $-\omega_-$ is positive as required by (C.2.59) and forms a lower bound.

b) For $|\mathbf{q}| < |\omega| < \sqrt{\mathbf{q}^2 + m_{\phi}^2}$ both $-\omega_{\pm}$ are positive and solutions, due to its first order pole at $|\omega| = |\mathbf{q}|$ the solution $-\omega_+$ is now the larger one and in fact forms an upper limit, leading to $-\omega_- < \omega_1 < -\omega_+$.

c) For $|\omega| > \sqrt{\mathbf{q}^2 + m_\phi^2}$ both $-\omega_\pm$ are negative and not equality solutions of (C.2.60), there is no contribution to the integral from here.

Therefore

$$\int_3 d\omega_1 = \theta(-q^2) \int_{-\omega_-}^{\infty} d\omega_1 + \theta(q^2)\theta(m_\phi^2 - q^2) \int_{-\omega_-}^{-\omega_+}. \quad (\text{C.2.61})$$

Limits for $\delta_4 = \delta(|\omega| - \omega_1 + \omega_2)$

The situation here is exactly the same as for δ_1 , in particular $x_{04} = x_{01}$, except that the condition $|\omega| - \omega_1 > 0$ has to be replaced by

$$|\omega| - \omega_1 < 0, \quad (\text{C.2.62})$$

making $\omega_1 > |\omega|$. Again for $|\omega| < |\mathbf{q}|$ only ω_+ fulfills (C.2.55), imposing a lower bound on ω_1 and for $|\omega| > \sqrt{\mathbf{q}^2 + m_\phi^2}$ both ω_\pm are solutions with ω_+ being the upper and ω_- being the lower bound here while for $0 < q^2 < m_\phi^2$ none of ω_\pm is a valid solution. But this time the condition (C.2.62) selects out the region $q^2 < 0$ and one has

$$\int_4 d\omega_1 = \theta(-q^2) \int_{\omega_+}^{\infty} d\omega_1. \quad (\text{C.2.63})$$

Altogether this leads to

$$\begin{aligned} A_I = & \frac{\lambda^2}{16\pi|\mathbf{q}|} \left(\theta(q^2 - m_\phi^2) \left[\omega F_1 + G_1 \right]_{\omega_-}^{\omega_+} \right. \\ & + \theta(-q^2) \left[\omega F_3 - G_3 \right]_{-\omega_-}^{\infty} + \theta(q^2)\theta(m_\phi^2 - q^2) \left[\omega F_3 - G_3 \right]_{-\omega_-}^{-\omega_+} \\ & \left. + \theta(-q^2) \left[\omega F_4 + G_4 \right]_{\omega_+}^{\infty} \right), \end{aligned} \quad (\text{C.2.64})$$

and

$$\begin{aligned} B_I = & \frac{\lambda^2}{16\pi|\mathbf{q}|} \left(\theta(q^2 - m_\phi^2) \left[F_1 \right]_{\omega_-}^{\omega_+} \right. \\ & + \theta(-q^2) \left[F_3 \right]_{-\omega_-}^{\infty} + \theta(q^2)\theta(m_\phi^2 - q^2) \left[F_3 \right]_{-\omega_-}^{-\omega_+} \\ & \left. + \theta(-q^2) \left[F_4 \right]_{\omega_+}^{\infty} \right), \end{aligned} \quad (\text{C.2.65})$$

with

$$\begin{aligned} F_1 = & \frac{\omega_1}{\beta} \left(\ln(e^{\beta\omega_1} + 1) - \ln(1 - e^{\beta(\omega_1 - |\omega|)}) \right) \\ & + \frac{1}{\beta^2} \left(\text{Li}_2(-e^{\beta\omega_1}) - \text{Li}_2(e^{\beta(\omega_1 - |\omega|)}) \right), \\ F_3 = & \frac{\omega_1}{\beta} \left(\ln(1 - e^{\beta(\omega_1 + |\omega|)}) - \ln(e^{\beta\omega_1} + 1) \right) \end{aligned} \quad (\text{C.2.66})$$

$$+\frac{1}{\beta^2}\left(\text{Li}_2(e^{\beta(\omega_1+|\omega|)}) - \text{Li}_2(-e^{\beta\omega_1})\right), \quad (\text{C.2.67})$$

$$F_4 = F_1, \quad (\text{C.2.68})$$

and

$$\begin{aligned} G_1 &= \text{sign}(\omega)\frac{m_\phi^2 - q^2}{2\beta}\left(-\ln(1 + e^{\beta\omega_1}) + \ln(e^{\beta\omega_1} - e^{\beta|\omega|})\right) \\ &\quad + \frac{\omega\omega_1}{\beta}\left(\ln(1 - e^{\beta(\omega_1-|\omega|)}) - \ln(1 + e^{\beta\omega_1})\right) \\ &\quad + \frac{\omega}{\beta^2}\left(\text{Li}_2(e^{\beta(\omega_1-|\omega|)}) - \text{Li}_2(-e^{\beta\omega_1})\right), \end{aligned} \quad (\text{C.2.69})$$

$$\begin{aligned} G_3 &= \text{sign}(\omega)\frac{m_\phi^2 - q^2}{2\beta}\left(\ln(1 + e^{\beta\omega_1}) - \ln(e^{\beta(\omega_1+|\omega|)} - 1)\right) \\ &\quad + \frac{\omega\omega_1}{\beta}\left(\ln(1 - e^{\beta(\omega_1+|\omega|)}) - \ln(1 + e^{\beta\omega_1})\right) \\ &\quad + \frac{\omega}{\beta^2}\left(\text{Li}_2(e^{\beta(\omega_1+|\omega|)}) - \text{Li}_2(-e^{\beta\omega_1})\right), \end{aligned} \quad (\text{C.2.70})$$

$$G_4 = G_1. \quad (\text{C.2.71})$$

The F_i as displayed here are not real in all areas of the parameter space due to the choice of different branches of the (di)logarithms, but the additional terms always cancel since the choice of branch is always the same at both integration limits in (C.2.64,C.2.65).

Checks and Comparison to the Literature

In order to compare with the literature we now introduce the quantities

$$\Sigma_{(\pm)} = \frac{1}{2}\text{Tr}(\Sigma^R \Lambda_\pm \gamma_0) = a(\omega \pm |\mathbf{q}|) + b, \quad (\text{C.2.72})$$

with projectors

$$\Lambda_\pm = (1 \pm \gamma_0 \frac{\mathbf{q}}{|\mathbf{q}|} \boldsymbol{\gamma}). \quad (\text{C.2.73})$$

The figures C.3 and C.4 show $|\text{Im}\Sigma_{(+) }|$ for finite and zero spacial momentum \mathbf{q} and the same parameters as in figure 5 in [116]. The agreement is very good up to an overall minus sign that is hidden by plotting the absolute value. The imaginary part is in general to be understood in the discontinuity sense,

$$\text{Im}\Sigma_{(+)} = \frac{1}{2i} (\Sigma_{(+)}(\omega + i\epsilon) - \Sigma_{(+)}(\omega - i\epsilon)), \quad (\text{C.2.74})$$

meaning that the γ^μ matrices are treated as 'real' symbols and factors i that appear in their elements in any representation remain untouched. For $\Sigma_{(+)}$ this does not

make a difference since the trace has been taken, but for $\hat{\Sigma}$ this has to be kept in mind. From the analytic expression for $|\text{Im}\Sigma_{(+)}|$ one can obtain $|\text{Re}\Sigma_{(+)}|$ via the spectral representation.

$|\text{Re}\Sigma_{(+)}|$ for zero momentum is shown in figure C.5 and, up to the overall minus sign mentioned already, agrees perfectly with figure 4 in [116].

To perform a final consistency check, we compare our analytic formulae (C.2.64) and (C.2.65) to numerical solutions of (C.2.35) and its analogon for B_I . They agree very well as shown in figure C.6 and C.7.

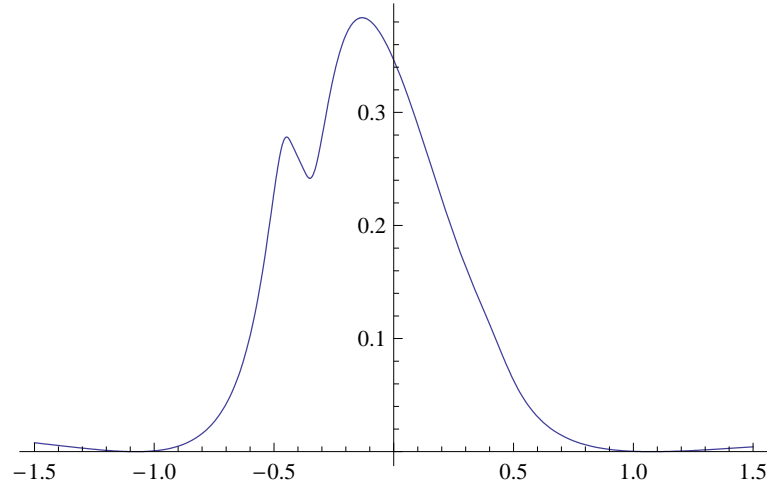


Figure C.3: $|\text{Im}\Sigma_{(+)}|$ as a function of ω for $|\mathbf{q}| = 0.4m_\phi$ and $T = 1.5m_\phi$ with $\lambda = 1$ for convenience

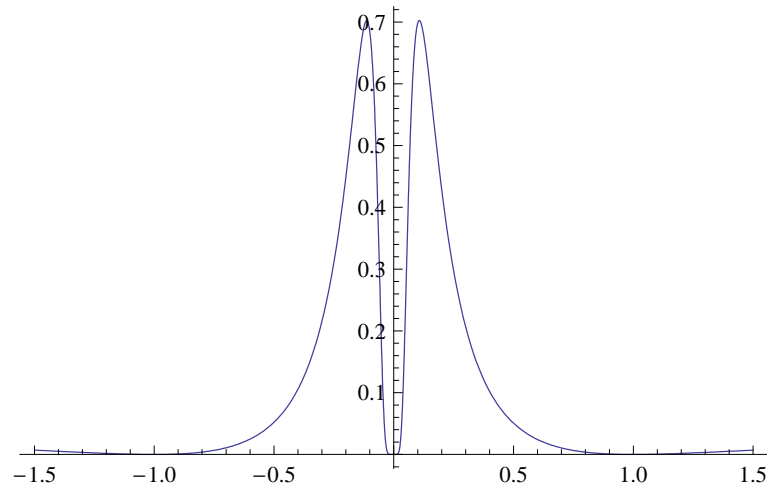


Figure C.4: $|\text{Im}\Sigma_{(+)}|$ as a function of ω for $|\mathbf{q}| = 0$ and $T = 1.5m_\phi$ with $\lambda = 1$ for convenience

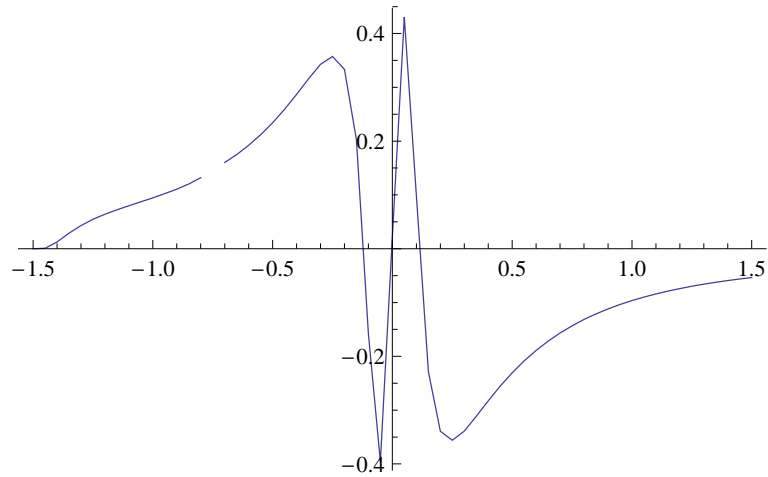


Figure C.5: $\text{Re}\Sigma_{(+)}$ as a function of ω for $|\mathbf{q}| = 0$ and $T = 1.5m_\phi$ with $\lambda = 1$ for convenience

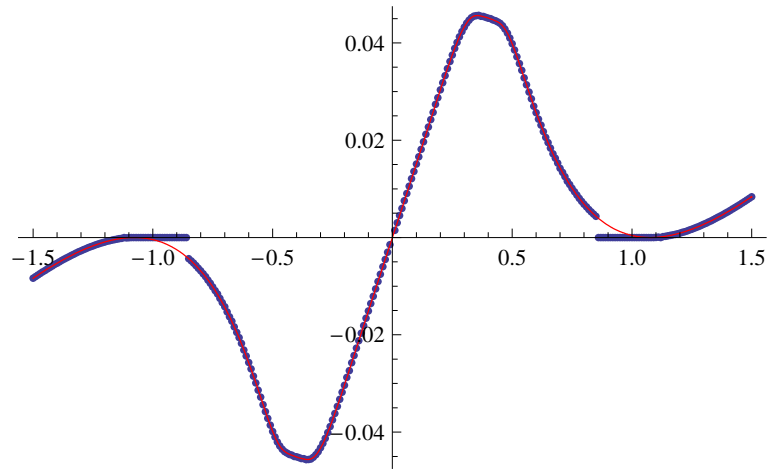


Figure C.6: comparison of the analytic formula (C.2.64) for A_I to the numerical solution as a function of ω for $|\mathbf{q}| = 0.4m_\phi$ and $T = 1.5m_\phi$ with $\lambda = 1$ for convenience

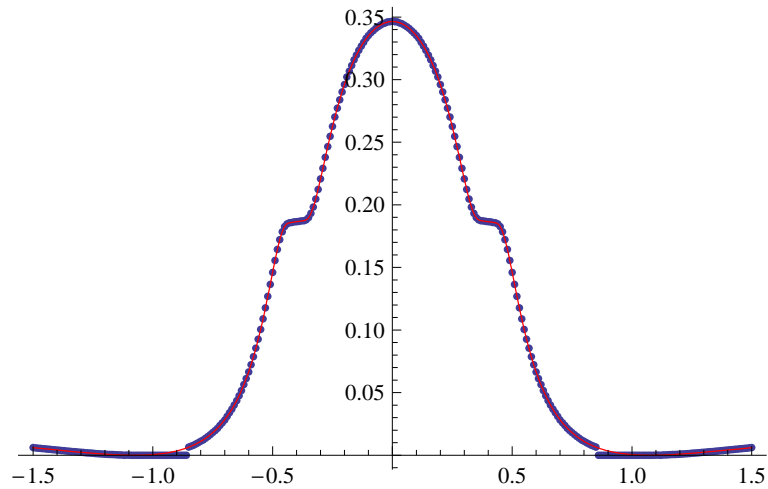


Figure C.7: comparison of the analytic formula (C.2.65) for B_I to the numerical solution as a function of ω for $|\mathbf{q}| = 0.4m_\phi$ and $T = 1.5m_\phi$ with $\lambda = 1$ for convenience

C.3 Computation of Γ

In the case of a Majorana neutrino in a Higgs lepton bath there appear additional factors C , P_L and P_R due to the Majorana nature of the particle and the coupling. This, however, does not change the analytic form of the self energy so that the pole structure of the spectral function is not influenced.

$$\rho_N = \frac{q(1+a_+) + \not{u}b_+ + M}{D_+} - \frac{q(1+a_-) + \not{u}b_- + M}{D_-}, \quad (\text{C.3.1})$$

with

$$D_{\pm} = q^2(1+a_{\pm})^2 + qu2b_{\pm}(1+a_{\pm}) + b_{\pm}^2 - M^2, \quad (\text{C.3.2})$$

$a_{\pm} = a_R \pm a_I$ and $b_{\pm} = b_R \pm b_I$. The D_{\pm} here have been written in the denominator because they commute with the numerator in the flavourless case. Furthermore the scalar particle in the thermal bath has a complex structure, but since the backreaction is small one can neglect the chemical potential induced by the CP violation in the heavy neutrino coupling. Then the Higgs can be treated like two real scalars. Finally, the coupling in this case is so tiny that the spectral function is effectively a δ function at $\pm\omega_{\mathbf{q}}$ with some finite Γ . A Lorentz decomposition of (C.3.1) gives the following coefficients

$$\begin{aligned} & \frac{1}{D_+D_-}((D_- - D_+)\gamma^0((D_-(1+a_+) - D_+(1+a_-))\omega - (D_-b_+ - D_+b_-)) \\ & - \gamma^i q_i (D_-(1+a_+) - D_+(1+a_-))M(D_- - D_+)). \end{aligned} \quad (\text{C.3.3})$$

Expanding the above of (C.3.1) to first order in a and b

$$\begin{aligned} & \frac{1}{D_+D_-}(\gamma^0(-2i)(a_I\omega(q^2 + M^2) + b_I(\omega^2 + \omega_{\mathbf{q}}^2)) \\ & + \not{\boldsymbol{\gamma}}\mathbf{p}2i(2b_I\omega + a_I(q^2 + M^2)) + M(-4i)(a_Iq^2 + b_I\omega)), \end{aligned} \quad (\text{C.3.4})$$

In order to obtain the pole structure we also expand D_{\pm} in a and b . This leads to

$$\begin{aligned} D_{\pm} &= \omega^2 - \omega_{\mathbf{q}}^2 + 2(\omega b_R + a_R(\omega^2 - \mathbf{q}^2) \pm i(b_I\omega + a_I(\omega^2 - \mathbf{q}^2))), \\ &= \omega^2 - \omega_{\mathbf{q}}^2 + 2(b_{\pm}\omega + a_{\pm}(\omega^2 - \mathbf{q}^2)). \end{aligned} \quad (\text{C.3.5})$$

The spectral propagator G^- will be computed after performing a Fourier transform in ω on (C.3.1). In principle the ω dependence of a and b is very complicated, but the extreme smallness of coupling gives ρ_N an almost δ function like shape with extremely narrow peaks near $\omega = \pm\omega_{\mathbf{q}}$. Since the integral is strongly dominated by the region around those peaks one can replace $a(\omega)$ and $b(\omega)$ by $a(\pm\omega_{\mathbf{q}})$ and $b(\pm\omega_{\mathbf{q}})$, making D_{\pm} second order polynomials. Now the integral can easily be evaluated using Cauchy's theorem. The solutions for $D_+ = 0$ are

$$\omega = \pm\sqrt{\omega_{\mathbf{q}}^2 - 2(\pm\omega_{\mathbf{q}}b_+(\pm\omega_{\mathbf{q}}) + (\omega_{\mathbf{q}}^2 - \mathbf{q}^2)a_+(\pm\omega_{\mathbf{q}}))}. \quad (\text{C.3.6})$$

We can neglect the real parts of a and b since they are small compared to $\omega_{\mathbf{q}}$, use the symmetry properties $a_I(-\omega) = -a_I(\omega)$ and $b_I(-\omega) = b_I(\omega)$ and expand to square root to find the poles

$$\omega_{01} = \omega_{\mathbf{q}} - i \left(b_I + a_I \frac{M^2}{\omega_{\mathbf{q}}} \right), \quad (\text{C.3.7})$$

$$\omega_{02} = -\omega_{\mathbf{q}} + i \left(b_I + a_I \frac{M^2}{\omega_{\mathbf{q}}} \right) = -\omega_{01}. \quad (\text{C.3.8})$$

In the same way we obtain from D_- :

$$\omega_{03} = \omega_{\mathbf{q}} + i \left(b_I + a_I \frac{M^2}{\omega_{\mathbf{q}}} \right) = \omega_{01}^*, \quad (\text{C.3.9})$$

$$\omega_{04} = -\omega_{\mathbf{q}} - i \left(b_I + a_I \frac{M^2}{\omega_{\mathbf{q}}} \right) = -\omega_{01}^*. \quad (\text{C.3.10})$$

with $a_I = a_I(\omega_{\mathbf{q}})$ and $b_I = b_I(\omega_{\mathbf{q}})$. Two of these poles are in the upper and two are in the lower half plane.

The time-dependent spectral function will then be given by the inverse Fourier transformation

$$G_{\mathbf{q}}^-(y) = \int \frac{d\omega}{2\pi} e^{-i\omega y} \rho_N(\omega, \mathbf{q}), \quad (\text{C.3.11})$$

When performing Cauchy integration, the convergence of the function is given by the imaginary part of the pole. Choosing the right contour one is lead to define the decay width

$$\Gamma_{\mathbf{q}} = -2 \left(b_I + a_I \frac{M^2}{\omega_{\mathbf{q}}} \right)_{\omega=\omega_{\mathbf{q}}} \quad (\text{C.3.12})$$

$\Gamma_{\mathbf{q}}$ can, for given masses, be plotted as a function of \mathbf{q} .

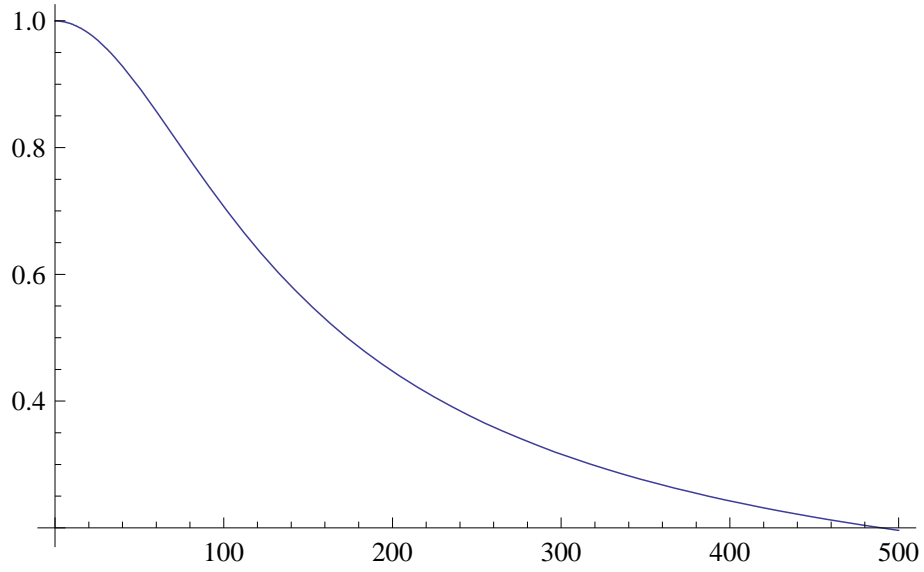


Figure C.8: The decay rate $\Gamma_{\mathbf{q}=0}$ normalized to $\Gamma_0 = \frac{K_{11}M_1}{8\pi}$ as a function of \mathbf{q} .

C.4 Calculation of the 2-loop self-energy

a) First diagram

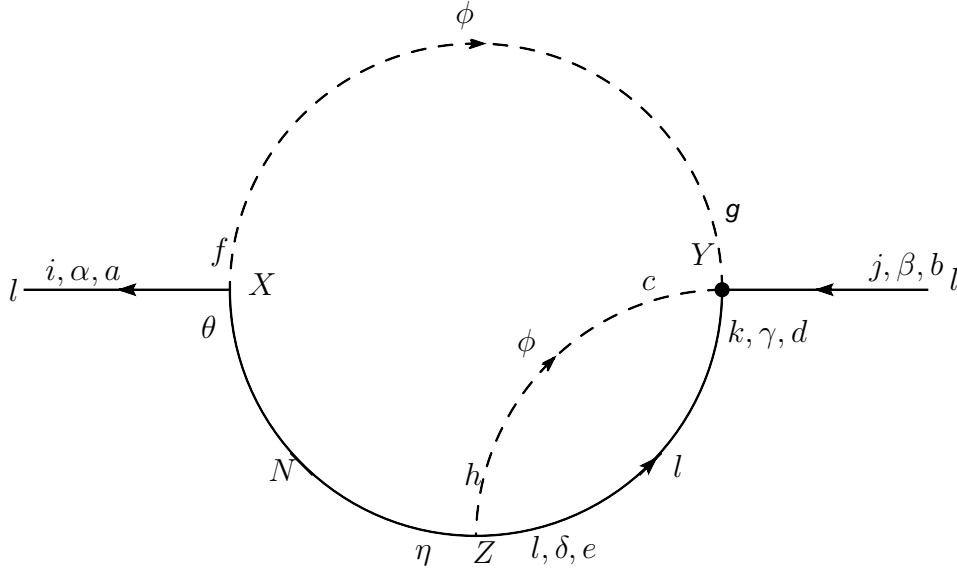


Figure C.9: 2-loop graph a)

Using Feynman rules we obtain

$$\begin{aligned} \Pi_{ij}^{ab}(x, y) = & -\frac{1}{2} \int d^4 z [i\lambda_{i1}^* \epsilon_{af} (P_R)_{\alpha\theta}] [iG_{\eta\theta}(z, x)] [i\lambda_{l1}^* \epsilon_{ch} (P_R)_{\delta\eta}] [i\delta_{kl} \delta_{de} S_{\gamma\delta}(y, z)] \\ & \times [i\eta_{kj} (\epsilon_{dc} \epsilon_{bg} + \epsilon_{dg} \epsilon_{bc}) (CP_L)_{\gamma\beta}] [i\Delta(y, z) \delta_{ch}] [i\Delta(y, x) \delta_{gf}] . \end{aligned} \quad (\text{C.4.1})$$

Rearranging

$$\begin{aligned} \Pi_{ij}^{ab}(x, y) = & -\frac{i}{2} \int d^4 z \epsilon_{ag} \epsilon_{dc} (\epsilon_{dc} \epsilon_{bg} + \epsilon_{dg} \epsilon_{bc}) \lambda_{i1}^* \lambda_{k1}^* \eta_{kj} \\ & \times (P_R)_{\alpha\theta} G_{\eta\theta}(z, x) (P_R)_{\delta\eta} S_{\gamma\delta}(y, z) (CP_L)_{\gamma\beta} \Delta(y, z) \Delta(y, x) . \end{aligned} \quad (\text{C.4.2})$$

Going to matrix for we get

$$\Pi_{ij}^{ab}(x, y) = -\frac{i}{2} \int d^4 z \epsilon_{ag} \epsilon_{dc} (\epsilon_{dc} \epsilon_{bg} + \epsilon_{dg} \epsilon_{bc}) \lambda_{i1}^* \lambda_{k1}^* \eta_{kj} \quad (\text{C.4.3})$$

$$\times P_R G^T(z, x) P_R^T S^T(y, z) CP_L \Delta(y, z) \Delta(y, x) . \quad (\text{C.4.4})$$

Using $G^T(z, x) = -G(x, z)$, introducing η_{kj} , renaming indices and suming over them we have

$$\Pi_{ij}^{ab}(x, y) = -\frac{i}{2} \sum_{k,p,c,d,e} \int d^4 z \epsilon_{ac} \epsilon_{ed} (\epsilon_{ed} \epsilon_{bc} + \epsilon_{ec} \epsilon_{bd}) \frac{1}{M_p} \lambda_{i1}^* \lambda_{k1}^* \lambda_{kp} \lambda_{pj} \quad (\text{C.4.5})$$

$$\times P_R G(x, z) P_R^T S^T(y, z) CP_L \Delta(y, z) \Delta(y, x) . \quad (\text{C.4.6})$$

Note that the propagator of the lepton field depends on P_L , and enters in $S^T(y, z) CP_L \rightarrow S^T(y, z) P_L^T CP_L$, this will not have any consequence when we use that $P_L^T C = CP_L$. Now, using some properties of ϵ

$$\epsilon_{ij} \epsilon_{mn} = \delta_{im} \delta_{jn} - \delta_{in} \delta_{jm} , \quad (\text{C.4.7})$$

$$\epsilon_{ac} \epsilon_{bc} = \delta_{ac} , \quad (\text{C.4.8})$$

$$\epsilon_{ac} \epsilon_{ed} \epsilon_{ec} \epsilon_{bd} = \delta_{ab} . \quad (\text{C.4.9})$$

These will lead us to

$$\begin{aligned} \Pi_{ij}^{ab}(x, y) = & -\frac{3i}{2} \sum_{k,p} \int d^4 z \frac{1}{M_p} \lambda_{i1}^* \lambda_{k1}^* \lambda_{kp} \lambda_{pj} \\ & \times P_R G(x, z) P_R^T S^T(y, z) CP_L \Delta(y, z) \Delta(y, x) \delta_{ab} . \end{aligned} \quad (\text{C.4.10})$$

In order to continue, we use the fact that $P_L^T C = CP_L$, $P_R^T C = CP_R$ and because the lepton is massless ($m_l = 0$), so that $S^T C = -CS$, we have

$$\begin{aligned} \Pi_{ij}^{ab}(x, y) = & -\frac{3i}{2} \sum_{k,p} \int d^4 z \frac{1}{M_p} \lambda_{i1}^* \lambda_{k1}^* \lambda_{kp} \lambda_{pj} \\ & \times P_R G(x, z) CP_R S(y, z) P_L \Delta(y, z) \Delta(y, x) \delta_{ab} . \end{aligned} \quad (\text{C.4.11})$$

In a general form, we can express the propagator of the Majorana neutrino as

$$G(x, z) = \left(\frac{T_{\mu\nu} \sigma^{\mu\nu} + V_\mu \Gamma^\mu + T_{\mu\nu} \sigma^{\mu\nu} + M}{D} \right) C^{-1} , \quad (\text{C.4.12})$$

where $C^* = -C$, D is a scalar denominator, V_μ a vector part and M the mass of the Majorana neutrino. We can see that there is no tensor part, so after some algebra we are left only with the scalar part of the propagator

$$P_R \left(\frac{V_\mu \Gamma^\mu + M}{D} \right) C^{-1} CP^R = -\frac{M}{D} P_R , \quad (\text{C.4.13})$$

$$= -G_S(x, z)P_R, \quad (\text{C.4.14})$$

where $G_S(x, s) = M/D$ is the scalar part of the Majorana propagator. We finally obtain

$$\begin{aligned} \Pi_{ij}^{ab}(x, y) = & -\frac{3i}{2} \sum_{k,p} \int d^4z \frac{1}{M_p} \lambda_{i1}^* \lambda_{k1}^* \lambda_{kp} \lambda_{pj} \\ & \times G_S S(x, z) S(y, z) P_L \Delta(y, z) \Delta(y, x) \delta_{ab}. \end{aligned} \quad (\text{C.4.15})$$

Writing $\lambda_{ij}^{ab} = -\frac{3}{2} \sum_{k,p} \frac{1}{M_p} \lambda_{i1}^* \lambda_{k1}^* \lambda_{kp} \lambda_{pj} \delta_{ab}$, and $dZ = dt_z d^3\mathbf{z}$ we have after performing momentum Fourier transforms

$$\begin{aligned} \Pi_{ij}^{ab}(x, y) = & i\lambda_{ij}^{ab} \int dt_z d^3\mathbf{z} \frac{d^3\mathbf{q}}{(2\pi)^3} e^{-i\mathbf{q}(\mathbf{y}-\mathbf{x})} \frac{d^3\mathbf{q}'}{(2\pi)^3} e^{-i\mathbf{q}'(\mathbf{y}-\mathbf{z})} \frac{d^3\mathbf{k}'}{(2\pi)^3} e^{-i\mathbf{k}'(\mathbf{y}-\mathbf{z})} \frac{d^3\mathbf{p}}{(2\pi)^3} e^{-i\mathbf{p}(\mathbf{x}-\mathbf{z})} \\ & \times G_{S\mathbf{p}}(t_x, t_z) C S_{\mathbf{k}'}(t_y - t_z) P_L \Delta_{\mathbf{q}'}(t_y - t_z) \Delta_{\mathbf{q}}(t_y - t_x). \end{aligned} \quad (\text{C.4.16})$$

We can arrange some exponentials to have

$$\int d^3\mathbf{z} e^{i(\mathbf{p}+\mathbf{q}'+\mathbf{k}')\mathbf{z}} = (2\pi)^3 \delta(\mathbf{q}' + \mathbf{k}' + \mathbf{p}). \quad (\text{C.4.17})$$

So now for the self energy can be written as

$$\begin{aligned} \Pi_{ij}^{ab}(x, y) = & i\lambda_{ij}^{ab} \int dt_z \frac{d^3\mathbf{q}}{(2\pi)^3} \frac{d^3\mathbf{q}'}{(2\pi)^3} \frac{d^3\mathbf{p}}{(2\pi)^3} e^{i(\mathbf{p}-\mathbf{q})(\mathbf{y}-\mathbf{x})} \\ & \times G_{S\mathbf{p}}(t_x, t_z) C S_{-(\mathbf{p}+\mathbf{q}')} (t_y - t_z) P_L \Delta_{\mathbf{q}'}(t_y - t_z) \Delta_{\mathbf{q}}(t_y - t_x). \end{aligned} \quad (\text{C.4.18})$$

Introducing the external momentum $\mathbf{k} = \mathbf{p} - \mathbf{q}$, we can make a Fourier transformation

$$\begin{aligned} \Pi_{\mathbf{k}ij}^{ab}(t_x, t_y) = & -i \int d^3(\mathbf{y} - \mathbf{x}) e^{i\mathbf{k}(\mathbf{y}-\mathbf{x})} \Pi_{ij}^{ab}(x, y), \\ = & i\lambda_{ij}^{ab} \int dt_z \frac{d^3\mathbf{q}}{(2\pi)^3} \frac{d^3\mathbf{q}'}{(2\pi)^3} \frac{d^3\mathbf{p}}{(2\pi)^3} d^3(\mathbf{z} - \mathbf{x}) e^{i(\mathbf{p}-\mathbf{q}+\mathbf{k})(\mathbf{y}-\mathbf{x})} \\ & \times G_{S\mathbf{p}}(t_x, t_z) C S_{-(\mathbf{p}+\mathbf{q}')} (t_y - t_z) P_L \Delta_{\mathbf{q}'}(t_y - t_z) \Delta_{\mathbf{q}}(t_y - t_x). \end{aligned} \quad (\text{C.4.19})$$

the integration over $d^3(\mathbf{y} - \mathbf{x})$ will give us a delta function $(2\pi)^3 \delta(\mathbf{K} - \mathbf{k} + \mathbf{q})$, so we are left with

$$\begin{aligned} -i\Pi_{\mathbf{k}ij}^{ab}(t_x, t_y) = & i\lambda_{ij}^{ab} \int dt_z \frac{d^3\mathbf{q}'}{(2\pi)^3} \frac{d^3\mathbf{p}}{(2\pi)^3} \\ & \times G_{S\mathbf{p}}(t_x, t_z) C S_{-(\mathbf{p}+\mathbf{q}')} (t_y - t_z) P_L \Delta_{\mathbf{q}'}(t_y - t_z) \Delta_{\mathbf{p}-\mathbf{k}}(t_y - t_x). \end{aligned} \quad (\text{C.4.20})$$

Going now to the countour we have

$$\begin{aligned} \Pi_{\mathbf{K}ij}^{ab>}(t_x, t_y) = & i\lambda_{ij}^{ab} \int dt_z \frac{d^3\mathbf{k}_1}{(2\pi)^3} \frac{d^3\mathbf{k}}{(2\pi)^3} \\ & \times [G_{S\mathbf{k}}^{>}(t_x, t_z) C S_{-(\mathbf{k}+\mathbf{k}_1)}^{11}(t_y - t_z) P_L \Delta_{\mathbf{k}_1}^{11}(t_y - t_z) \Delta_{\mathbf{k}-\mathbf{K}}^{<}(t_y - t_x) \\ & - G_{S\mathbf{k}}^{22}(t_x, t_z) C S_{-(\mathbf{k}+\mathbf{k}_1)}^{<}(t_y - t_z) P_L \Delta_{\mathbf{k}_1}^{<}(t_y - t_z) \Delta_{\mathbf{k}-\mathbf{K}}^{<}(t_y - t_x)]. \end{aligned} \quad (\text{C.4.21})$$

$$\begin{aligned} \Pi_{\mathbf{K}ij}^{ab<}(t_x, t_y) = & i\lambda_{ij}^{ab} \int dt_z \frac{d^3\mathbf{k}_1}{(2\pi)^3} \frac{d^3\mathbf{k}}{(2\pi)^3} \\ & \times [G_{S\mathbf{k}}^{11}(t_x, t_z) C S_{-(\mathbf{k}+\mathbf{k}_1)}^{>}(t_y - t_z) P_L \Delta_{\mathbf{k}_1}^{>}(t_y - t_z) \Delta_{\mathbf{k}-\mathbf{K}}^{>}(t_y - t_x) \\ & - G_{S\mathbf{k}}^{<}(t_x, t_z) C S_{-(\mathbf{k}+\mathbf{k}_1)}^{22}(t_y - t_z) P_L \Delta_{\mathbf{k}_1}^{22}(t_y - t_z) \Delta_{\mathbf{k}-\mathbf{K}}^{>}(t_y - t_x)]. \end{aligned} \quad (\text{C.4.22})$$

b) Second diagram

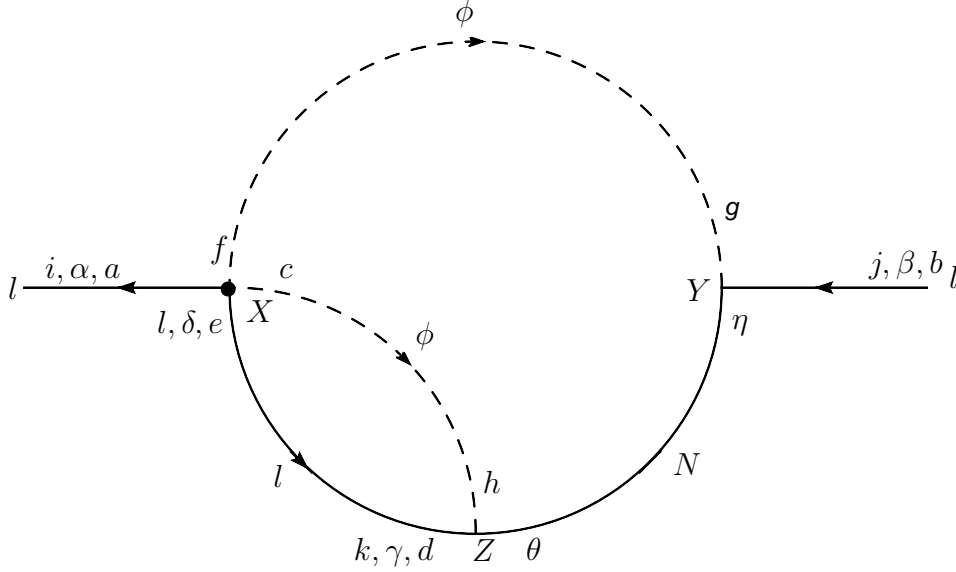


Figure C.10: 2-loop graph b)

$$\begin{aligned} \Pi_{ij}^{ab} = & -\frac{1}{2} \int d^4z [i\eta_{il}^*(\epsilon_{af}\epsilon_{ec} + \epsilon_{ac}\epsilon_{ef})(P_R C)_{\alpha\delta}] [i\delta_{lk}\delta_{ed}S_{\gamma\delta}(z, x)] [i\lambda_{k1}\epsilon_{dh}(CP_L)_{\theta\gamma}] \\ & \times [iG_{\eta\theta}(y, z)] [i\lambda_{j1}\epsilon_{bg}(CP_L)_{\theta\gamma}] [i\Delta(y, x)\delta_{gf}] [i\Delta(z, x)\delta_{ch}] ; \dots \quad (\text{C.4.23}) \end{aligned}$$

Which will give

$$\Pi_{ij}^{ab} = -\frac{3i}{2} \sum_{k,p} \int d^4z \frac{1}{M_p} \lambda_{ip}^* \lambda_{pl}^* \lambda_{l1} \lambda_{j1} S(z, x) G_S(z, y) CP_L \Delta(z, x) \Delta(y, x) \delta_{ab} . \quad (\text{C.4.24})$$

All Green's functions so far are taken on the Keldysh contour. The $\int d^4z$ has to be read as $\int_C dt_z \int_{-\infty}^{-\infty} dz^3$. In order to practically perform the integration one has to break the Keldysh contour into a forward and backward piece. Then propagators and self energies turn into matrices S_{ij} , Σ_{ij} etc. The indices indicate the part of the contour that the first and second time argument on the function lies on.

$$\begin{aligned} \Pi_{\mathbf{k}ij}^{ab>}(t_x, t_y) = & i (\lambda_{ij}^{ab})^* \int dt_z \frac{d^3\mathbf{q}'}{(2\pi)^3} \frac{d^3\mathbf{p}}{(2\pi)^3} \quad (\text{C.4.25}) \\ & \times [S_{-(\mathbf{p}+\mathbf{q}')}^{22}(t_z - t_x) G_{S\mathbf{k}}^{>}(t_z, t_x) CP_L \Delta_{\mathbf{q}'}^{22}(t_z - t_x) \Delta_{\mathbf{p}-\mathbf{k}}^{<}(t_y - t_x) \\ & - S_{-(\mathbf{p}+\mathbf{q}')}^{<}(t_z - t_x) G_{S\mathbf{p}}^{11}(t_z, t_y) CP_L \Delta_{\mathbf{q}'}^{<}(t_z - t_x) \Delta_{\mathbf{p}-\mathbf{k}}^{<}(t_y - t_x)] , \end{aligned}$$

$$\begin{aligned} \Pi_{\mathbf{k}ij}^{ab<}(t_x, t_y) = & i (\lambda_{ij}^{ab})^* \int dt_z \frac{d^3\mathbf{q}'}{(2\pi)^3} \frac{d^3\mathbf{p}}{(2\pi)^3} \quad (\text{C.4.26}) \\ & \times [S_{-(\mathbf{p}+\mathbf{q}')}^{>}(t_z - t_x) G_{S\mathbf{p}}^{22}(t_z, t_y) CP_L \Delta_{\mathbf{q}'}^{>}(t_z - t_x) \Delta_{\mathbf{p}-\mathbf{k}}^{>}(t_y - t_x) \\ & - S_{-(\mathbf{p}+\mathbf{q}')}^{11}(t_z - t_x) G_{S\mathbf{p}}^{<}(t_z, t_x) CP_L \Delta_{\mathbf{q}'}^{11}(t_z - t_x) \Delta_{\mathbf{p}-\mathbf{k}}^{>}(t_y - t_x)] . \end{aligned}$$

Appendix D

List of propagators

Free propagators

- Scalar

$$\begin{aligned}\Delta_{\mathbf{q}}^{F,-}(y) &= \frac{1}{\omega_{\mathbf{q}}} \sin(\omega_{\mathbf{q}}y) , \\ \Delta_{\mathbf{q}}^{F,+}(y) &= \frac{1}{2\omega_{\mathbf{q}}} \coth\left(\frac{\beta\omega_{\mathbf{q}}}{2}\right) \cos(\omega_{\mathbf{q}}y) , \\ \Delta_{\mathbf{q}}^{F,11}(y) &= \frac{1}{2\omega_{\mathbf{q}}} \left(\coth\left(\frac{\beta\omega_{\mathbf{q}}}{2}\right) \cos(\omega_{\mathbf{q}}y) - i \sin(\omega_{\mathbf{q}}|y|) \right) , \\ \Delta_{\mathbf{q}}^{F,22}(y) &= (\Delta_{\mathbf{q}}^{F,11}(y))^* , \\ \Delta_{\mathbf{q}}^{F,>}(y) &= \frac{1}{2\omega_{\mathbf{q}}} \left(\coth\left(\frac{\beta\omega_{\mathbf{q}}}{2}\right) \cos(\omega_{\mathbf{q}}y) - i \sin(\omega_{\mathbf{q}}y) \right) , \\ \Delta_{\mathbf{q}}^{F,<}(y) &= (\Delta_{\mathbf{q}}^{F,>}(y))^* .\end{aligned}$$

- Fermion

$$\begin{aligned}S_{\mathbf{k}}^{F,-}(y) &= i\gamma_0 \cos(\omega_{\mathbf{k}}y) + \frac{M - \mathbf{k}\gamma}{\omega_{\mathbf{k}}} \sin(\omega_{\mathbf{k}}y) , \\ S_{\mathbf{k}}^{F,+}(y) &= -\frac{\tanh\left(\frac{\beta\omega_{\mathbf{k}}}{2}\right)}{2} \left(i\gamma_0 \sin(\omega_{\mathbf{k}}y) - \frac{M - \mathbf{k}\gamma}{\omega_{\mathbf{k}}} \cos(\omega_{\mathbf{k}}y) \right) , \\ S_{\mathbf{k}}^{F,11}(y) &= \frac{\gamma_0}{2} \left(\cos(\omega_{\mathbf{k}}y) \text{sign}(y) - i \tanh\left(\frac{\beta\omega_{\mathbf{k}}}{2}\right) \sin(\omega_{\mathbf{k}}y) \right) \\ &\quad + \frac{M - \mathbf{k}\gamma}{2\omega_{\mathbf{k}}} \left(\tanh\left(\frac{\beta\omega_{\mathbf{k}}}{2}\right) \cos(\omega_{\mathbf{k}}y) - i \sin(\omega_{\mathbf{k}}|y|) \right) , \\ S_{\mathbf{k}}^{F,22}(y) &= (S_{\mathbf{k}}^{F,11}(-y))^* , \\ S_{\mathbf{k}}^{F,>}(y) &= \frac{\gamma_0}{2} \left(\cos(\omega_{\mathbf{k}}y) - i \tanh\left(\frac{\beta\omega_{\mathbf{k}}}{2}\right) \sin(\omega_{\mathbf{k}}y) \right) \\ &\quad + \frac{M - \mathbf{k}\gamma}{2\omega_{\mathbf{k}}} \left(\tanh\left(\frac{\beta\omega_{\mathbf{k}}}{2}\right) \cos(\omega_{\mathbf{k}}y) - i \sin(\omega_{\mathbf{k}}y) \right) ,\end{aligned} \tag{D.0.1}$$

$$S_{\mathbf{k}}^{F,<}(y) = \frac{\gamma_0}{2} \left(-\cos(\omega_{\mathbf{k}}y) - i \tanh\left(\frac{\beta\omega_{\mathbf{k}}}{2}\right) \sin(\omega_{\mathbf{k}}y) \right) + \frac{M - \mathbf{k}\gamma}{2\omega_{\mathbf{k}}} \left(\tanh\left(\frac{\beta\omega_{\mathbf{k}}}{2}\right) \cos(\omega_{\mathbf{k}}y) + i \sin(\omega_{\mathbf{k}}y) \right).$$

For massless SM leptons, then the mass should be set to zero $M \rightarrow 0$, the energy $\omega_{\mathbf{k}} \rightarrow k$ and a left-handed projector should be multiplied to the r.h.s of each equation

- Majorana

$$\begin{aligned} G_{\mathbf{p}}^{F,-}(y) &= \left(i\gamma_0 \cos(\omega_{\mathbf{p}}y) + \frac{M - \mathbf{p}\gamma}{\omega_{\mathbf{p}}} \sin(\omega_{\mathbf{p}}y) \right) C^{-1}, \\ G_{\mathbf{p}}^{F,+}(y) &= -\frac{\tanh\left(\frac{\beta\omega_{\mathbf{p}}}{2}\right)}{2} \left(i\gamma_0 \sin(\omega_{\mathbf{p}}y) - \frac{M - \mathbf{p}\gamma}{\omega_{\mathbf{p}}} \cos(\omega_{\mathbf{p}}y) \right) C^{-1}, \\ G_{\mathbf{p}}^{F,11}(y) &= \left[\frac{\gamma_0}{2} \left(\cos(\omega_{\mathbf{p}}y) \text{sign}(y) - i \tanh\left(\frac{\beta\omega_{\mathbf{p}}}{2}\right) \sin(\omega_{\mathbf{p}}y) \right) + \frac{M - \mathbf{p}\gamma}{2\omega_{\mathbf{p}}} \left(\tanh\left(\frac{\beta\omega_{\mathbf{p}}}{2}\right) \cos(\omega_{\mathbf{p}}y) - i \sin(\omega_{\mathbf{p}}|y|) \right) \right] C^{-1}, \\ G_{\mathbf{p}}^{F,22}(y) &= (G_{\mathbf{p}}^{F,11}(-y))^*, \\ G_{\mathbf{p}}^{F,>}(y) &= \left[\frac{\gamma_0}{2} \left(\cos(\omega_{\mathbf{p}}y) - i \tanh\left(\frac{\beta\omega_{\mathbf{p}}}{2}\right) \sin(\omega_{\mathbf{p}}y) \right) + \frac{M - \mathbf{p}\gamma}{2\omega_{\mathbf{p}}} \left(\tanh\left(\frac{\beta\omega_{\mathbf{p}}}{2}\right) \cos(\omega_{\mathbf{p}}y) - i \sin(\omega_{\mathbf{p}}y) \right) \right] C^{-1}, \\ G_{\mathbf{p}}^{F,<}(y) &= \left[\frac{\gamma_0}{2} \left(-\cos(\omega_{\mathbf{p}}y) - i \tanh\left(\frac{\beta\omega_{\mathbf{p}}}{2}\right) \sin(\omega_{\mathbf{p}}y) \right) + \frac{M - \mathbf{p}\gamma}{2\omega_{\mathbf{p}}} \left(\tanh\left(\frac{\beta\omega_{\mathbf{p}}}{2}\right) \cos(\omega_{\mathbf{p}}y) + i \sin(\omega_{\mathbf{p}}y) \right) \right] C^{-1}. \end{aligned}$$

Equilibrium propagators

- scalar

$$\begin{aligned} \Delta_{\mathbf{q}}^{eq,-}(y) &= \frac{1}{\omega_{\mathbf{q}}} \sin(\omega_{\mathbf{q}}y) e^{-\frac{\Gamma_{\mathbf{q}}|y|}{2}}, \\ \Delta_{\mathbf{q}}^{eq,+}(y) &= \frac{1}{2\omega_{\mathbf{q}}} \coth\left(\frac{\beta\omega_{\mathbf{q}}}{2}\right) \cos(\omega_{\mathbf{q}}y) e^{-\frac{\Gamma_{\mathbf{q}}|y|}{2}}, \\ \Delta_{\mathbf{q}}^{eq,11}(y) &= \frac{1}{2\omega_{\mathbf{q}}} \left(\coth\left(\frac{\beta\omega_{\mathbf{q}}}{2}\right) \cos(\omega_{\mathbf{q}}y) - i \sin(\omega_{\mathbf{q}}|y|) \right) e^{-\frac{\Gamma_{\mathbf{q}}|y|}{2}}, \\ \Delta_{\mathbf{q}}^{eq,22}(y) &= (\Delta_{\mathbf{q}}^{eq,11}(y))^*, \\ \Delta_{\mathbf{q}}^{eq,>}(y) &= \frac{1}{2\omega_{\mathbf{q}}} \left(\coth\left(\frac{\beta\omega_{\mathbf{q}}}{2}\right) \cos(\omega_{\mathbf{q}}y) - i \sin(\omega_{\mathbf{q}}y) \right) e^{-\frac{\Gamma_{\mathbf{q}}|y|}{2}}, \\ \Delta_{\mathbf{q}}^{eq,<}(y) &= (\Delta_{\mathbf{q}}^{eq,>}(y))^*. \end{aligned}$$

- Fermion

$$\begin{aligned}
S_{\mathbf{k}}^{eq,-}(y) &= \left(i\gamma_0 \cos(\omega_{\mathbf{k}}y) + \frac{M - \mathbf{k}\gamma}{\omega_{\mathbf{k}}} \sin(\omega_{\mathbf{k}}y) \right) e^{-\frac{\Gamma_{\mathbf{k}}|y|}{2}}, \\
S_{\mathbf{k}}^{eq,+}(y) &= -\frac{\tanh\left(\frac{\beta\omega_{\mathbf{k}}}{2}\right)}{2} \left(i\gamma_0 \sin(\omega_{\mathbf{k}}y) - \frac{M - \mathbf{k}\gamma}{\omega_{\mathbf{k}}} \cos(\omega_{\mathbf{k}}y) \right) e^{-\frac{\Gamma_{\mathbf{k}}|y|}{2}}, \\
S_{\mathbf{k}}^{eq,11}(y) &= \left[\frac{\gamma_0}{2} \left(\cos(\omega_{\mathbf{k}}y) \text{sign}(y) - i \tanh\left(\frac{\beta\omega_{\mathbf{k}}}{2}\right) \sin(\omega_{\mathbf{k}}y) \right) \right. \\
&\quad \left. + \frac{M - \mathbf{k}\gamma}{2\omega_{\mathbf{k}}} \left(\tanh\left(\frac{\beta\omega_{\mathbf{k}}}{2}\right) \cos(\omega_{\mathbf{k}}y) - i \sin(\omega_{\mathbf{k}}|y|) \right) \right] e^{-\frac{\Gamma_{\mathbf{k}}|y|}{2}}, \\
S_{\mathbf{k}}^{eq,22}(y) &= (S_{\mathbf{k}}^{eq,11}(-y))^*, \\
S_{\mathbf{k}}^{eq,>}(y) &= \left[\frac{\gamma_0}{2} \left(\cos(\omega_{\mathbf{k}}y) - i \tanh\left(\frac{\beta\omega_{\mathbf{k}}}{2}\right) \sin(\omega_{\mathbf{k}}y) \right) \right. \\
&\quad \left. + \frac{M - \mathbf{k}\gamma}{2\omega_{\mathbf{k}}} \left(\tanh\left(\frac{\beta\omega_{\mathbf{k}}}{2}\right) \cos(\omega_{\mathbf{k}}y) - i \sin(\omega_{\mathbf{k}}y) \right) \right] e^{-\frac{\Gamma_{\mathbf{k}}|y|}{2}}, \\
S_{\mathbf{k}}^{eq,<}(y) &= \left[\frac{\gamma_0}{2} \left(-\cos(\omega_{\mathbf{k}}y) - i \tanh\left(\frac{\beta\omega_{\mathbf{k}}}{2}\right) \sin(\omega_{\mathbf{k}}y) \right) \right. \\
&\quad \left. + \frac{M - \mathbf{k}\gamma}{2\omega_{\mathbf{k}}} \left(\tanh\left(\frac{\beta\omega_{\mathbf{k}}}{2}\right) \cos(\omega_{\mathbf{k}}y) + i \sin(\omega_{\mathbf{k}}y) \right) \right] e^{-\frac{\Gamma_{\mathbf{k}}|y|}{2}}.
\end{aligned}$$

- Majorana

$$\begin{aligned}
G_{\mathbf{p}}^{eq,-}(y) &= \left(i\gamma_0 \cos(\omega_{\mathbf{p}}y) + \frac{M - \mathbf{p}\gamma}{\omega_{\mathbf{p}}} \sin(\omega_{\mathbf{p}}y) \right) e^{-\frac{\Gamma_{\mathbf{p}}|y|}{2}} C^{-1}, \\
G_{\mathbf{p}}^{eq,+}(y) &= -\frac{\tanh\left(\frac{\beta\omega_{\mathbf{p}}}{2}\right)}{2} \left(i\gamma_0 \sin(\omega_{\mathbf{p}}y) - \frac{M - \mathbf{p}\gamma}{\omega_{\mathbf{p}}} \cos(\omega_{\mathbf{p}}y) \right) e^{-\frac{\Gamma_{\mathbf{p}}|y|}{2}} C^{-1}, \\
G_{\mathbf{p}}^{eq,11}(y) &= \left[\frac{\gamma_0}{2} \left(\cos(\omega_{\mathbf{p}}y) \text{sign}(y) - i \tanh\left(\frac{\beta\omega_{\mathbf{p}}}{2}\right) \sin(\omega_{\mathbf{p}}y) \right) \right. \\
&\quad \left. + \frac{M - \mathbf{p}\gamma}{2\omega_{\mathbf{p}}} \left(\tanh\left(\frac{\beta\omega_{\mathbf{p}}}{2}\right) \cos(\omega_{\mathbf{p}}y) - i \sin(\omega_{\mathbf{p}}|y|) \right) \right] e^{-\frac{\Gamma_{\mathbf{p}}|y|}{2}} C^{-1}, \\
G_{\mathbf{p}}^{eq,22}(y) &= (G_{\mathbf{p}}^{eq,11}(-y))^*, \\
G_{\mathbf{p}}^{eq,>}(y) &= \left[\frac{\gamma_0}{2} \left(\cos(\omega_{\mathbf{p}}y) - i \tanh\left(\frac{\beta\omega_{\mathbf{p}}}{2}\right) \sin(\omega_{\mathbf{p}}y) \right) \right. \\
&\quad \left. + \frac{M - \mathbf{p}\gamma}{2\omega_{\mathbf{p}}} \left(\tanh\left(\frac{\beta\omega_{\mathbf{p}}}{2}\right) \cos(\omega_{\mathbf{p}}y) - i \sin(\omega_{\mathbf{p}}y) \right) \right] e^{-\frac{\Gamma_{\mathbf{p}}|y|}{2}} C^{-1}, \\
G_{\mathbf{p}}^{eq,<}(y) &= \left[\frac{\gamma_0}{2} \left(-\cos(\omega_{\mathbf{p}}y) - i \tanh\left(\frac{\beta\omega_{\mathbf{p}}}{2}\right) \sin(\omega_{\mathbf{p}}y) \right) \right. \\
&\quad \left. + \frac{M - \mathbf{p}\gamma}{2\omega_{\mathbf{p}}} \left(\tanh\left(\frac{\beta\omega_{\mathbf{p}}}{2}\right) \cos(\omega_{\mathbf{p}}y) + i \sin(\omega_{\mathbf{p}}y) \right) \right] e^{-\frac{\Gamma_{\mathbf{p}}|y|}{2}} C^{-1}.
\end{aligned}$$

Non-equilibrium

- Fermion

$$\begin{aligned}
S_{\mathbf{k}}^-(y) &= \left(i\gamma_0 \cos(\omega_{\mathbf{k}}y) + \frac{M - \mathbf{k}\gamma}{\omega_{\mathbf{k}}} \sin(\omega_{\mathbf{k}}y) \right) e^{-\Gamma_{\mathbf{k}}|y|/2}, \\
S_{\mathbf{k}}^+(y, t) &= - \left(i\gamma_0 \sin(\omega_{\mathbf{k}}y) - \frac{M - \mathbf{k}\gamma}{\omega_{\mathbf{k}}} \cos(\omega_{\mathbf{k}}y) \right) \\
&\quad \times \left(\frac{\tanh\left(\frac{\beta\omega_{\mathbf{k}}}{2}\right)}{2} e^{-\Gamma_{\mathbf{k}}|y|/2} + f_l^{eq}(\omega_{\mathbf{k}}) e^{-\Gamma_{\mathbf{k}}t} \right), \\
S_{\mathbf{k}}^{11}(y, t) &= - \frac{\gamma_0}{2} \left(2i \sin(\omega_{\mathbf{k}}y) \left(\frac{\tanh\left(\frac{\beta\omega_{\mathbf{k}}}{2}\right)}{2} e^{-\Gamma_{\mathbf{k}}|y|/2} + f_l^{eq}(\omega_{\mathbf{k}}) e^{-\Gamma_{\mathbf{k}}t} \right) \right. \\
&\quad \left. - \cos(\omega_{\mathbf{k}}y) \text{sign}(y) e^{-\Gamma_{\mathbf{k}}|y|/2} \right) \\
&\quad + \frac{M - \mathbf{k}\gamma}{2\omega_{\mathbf{k}}} \left(2 \cos(\omega_{\mathbf{k}}y) \left(\frac{\tanh\left(\frac{\beta\omega_{\mathbf{k}}}{2}\right)}{2} e^{-\Gamma_{\mathbf{k}}|y|/2} + f_l^{eq}(\omega_{\mathbf{k}}) e^{-\Gamma_{\mathbf{k}}t} \right) \right. \\
&\quad \left. - i \sin(\omega_{\mathbf{k}}|y|) e^{-\Gamma_{\mathbf{k}}|y|/2} \right), \\
S_{\mathbf{k}}^{22}(y, t) &= (S_{\mathbf{k}}^{11}(y, t))^*, \\
S_{\mathbf{k}}^>(y, t) &= - \frac{\gamma_0}{2} \left(2i \sin(\omega_{\mathbf{k}}y) \left(\frac{\tanh\left(\frac{\beta\omega_{\mathbf{k}}}{2}\right)}{2} e^{-\Gamma_{\mathbf{k}}|y|/2} + f_l^{eq}(\omega_{\mathbf{k}}) e^{-\Gamma_{\mathbf{k}}t} \right) \right. \\
&\quad \left. - \cos(\omega_{\mathbf{k}}y) e^{-\Gamma_{\mathbf{k}}|y|/2} \right) \\
&\quad + \frac{M - \mathbf{k}\gamma}{2\omega_{\mathbf{k}}} \left(2 \cos(\omega_{\mathbf{k}}y) \left(\frac{\tanh\left(\frac{\beta\omega_{\mathbf{k}}}{2}\right)}{2} e^{-\Gamma_{\mathbf{k}}|y|/2} + f_l^{eq}(\omega_{\mathbf{k}}) e^{-\Gamma_{\mathbf{k}}t} \right) \right. \\
&\quad \left. - i \sin(\omega_{\mathbf{k}}y) e^{-\Gamma_{\mathbf{k}}|y|/2} \right), \\
S_{\mathbf{k}}^<(y, t) &= - \frac{\gamma_0}{2} \left(2i \sin(\omega_{\mathbf{k}}y) \left(\frac{\tanh\left(\frac{\beta\omega_{\mathbf{k}}}{2}\right)}{2} e^{-\Gamma_{\mathbf{k}}|y|/2} + f_l^{eq}(\omega_{\mathbf{k}}) e^{-\Gamma_{\mathbf{k}}t} \right) \right. \\
&\quad \left. + \cos(\omega_{\mathbf{k}}y) e^{-\Gamma_{\mathbf{k}}|y|/2} \right) \\
&\quad + \frac{M - \mathbf{k}\gamma}{2\omega_{\mathbf{k}}} \left(2 \cos(\omega_{\mathbf{k}}y) \left(\frac{\tanh\left(\frac{\beta\omega_{\mathbf{k}}}{2}\right)}{2} e^{-\Gamma_{\mathbf{k}}|y|/2} + f_l^{eq}(\omega_{\mathbf{k}}) e^{-\Gamma_{\mathbf{k}}t} \right) \right. \\
&\quad \left. + i \sin(\omega_{\mathbf{k}}y) e^{-\Gamma_{\mathbf{k}}|y|/2} \right).
\end{aligned}$$

- Majorana

$$\begin{aligned}
G_{\mathbf{p}}^{-}(y) &= \left(i\gamma_0 \cos(\omega_{\mathbf{p}}y) + \frac{M - \mathbf{p}\gamma}{\omega_{\mathbf{p}}} \sin(\omega_{\mathbf{p}}y) \right) e^{-\Gamma_{\mathbf{p}}|y|/2} C^{-1}, \\
G_{\mathbf{p}}^{+}(y, t) &= - \left(i\gamma_0 \sin(\omega_{\mathbf{p}}y) - \frac{M - \mathbf{p}\gamma}{\omega_{\mathbf{p}}} \cos(\omega_{\mathbf{p}}y) \right) \\
&\quad \times \left(\frac{\tanh\left(\frac{\beta\omega_{\mathbf{p}}}{2}\right)}{2} e^{-\Gamma_{\mathbf{p}}|y|/2} + f_N^{eq}(\omega_{\mathbf{p}}) e^{-\Gamma_{\mathbf{p}}t} \right) C^{-1}, \\
G_{\mathbf{p}}^{11}(y, t) &= - \frac{\gamma_0}{2} \left(2i \sin(\omega_{\mathbf{p}}y) \left(\frac{\tanh\left(\frac{\beta\omega_{\mathbf{p}}}{2}\right)}{2} e^{-\Gamma_{\mathbf{p}}|y|/2} + f_N^{eq}(\omega_{\mathbf{p}}) e^{-\Gamma_{\mathbf{p}}t} \right) \right. \\
&\quad \left. - \cos(\omega_{\mathbf{p}}y) \text{sign}(y) e^{-\Gamma_{\mathbf{p}}|y|/2} \right) C^{-1} \\
&\quad + \frac{M - \mathbf{p}\gamma}{2\omega_{\mathbf{p}}} \left(2 \cos(\omega_{\mathbf{p}}y) \left(\frac{\tanh\left(\frac{\beta\omega_{\mathbf{p}}}{2}\right)}{2} e^{-\Gamma_{\mathbf{p}}|y|/2} + f_N^{eq}(\omega_{\mathbf{p}}) e^{-\Gamma_{\mathbf{p}}t} \right) \right. \\
&\quad \left. - i \sin(\omega_{\mathbf{p}}|y|) e^{-\Gamma_{\mathbf{p}}|y|/2} \right) C^{-1}, \\
G_{\mathbf{p}}^{22}(y, t) &= (G_{\mathbf{p}}^{11}(y, t))^*, \\
G_{\mathbf{p}}^{>}(y, t) &= - \frac{\gamma_0}{2} \left(2i \sin(\omega_{\mathbf{p}}y) \left(\frac{\tanh\left(\frac{\beta\omega_{\mathbf{p}}}{2}\right)}{2} e^{-\Gamma_{\mathbf{p}}|y|/2} + f_N^{eq}(\omega_{\mathbf{p}}) e^{-\Gamma_{\mathbf{p}}t} \right) \right. \\
&\quad \left. - \cos(\omega_{\mathbf{p}}y) e^{-\Gamma_{\mathbf{p}}|y|/2} \right) C^{-1} \\
&\quad + \frac{M - \mathbf{p}\gamma}{2\omega_{\mathbf{p}}} \left(2 \cos(\omega_{\mathbf{p}}y) \left(\frac{\tanh\left(\frac{\beta\omega_{\mathbf{p}}}{2}\right)}{2} e^{-\Gamma_{\mathbf{p}}|y|/2} + f_N^{eq}(\omega_{\mathbf{p}}) e^{-\Gamma_{\mathbf{p}}t} \right) \right. \\
&\quad \left. - i \sin(\omega_{\mathbf{p}}y) e^{-\Gamma_{\mathbf{p}}|y|/2} \right) C^{-1},
\end{aligned}$$

$$\begin{aligned}
G_{\mathbf{p}}^<(y, t) = & - \frac{\gamma_0}{2} \left(2i \sin(\omega_{\mathbf{p}} y) \left(\frac{\tanh\left(\frac{\beta\omega_{\mathbf{p}}}{2}\right)}{2} e^{-\Gamma_{\mathbf{p}}|y|/2} + f_N^{eq}(\omega_{\mathbf{p}}) e^{-\Gamma_{\mathbf{p}} t} \right) \right. \\
& \left. + \cos(\omega_{\mathbf{p}} y) e^{-\Gamma_{\mathbf{p}}|y|/2} \right) C^{-1} \\
& + \frac{M - \mathbf{p}\gamma}{2\omega_{\mathbf{p}}} \left(2 \cos(\omega_{\mathbf{p}} y) \left(\frac{\tanh\left(\frac{\beta\omega_{\mathbf{p}}}{2}\right)}{2} e^{-\Gamma_{\mathbf{p}}|y|/2} + f_N^{eq}(\omega_{\mathbf{p}}) e^{-\Gamma_{\mathbf{p}} t} \right) \right. \\
& \left. + i \sin(\omega_{\mathbf{p}} y) e^{-\Gamma_{\mathbf{p}}|y|/2} \right) C^{-1} .
\end{aligned}$$

Bibliography

- [1] C. Amsler *et al.*, *Review of Particle Physics*, Phys. Lett. **B667** (2008).
- [2] E. Komatsu *et al.*, *Seven-Year Wilkinson Microwave Anisotropy Probe (WMAP) Observations: Cosmological Interpretation*, arXiv:1001.4538 (2010).
- [3] M. Yoshimura, *Unified Gauge Theories and the Baryon Number of the Universe*, Phys. Rev. Lett. **41** (1978) 281.
- [4] A. Yu. Ignatiev, N. V. Krasnikov, V. A. Kuzmin, V. A. and A. N. Tavkhelidze, *Universal CP Noninvariant Superweak Interaction and Baryon Asymmetry of the Universe*, Phys. Lett. **B76** (1978) 436.
- [5] D. Toussaint, S. B. Treinman, F. Wilczek and A. Zee, *Matter - Antimatter Accounting, Thermodynamics, and Black Hole Radiation*, Phys. Rev. **D19** (1979) 1036.
- [6] S. Dimopoulos and L. Susskind, *On the Baryon Number of the Universe*, Phys. Rev. **D18** (1978) 4500.
- [7] J. R. Ellis, M. K. Gaillard and D. V. Nanopoulos, *Baryon Number Generation in Grand Unified Theories*, Phys. Lett. **B80** (1979) 360.
- [8] S. Weinberg, *Cosmological Production Of Baryons*, Phys. Rev. Lett. **42** (1979) 850.
- [9] S. M. Barr, G. Segre, and H. A. Weldon, H. Arthur, *The Magnitude of the Cosmological Baryon Asymmetry*, Phys. Rev. **D20** (1979) 2494.
- [10] A. Yildiz and P. H. Cox, *Net Baryon Number, CP Violation with Unified Fields*, Phys. Rev. **D21** (1980) 906.
- [11] V. A. Rubakov and M. E. Shaposhnikov, *Elektroweak Baryon Number non-Conservation in the Early Universe and in High-Energy Collisions*, Usp. Fiz. Nauk. **166** (1996) 493.
- [12] A. Riotto and M. Trodden, *Recent Progress in Baryogenesis*, Ann. Rev. Nucl. Part. Sci. **49** (1999) 35.
- [13] J. M. Cline, *Baryogenesis*, hep-ph/0609145 (2006).
- [14] K. Kajantie, M. Laine, K. Rummukainen M. E. and Shaposhnikov, *The Electroweak Phase Transition: A Non-Perturbative Analysis*, Nucl. Phys. **B466** (1996) 189.

- [15] M. B Gavela, M. Lozano, J. Orloff O. and Pene, *Standard Model CP Violation and Baryon Asymmetry. Part 1: Zero Temperature*, Nucl. Phys. **B430** (1994) 345.
- [16] M. B. Gavela, P. Hernandez, J. Orloff O. and Pene, *Standard Model CP-Violation and Baryon Asymmetry*, Mod. Phys. Lett. **A9** (1994) 795.
- [17] M. Losada, *High Temperature Dimensional Reduction of the MSSM and Other Multi-Scalar Models*, Phys. Rev. **D56** (1997) 2893.
- [18] M. S. Carena, M. Quiros and C. E. M. Wagner, *Opening the Window for Electroweak Baryogenesis*, Phys. Lett. **B380** (1996) 81.
- [19] D. Delepine, J. M. Gerard, F. R. J. Gonzalez and J. Weyers, *A Light stop and Electroweak Baryogenesis*, Phys. Lett. **Phys. Lett** (1996) 183.
- [20] I. Affleck and M. Dine, *A New Mechanism for Baryogenesis*, Nucl. Phys. **B249** (1985) 361.
- [21] M. Fujii, K. Hamaguchi and T. Yanagida, *Affleck-Dine baryogenesis / leptogenesis with a gauged $U(1)(B-L)$* , Phys. Rev. **D64** (2001) 123526.
- [22] K. Hamaguchi, *Cosmological baryon asymmetry and neutrinos: Baryogenesis via leptogenesis in supersymmetric theories*, hep-ph/0212305 (2002).
- [23] T. Asaka and M. Shaposhnikov, *The ν MSSM, Dark Matter and Baryon Asymmetry of the Universe*, Phys. Lett. **B620** (2005) 17.
- [24] A. D. Sakharov, *Violation of CP Invariance, C Asymmetry, and Baryon Asymmetry of the Universe*, JETP Lett. **5** (1967) 24.
- [25] M. Fukugita and T. Yanagida, *Baryogenesis Without Grand Unification*, Phys. Lett. **B5** (1967) 24.
- [26] W. Buchmuller, R. D. Peccei and T. Yanagida, *Leptogenesis as the Origin of Matter*, Ann. Rev. Nucl. Part. Sci. **55** (2005) 311.
- [27] W. Buchmuller, P. Di Bari and M. Plumacher, *Leptogenesis for Pedestrians*, Ann. Phys. **315** (2005) 305.
- [28] G. F. Giudice, A. Notari, M. Raidal, A. Riotto, A. Strumia, *Radiative Leptogenesis in Minimal Seesaw Models*, Nucl. Phys. **B685** (2004) 89.
- [29] T. Yanagida, *Horizontal Symmetry and Masses of Neutrinos*, Prog. Theor. Phys. **63** (1980) 1103.
- [30] M. Gell-Mann, P. Ramond and R. Slansky, *in Supergravity*, Freedman et al. North Holland (1979).
- [31] V. A. Kuzmin, V. A. Rubakov and M. E. Shaposhnikov, *On the Anomalous Electroweak Baryon Number Nonconservation in the Early Universe*, Phys. Lett. **B155** (1985) 36.

- [32] G. 't Hooft, *Symmetry Breaking through Bell-Jackiw Anomalies*, Phys. Rev. Lett. **37** (1976) 8.
- [33] M. Kawasaki, K. Kohri and T. Moroi, *Big-Bang Nucleosynthesis and Hadronic Decay of Long-Lived Massive Particles*, Phys. Rev. **D71** (2005) 083502.
- [34] R. H. Cyburt, J. Ellis, B. D. Fields, F. Luo, K. A. Olive and V. C. Spanos, *Nucleosynthesis Constraints on a Massive Gravitino in Neutralino Dark Matter Scenarios*, JCAP **0910** (2009) 021.
- [35] K. Jedamzik, *Big Bang Nucleosynthesis Constraints on Hadronically and Electromagnetically Decaying Relic Neutral Particles*, Phys. Rev. **D74** (2006) 103509.
- [36] M. Pospelov, *Particle Physics Catalysis of Thermal Big Bang Nucleosynthesis*, Phys. Rev. Lett. **98** (2007) 231301.
- [37] K. Kohri and F. Takayama, *Big Bang Nucleosynthesis with Long Lived Charged Massive Particles*, Phys. Rev. **D76**, 063507 (2007).
- [38] M. Kaplinghat and A. Rajaraman, *Big Bang Nucleosynthesis with Bound States of Long-lived Charged Particles*, Phys. Rev. **D74**, 103004 (2006).
- [39] R. H. Cyburt *et al.*, *Bound-State Effects on Light-Element Abundances in Gravitino Dark Matter Scenarios*, JCAP **0611**, 014 (2006).
- [40] K. Hamaguchi *et al.*, *Stau-Catalyzed Li-6 Production in Big-Bang Nucleosynthesis*, Phys. Lett. **B650** (2007) 268.
- [41] J. Pradler and F. D. Steffen, *Implications of Catalyzed BBN in the CMSSM with Gravitino Dark Matter*, Phys. Lett. **B666**, 181 (2008).
- [42] M. Pospelov, J. Pradler and F. D. Steffen, *Constraints on Supersymmetric Models from Catalytic Primordial Nucleosynthesis of Beryllium*, JCAP **0811** (2008) 020.
- [43] W. Buchmüller, L. Covi, K. Hamaguchi, A. Ibarra and T. Yanagida, *Gravitino Dark Matter in R-Parity Breaking Vacua*, JHEP **0703**, 037 (2007).
- [44] A. De Simone, M. Garny, A. Ibarra and C. Weniger, *Supersymmetric Leptogenesis with a Hidden Sector*, arXiv:1004.4890 [hep-ph].
- [45] C. Cheung, J. Mardon, Y. Nomura and J. Thaler, *A Definitive Signal of Multiple Supersymmetry Breaking at the LHC*, arXiv:1004.4637 [hep-ph].
- [46] J. Pradler and F. D. Steffen, *Constraints on the Reheating Temperature in Gravitino Dark Matter Scenarios*, Phys. Lett. **B648** (2007) 224.
- [47] E. W. Kolb and M. S. Turner, *The Early Universe*, Addison-Wesley, New York (1990).
- [48] V. Mukhanov, *Physical Foundations of Cosmology*, Cambridge University Press, Cambridge (2005).

- [49] P. Danielewicz, *Quantum Theory of Nonequilibrium Processes. 1*, Ann. Phys. **152** (1984) 239.
- [50] Y. B. Ivanov, J. Knoll and D. N. Voskresensky *Resonance Transport and Kinetic Entropy*, Nucl. Phys. **A672** (2000) 313.
- [51] Y. B. Ivanov, J. Knoll and D. N. Voskresensky *Exact Conservation Laws of the Gradient Expanded Kadanoff-Baym Equations*, Ann. Phys. **293** (2001) 126.
- [52] J.-P. Blaizot and E. Iancu *The Quark gluon plasma: Collective Dynamics and Hard Thermal Loops*, Phys. Rept. **359** (2002) 355.
- [53] G. F. Giudice, A. Notari, M. Raidal, A. Riotto, A. Strumia, *Towards a Complete Theory of Thermal Leptogenesis in the SM and MSSM*, Nucl. Phys. **B685** (2005) 89.
- [54] A. De Simone and A. Riotto, *Quantum Boltzmann Equations and Leptogenesis*, JCAP **0708** (2007) 002.
- [55] M. Garny, A. Hohenegger, A. Kartavtsev and M. Lindner, *Systematic Approach to Leptogenesis in Nonequilibrium QFT: Vertex Contribution to the CP-Violating Parameter*, Phys. Rev. **D80** (2009) 125027.
- [56] M. Garny, A. Hohenegger, A. Kartavtsev and M. Lindner, *Systematic Approach to Leptogenesis in Nonequilibrium QFT: Self-Energy Contribution to the CP-Violating Parameter*, Phys. Rev. **D81** (2010) 085027.
- [57] M. Garny, A. Hohenegger and A. Kartavtsev, *Quantum Corrections to Leptogenesis from the Gradient Expansion*, 1005.5385 [hep-ph] (2010).
- [58] J. F. Koksma, T. Prokopec and M. G. Schmidt, *Decoherence in an Interacting Quantum Field Theory: The Vacuum Case*, Phys. Rev. **D81** (2010) 065030.
- [59] E. Nardi, Y. Nir, E. Roulet and J. Racker, *The Importance of Flavor in Leptogenesis*, JHEP **01** (2006) 164.
- [60] A. Abada, S. Davidson, F-X. Josse-Michaux, M. Losada and A. Riotto, *Flavor Issues in Leptogenesis*, JCAP **0604** (2006) 004.
- [61] A. Abada *et al.*, *Flavour matters in leptogenesis*, JHEP **09** (2006) 010.
- [62] R. Barbieri, P. Creminelli, A. Strumia and N. Tetradis, *Baryogenesis Through Leptogenesis*, Nucl. Phys. **B575** (2000) 61.
- [63] S. Blanchet and P. Di Bari, *Flavor Effects on Leptogenesis Predictions*, JCAP **0703** (2007) 018.
- [64] S. Blanchet and P. Di Bari, *Flavor Effects in Thermal Leptogenesis*, Nucl. Phys. Proc. Suppl. **168** (2007) 372.
- [65] A. Anisimov, S. Blanchet and P. Di Bari, *Viability of Dirac Phase Leptogenesis*, JCAP **0804** (2008) 033.

- [66] S. Antusch and A. M. Teixeira, *Towards Constraints on the SUSY Seesaw from Flavour-dependent Leptogenesis*, JCAP **0702** (2007) 024.
- [67] S. Antusch, S. F. King and A. Riotto, *Flavour-Dependent Leptogenesis with Sequential Dominance*, JCAP **0611** (2006) 011.
- [68] A. Pilaftsis and T. E. J. Underwood, *Resonant Leptogenesis*, Nucl. Phys. **B692** (2004) 303.
- [69] A. Pilaftsis and T. E. J. Underwood, *Electroweak-Scale Resonant Leptogenesis*, Phys. Rev. **D72** (2005) 113001.
- [70] A. Anisimov, A. Broncano and M. Plumacher, *The CP-Asymmetry in Resonant Leptogenesis*, Nucl. Phys. **B737** (2006) 176.
- [71] A. De Simone and A. Riotto, *On Resonant Leptogenesis*, JCAP **0708** (2007) 013.
- [72] M. Drewes, *Quantum Aspects of Early Universe Thermodynamics* Ph.D. Thesis.
- [73] W. Buchmuller and S. Fredenhagen, *Quantum Mechanics of Baryogenesis*, Phys. Lett. **B483** (2000) 217.
- [74] L. P. Kadanoff and G. Baym, *Quantum Statistical Mechanics*, Benjamin, New York (1962).
- [75] J. Schwinger, *Brownian Motion of a Quantum Oscillator*, J. Math. Phys. **2** (1961) 407.
- [76] P. M. Bakschi and K. T. Mahanthappa, *Expectation Value in Formalism in Quantum Field Theory. 1*, J. Math. Phys. **4** (1963) 1.
- [77] P. M. Bakschi and K. T. Mahanthappa, *Expectation Value in Formalism in Quantum Field Theory. 2*, J. Math. Phys. **4** (1963) 12.
- [78] L. V. Keldysh, *Diagram Technique for Nonequilibrium Processes*, Zh. Eksp. Teor. Fiz. **47** (1964) 1515 [Sov. Phys. JETP **20** (1965) 1018].
- [79] M. Le Bellac, *Thermal Field Theory*, Cambridge University Press, Cambridge, (1996).
- [80] J. Berges, *Introduction to Nonequilibrium Quantum Field Theory*, AIP Conf. Proc. **739** (2005) 3.
- [81] K. c. Chou, Z. b. Su, B. l. Hao and L. Yu, *Equilibrium And Nonequilibrium Formalisms Made Unified*, Phys. Rept. **118** (1985) 1.
- [82] J. Zinn-Justin, *Quantum Field Theory and Critical Phenomena*, Int. Ser. Monogr. Phys. **85** (1993) 1.
- [83] J. Yokoyama, *Fate of Oscillating Scalar Fields in the Thermal Bath and Their Cosmological Implications*, Phys. Rev. D **70** (2004) 103511.

- [84] D. Boyanovsky, K. Davey and C. M. Ho, *Particle abundance in a thermal plasma: Quantum kinetics vs. Boltzmann equation*, Phys. Rev. D **71** (2005) 023523.
- [85] E. Peskin and V. Schroeder, *An Introduction to Quantum Field Theory*, Westview Press (1995).
- [86] A. Anisimov, W. Buchmueller, M. Drewes and S. Mendizabal, *Nonequilibrium Dynamics of Scalar Fields in a Thermal Bath*, Annals Phys. **324** (2009) 1234.
- [87] A. Anisimov, W. Buchmueller, M. Drewes and S. Mendizabal, *Leptogenesis from Quantum Interference in a Thermal Bath*, Phys. Rev. Lett. **104** (2010) 121102.
- [88] M. Kobayashi and T. Maskawa, *CP Violation In The Renormalizable Theory Of Weak Interaction*, Prog. Theor. Phys. **49** (1973) 652.
- [89] R. N. Mohapatra and G. Senjanovic, *Neutrino Masses and Mixings in Gauge Models with Spontaneous Parity Violation*, Phys. Rev. **D23** (1981) 165.
- [90] M. Magg and C. Wetterich, *Neutrino Mass Problem and Gauge Hierarchy*, Phys. Lett. **B94** (1980) 61.
- [91] G. Lazarides and Q. Shafi, *Neutrino Masses in SU(5)*, Phys. Lett. **B99** (1981) 113.
- [92] R. Foot, H. Lew, X. G. He and G. C. Joshi, *Seesaw Neutrino Masses Induced by a Triplet of Leptons*, Z. Phys. **C44** (1989) 441.
- [93] B. Bajc, M. Nemevsek and G. Senjanovic, *Probing Seesaw at LHC*, Phys. Rev. **D76** (2007) 055011.
- [94] I. Dorsner and P. Fileviez Perez, *Upper Bound on the Mass of the Type III Seesaw Triplet in an SU(5) Model*, JHEP **06** (2007) 029.
- [95] P. B. Arnold, D. Son and L. G. Yaffe, *The Hot Baryon Violation Rate is $O(\alpha(w)^5 T^4)$* , Phys. Rev. **D55** (1997) 6264.
- [96] P. B. Arnold, D. Son and L. G. Yaffe, *Hot B Violation, Color Conductivity, and $\log(1/\alpha)$ Effects*, Phys. Rev. **D59** (1999) 105020.
- [97] D. Bodeker, *On the Effective Dynamics of Soft non-Abelian Gauge Fields at Finite Temperature*, Phys. Lett. **B426** (1998) 351.
- [98] D. Bodeker, *From hard Thermal Loops to Langevin Dynamics*, Nucl. Phys. **B559** (1999) 502.
- [99] K. Huang, *Statistical Mechanics*, Wiley (1987).
- [100] M. E. Shaposhnikov, *Possible Appearance of the Baryon Asymmetry of the Universe in an Electroweak Theory*, Phys. Rev. Lett. **44** (1986) 465.
- [101] C. Jarlskog, *Commutator of the Quark Mass Matrices in the Standard Electroweak Model and a Measure of Maximal CP Violation*, JETP Lett. **55** (1985) 1039.

- [102] L. Covi, E. Roulet and F. Vissani, *CP Violating Decays in Leptogenesis Scenarios*, Phys. Lett. **B384** (1996) 169.
- [103] L. Covi and E. Roulet, *Baryogenesis From Mixed Particle Decays*, Phys. Lett. **B399** (1997) 113.
- [104] M. Flanz, E. A. Paschos, U. Sarkar, J. Weiss, *Baryogenesis Through Mixing of Heavy Majorana Neutrinos*, Phys. Lett. **B389** (1996) 693.
- [105] S. Davidson and A. Ibarra, *A Lower Bound on the Right-Handed Neutrino Mass from Leptogenesis*, Phys. Lett. **B535** (2002) 25.
- [106] L. Covi, N. Rius, E. Roulet and F. Vissani, *Finite Temperature Effects on CP Violating Asymmetries*, Phys. Lett. **D57** (1998) 93.
- [107] T. Matsubara, *A New Approach to Quantum Statistical Mechanics*, Progr. Theoret. Phys. **14** (1955) 351.
- [108] H. A. Weldon, *Simple Rules For Discontinuities In Finite Temperature Field Theory*, Phys. Rev. **D28** (1983) 2007.
- [109] J. Morales and C. Quimbay and F. Fonseca, *Fermionic Dispersion Relations at Finite Temperature and non-vanishing Chemical Potentials in the Minimal Standard Model*, Nucl. Phys. **B560** (1999) 601.
- [110] M. Beneke and B. Garbrecht and M. Herranen and P. Schwaller, *Finite Number Density Corrections to Leptogenesis*, arXiv:1002.1326 [hep-ph].
- [111] M. Garny and M. M. Muller, *Kadanoff-Baym Equations with Non-Gaussian Initial Conditions: The Equilibrium Limit*, arXiv:0904.3600 [hep-ph].
- [112] P. Arnold, G. D. Moore and L. G. Yaffe, *Effective Kinetic Theory for High Temperature Gauge Theories*, JHEP **0301** (2003) 030.
- [113] A. Hohenegger, A. Kartavtsev M. and Lindner, *Deriving Boltzmann Equations from Kadanoff-Baym Equations in Curved Space-Time*, Phys. Rev. **D78** (2008) 085027.
- [114] M. Laine and O. Philipsen and M. Tassler, *Wilson Loop in classical Lattice Gauge Theory and the Thermal Width of Heavy Quarkonium*, Pos LAT2007 (2007) 230.
- [115] O. Philipsen, *Lattice QCD at finite Temperature and Density*, Eur. Phys. J. ST **152** (2007) 29.
- [116] M. Kitazawa and T. Kunihiro and Y. Nemoto, *Novel Collective Excitations and the Quasi-Particle Picture of Quarks with a Massive Boson at Finite Temperature*, Prog. Theor. Phys. **117** (2007) 103.